

University of Southampton Research Repository ePrints Soton

Copyright © and Moral Rights for this thesis are retained by the author and/or other copyright owners. A copy can be downloaded for personal non-commercial research or study, without prior permission or charge. This thesis cannot be reproduced or quoted extensively from without first obtaining permission in writing from the copyright holder/s. The content must not be changed in any way or sold commercially in any format or medium without the formal permission of the copyright holders.

When referring to this work, full bibliographic details including the author, title, awarding institution and date of the thesis must be given e.g.

AUTHOR (year of submission) "Full thesis title", University of Southampton, name of the University School or Department, PhD Thesis, pagination

UNIVERSITY OF SOUTHAMPTON
FACULTY OF ENGINEERING SCIENCE AND MATHEMATICS
OPTOELECTRONICS RESEARCH CENTRE

Photodarkening in Ytterbium doped silica fibers
under 488 nm CW irradiation

by

Chandrajit Basu

Thesis for the degree of Master of Philosophy

September 2010

UNIVERSITY OF SOUTHAMPTON

ABSTRACT

FACULTY OF ENGINEERING, SCIENCE & MATHEMATICS

OPTOELECTRONICS RESEARCH CENTRE

Master of Philosophy

PHOTODARKENING IN YTTERBIUM DOPED SILICA FIBERS UNDER
488 NM CW IRRADIATION

By
Chandrajit Basu

Generation of high power 1178 nm laser line from an Yb-doped aluminosilicate fiber laser and subsequent frequency doubling for generating 589 nm laser, can be a smarter alternative to the more complicated approaches utilized for laser guide stars till date. Since high power Yb-doped aluminosilicate fiber lasers suffer from photodarkening, it is of great importance to understand photodarkening thoroughly and mitigate it accordingly.

Non-resonant 488 nm CW laser radiation induced photodarkening in Yb-doped aluminosilicate fibers was investigated as a major part of this project. The 488 nm CW irradiation induced excess background loss, in the visible (VIS) and near infrared (NIR) regions, was observed. Temporal evolution of excess background loss, in VIS and NIR regions, even after stopping the 488 nm irradiation, was also observed, using white light source, 638.7 nm laser diode source, He-Ne source and 1285 nm LED based OTDR accordingly. An Yb-doped phosphosilicate fiber was observed to be highly resistant to photodarkening. Photodarkening results in several aluminosilicate fibers with varied Yb-doping concentration were compared.

Effects of external heating, during and after 488 nm CW irradiation, were investigated. An important observation was the post-irradiation temporal growth in photodarkening which means that photodarkening doesn't 'freeze' immediately after stopping the 488 nm CW irradiation. Variation of this post-irradiation loss dynamics with external heating was also studied.

NIR pump induced photodarkening was also studied to a certain extent and a bluish fluorescence from the fibers was observed, which could be related to Yb ion-pair effect. Effects of hydrogen loading on Yb-doped aluminosilicate fibers, in the context of photodarkening, were also studied briefly.

Contents

Abstract	i
List of Figures & Tables	iv
Declaration of Authorship.....	viii
Acknowledgements.....	ix
List of Abbreviations	xi
1. Introduction	
1.1 Introduction & Motivation.....	1
1.2 Thesis Outline.....	3
2. Ytterbium Doped Fiber Lasers	
2.1 Ytterbium doped fiber lasers: A brief introduction	5
2.2 Spectroscopic properties of ytterbium-doped silica: a brief overview.....	5
2.3 Double clad fiber (DCF) structure & High power fiber laser (HPFL)	7
2.4 Ytterbium doped fiber: MCVD fabrication technique	9
2.5 Solution doping technique	11
2.6 Fiber drawing	12
2.7 Conclusions	14
Bibliography	15
3. Laser Guide Stars	
3.1 Laser Guide Stars: A brief knowhow & the possibilities for frequency doubled YDFL as a source	17
3.2 Status of LGS	18
3.3 Sodium beacon & laser requirements.....	19
3.4 Yb-doped fiber laser operating at 1178 nm	20
Bibliography.....	23
4. Photodarkening in Ytterbium Fiber Lasers: Literature review and brief theoretical background	
4.1 Background loss in optical fibers	25
4.2 Literature review and the status of the topic area	26
4.2.1 Photodarkening in Yb-doped silica fibers.....	26
4.2.1(a) Materials related facts on photodarkening of Yb-doped fibers	27
4.2.1(b) Photobleaching.....	28
Bibliography.....	30
5. Photodarkening in YDF by 488 nm CW irradiation	31
5.1 Introduction.....	34
5.2.1 Photodarkening experiment.....	35
5.2.2 Experimental results with fiber F628-LF235	37
5.2.3 Experimental results with fiber T0155-L30100	41
5.2.4 Phosphosilicate fiber	44
5.3 Photodarkening experiments with simultaneous probing at 633 nm.....	47

5.3.1 No heating of fibre during or after irradiation by 488 nm CW source	48
5.3.2 Influence of heat on photodarkening of normal Yb-doped fibers.....	51
5.3.2.1 Heating during irradiation.....	51
5.3.2.2 Heating after irradiation.....	53
5.4 Influence of probing sources on pristine Yb-doped fibers.....	57
5.5 Conclusion.....	58
Bibliography.....	60
6. NIR pump induced photodarkening.....	61
6.1 Introduction.....	61
6.2 Experimental setup and results	61
6.3 Pumping at 1047 nm and external heating effect on YDF.....	69
6.4 Simulation of YDFA.....	71
6.5 Conclusions.....	73
Bibliography.....	74
7. Hydrogen loaded fibers.....	76
7.1 Photodarkening in hydrogen loaded fibers under 488 nm irradiation	76
7.2 Hydrogen loading and effect on the coating material.....	78
7.3 Discussion & Conclusion.....	81
Bibliography.....	82
8. Conclusions.....	83
8.1 Summary and Conclusions.....	83
8.2 Future work.....	85
Bibliography.....	87
Appendix A	
List of Publications.....	88

List of Figures & Tables

Fig.2.1: Absorption and emission bands of Yb ³⁺	page 6
Fig.2.2: Absorption and emission cross-sections of Yb ³⁺	page 7
Fig.2.3: Double-clad optical fiber schematics.....	page 8
Fig.2.4: Schematic diagram of a typical MCVD preform fabrication system...page	10
Fig.2.5: Schematics of Solution Doping Technique.....	page 11
Fig.2.6: Schematics of optical fiber drawing tower system.....	page 13
Fig.2.7: MCVD & Solution doping based fiber manufacturing schematics.....	page 14
Fig.3.1: Sodium doublet energy diagram	page 17
Fig.3.2: A Simplified schematic diagram of LGS base AOI.....	page 18
Fig.5.1: Schematic description of the main photodarkening experiments performed	page 34
Fig.5.2: Schematic diagram of the photodarkening experimental setup	page 35
Fig.5.3: Typical photodarkening trend in Yb-doped fiber (F628-LF235) irradiated with 488 nm CW source	page 39
Fig.5.4: Post-irradiation temporal evolution of loss in F628-LF235, observed on OSA	page 39
Fig.5.5: Loss evolution probed with 638.7 nm source on F628-LF235 fiber... page	40
Fig 5.6: Background loss in F628-LF235 observed using cutback technique with a 638.7 nm source: comparison between a pristine and a photodarkened fiber...page	40
Fig.5.7: Post-irradiation temporal evolution of loss measured by OTDR	page 41
Fig.5.8: Drop in throughput power in the fiber T0155-L30100	page 42
Fig.5.9: Post irradiation loss evolution in fiber T0155 L30100	page 43
Fig.5.10: Loss comparison by cutback technique	page 43
Fig.5.11: Post-irradiation temporal loss evolution observed on OTDR	page 44
Fig.5.12: Loss comparison by cutback technique (at 1047 nm)	page 45
Fig.5.13: Loss comparison by cutback technique (at 633 nm)	page 45

Fig.5.14: Photodarkening by 488 nm CW irradiation and simultaneous probing at 633 nmpage 47

Fig.5.15: Throughput power drop at 488 nm due to photodarkening, without any external heatingpage 49

Fig.5.16: Throughput power drop of the probe (633 nm) due to photodarkening, without any external heatingpage 49

Fig.5.17 Post irradiation temporal loss evolution observed on OSA (using a white light source)page 50

Fig.5.18: Fitting to identify Rayleigh scattering centrespage 51

Fig.5.19: Photodarkening in a fiber under external heating during 488nm irradiationpage 52

Fig.5.20: Drop in the probe (633 nm) throughput power in T0155L30100 fiber, during 488 nm irradiation with simulatenous external heating and afterwardspage 53

Fig.5.21: Drop in throughput power of the 488 nm irradiation in T0155L30100 fiber. The fiber samples were heated after finishing 488 nm irradiationpage 55

Fig.5.22: Post-irradiation heating and effect on temporal loss evolution observed on an OSA, using a white light sourcepage 55

Fig.5.23: Plot to identify whether Rayleigh scattering centres are formed and are dominant in the post irradiation temporal loss evolution process, Please see text for detailspage 56

Fig.5.24: Effect of external heating on post-irradiation temporal loss evolution.....page 56

Fig.5.25: Schematic of a probable path for post-irradiation temporal loss evolution.....page 57

Fig.5.26: Pristine YDF monitored on an OSA, using a white light sourcepage 58

Fig.5.27: Optical absorption in an Yb-doped fiber preform before and after 488 nm irradiation (Inset: enlarged section to highlight the ODC peak at 220 nm)page 59

Fig.6.1: Schematic Diagram of NIR pumped photodarkening setuppage 62

Fig.6.2: WDM characterizationpage 62

Fig.6.3: WDM characterizationpage 62

Fig.6.4: bluish fluorescence from (a) 17000 ppm YDF(aluminosilicate) & (b) 3500 ppm YDF(aluminosilicate)	page 63
Fig.6.5: Very faint bluish fluorescence from 20000 ppm YDF (phosphosilicate).....	page 64
Fig.6.6: Faint bluish fluorescence from H-loaded 17000 ppm YDF. The loss was so high that the fluorescence is visible only from the initial portion (from launching end) of the FUT	page 64
Fig.6.7: Power calibration of the pump diode (977 nm)	page 65
Fig.6.8: Output spectrum observed on the OSA: 17000 ppm YDF(aluminosilicate)	page 65
Fig.6.9: Output spectrum observed on the OSA: 3500 ppm YDF(aluminosilicate)	page 66
Fig.6.10: Output spectrum observed on the OSA: 15 cm long, 20000 ppm YDF (phosphosilicate)	page 66
Fig.6.11: Output spectra of the phosphosilicate YDF at different pump / probe conditions	page 67
Fig.6.12: Output spectrum from an HL fiber under 977 nm pump and 633 nm probe	page 67
Fig.6.13: Temporal power drop at NIR (pump and ASE combined).....	page 68
Fig.6.14: Power calibration of the 1047 nm Nd:YLF source	page 68
Fig.6.15: Throughput power stability (No photodarkening observed)	page 69
Fig.6.16: Schematic diagram of the setup for monitoring ASE variation with temperature.....	page 69
Fig.6.17: Variation of throughput spectrum on heating the FUT	page 70
Fig.6.18: Zoomed in version of Fig. 5.17	page 71
Fig.6.19: Simulation of inversion vs pump power in a YDF	page 72
Fig.7.1: Normalized drop in throughput power (@488 nm) in HL YDF samples (T0155L30100)	page 77
Fig.7.2: Drop in the throughput power of the probe (@633 nm) in HL YDF samples (T0155L30100)	page 77

Fig.7.3: White light throughput spectra in an HL pristine YDF sample (straight & twisted) and comparison with a non-HL pristine samplepage 79

Fig.7.4: Whitelight throughput spectra, around the Yb³⁺ absorption band in an HL pristine YDF sample (straight & twisted) and comparison with a non-HL pristine samplepage 80

Fig.7.5: Refractive index profile comparison between a pristine HL fiber sample and the same after being irradiated by 488 nm laser sourcepage 80

Table T5.1: Summary of photodarkening in Yb-doped aluminosilicate fibers under 488 nm CW irradiationpage 46

Table T5.2: Summary of PD induced loss in T0155L30100 fiber without external heating. The cutback loss, measured with a pristine sample @633 nm, was 1.06 dB/mpage 50

Table T5.3: Summary of the PD loss in T0155L30100 fiber due to 488 nm irradiation with simultaneous external heatingpage 53

Table T7.1: Summary of the results related to the data shown in Fig.1 & Fig.2page 78

Declaration of Authorship

I, *Chandrajit Basu*, declare that this thesis entitled

'Photodarkening in Ytterbium doped silica fibers under 488 nm CW irradiation ',

and the work presented in the thesis are both my own, and have been generated by me as a result of my own original research. I confirm that:

- this work was done wholly or mainly while in candidature for a research degree at this University;
- where any part of this thesis has previously been submitted for a degree or any other qualification at this University or any other institution, this has been clearly stated;
- where I have consulted the published work of others, this is always clearly attributed;
- where I have quoted from the work of others, the source is always given. With the exception of such quotations, this thesis is entirely my own work;
- I have acknowledged all main sources of help;
- where the thesis is based on work done by myself jointly with others, I have made clear exactly what was done by others and what I have contributed myself;
- parts of this work have been published as: Refer to Appendix A (List of Publications).

Signed:

Date:.....

Acknowledgements

First of all, I would like to express my heartfelt thanks to my supervisor, Dr. Jayanta Kumar Sahu for his invaluable guidance, support and encouragement. He has always been very patient in discussing the technical and scientific issues at length and I am really grateful to him for everything.

I'm grateful to my group mates, Dr. Alexander Boyland, Dr. Seongwoo Yoo, Mr. Andrew Webb, Mr. Robert J Standish and Mridu P Kalita for their active support in scientific and technical matters and also for providing me with a friendly work environment within the group.

I'm also thankful to Prof. David Payne, Prof. David Richardson, Prof. Rob Eason, Prof. Johan Nilsson, Prof. David Shepherd, Dr. Bill Brocklesby, Dr. Senthil Ganapathy and Dr. Eleanor Tarbox for their encouragement and support. Special thanks to Dr. Morten Ibsen who helped me immensely by providing hydrogen loaded fibers. I'm grateful to Dr. Collin Sones and Dr. Sakellaris Mailis for their advice and help with the Argon laser source and beyond. Thanks to Dr. Ping Hua for providing me with a diode laser source for my experiments.

ORC has been a wonderful place to work and apart from the world class scientific environment and facilities, I will always remember the friendly staff and the fellow students for making me feel at home in Southampton. My heartfelt thanks to the one and only, Mrs. Eveline Smith, who always addressed the official issues with stunning speed but with a smiling face and I'll always remember her for her supportive and caring attitude.

Thanks to ORC for providing me with a full scholarship for successfully carrying out my research work.

I would like to thank my parents, grandparents and my friends for their encouragement and support. My father deserves special thanks for propelling me towards a career in scientific research and my grandpa deserves the same for funding my ‘crazy projects’ in my childhood.

I am grateful to Prof. P K Datta, Dept. of Physics & Meteorology, IIT Kharagpur, India, who introduced to me the fascinating world of Optoelectronics and also recommended my postgraduate study at the ORC, University of Southampton.

This work is dedicated to all the loving and caring people I have ever come across in life.

Chandrajit Basu

List of abbreviations

AOI	Adaptive Optical Imaging
ASE	Amplified Spontaneous Emission
CW	Continuous Wave
DCF	Double Clad Fiber
DM	Dichroic Mirror
DMM	Digital Multimeter
DND	Direct Nanoparticle Deposition
ESO	European Southern Observatory
FBG	Fiber Bragg Grating
FUT	Fiber Under Test
HL	Hydrogen Loaded
IR	Infra-Red
LED	Light Emitting Diode
LGS	Laser Guide Star
MCVD	Modified Chemical Vapour Deposition
MFC	Mass Flow Controller
MMTO	Multiple Mirror Telescope Observatory
NBOHC	Non-Bridging Oxygen Hole Centre
NDFL	Neodymium Doped Fiber Laser
NIR	Near Infra-Red
ODC	Oxygen Deficient Centre
OSA	Optical Spectrum Analyzer
OTDR	Optical Time Domain Reflectometer
OVD	Outside Vapour Deposition
PBGF	Photonic Band Gap Fiber
PD	Photodarkening/Photodarkened
PPM	Parts Per Million
SHG	Second Harmonic Generation
SM	Single Mode
UV	Ultra Violet
VAD	Vapour Axial Deposition
VIS	Visible
VLT	Very Large Telescope
WDM	Wavelength Division Multiplexer
WHT	William Herschel Telescope
YDF	Ytterbium Doped Fiber
YDFL	Ytterbium Doped Fiber Laser

Chapter 1

Introduction

1.1 Introduction and Motivation:

The fascinating world of Fiber Optics can be broadly divided into four areas:

- a) Optical Fiber Communication
- b) Fiber Lasers & Amplifiers
- c) Fiber Sensors
- d) Imaging (e.g. endoscopy)

Optical fibers completely revolutionized the world of communication. On the other hand, tiny and compact fiber lasers came up as a promising alternative to the gigantic solid state or gas lasers. Rare-earth doped fiber cores behave like any bulk solid state active media, but with some extraordinary features. Excellent optical-to-optical efficiency, single polarization, single spatial mode operation, easy thermal load handling – make them very attractive for industrial applications. Ytterbium doped fiber lasers (YDFLs) have been reported to be competing at the kW level in the continuous wave (CW) mode and hundreds of watts in the pulsed mode. In the recent years, power scaling has become very competitive in this domain.

After conquering the industrial arena for metal cutting, welding and such material processing related applications, YDFLs have also drawn significant attention from the Laser Guide Star (LGS) community. Most of the present LGS sources are solid state bulky lasers which demand a lot of complicated optical design and maintenance, let alone the costs involved. Having a compact fiber laser source for an LGS would definitely be an interesting target. YDFLs typically operate in the 1030-1080 nm region and, in order to generate 589 nm line for an LGS, one may go for second harmonic generation (SHG) from the 1178 nm line. That means pushing the emission cross-section of the YDFLs towards the higher wavelength region. This is a challenging task, keeping in mind the requirements of the LGS. Researchers have successfully demonstrated various routes to generate 1178 nm from YDFLs and

these findings are discussed in chapter 2 of the thesis. Having said about the positive and promising sides of YDFs briefly, let us have a look at the challenges now. Apart from Stimulated Brillouin Scattering (SBS), ‘Photodarkening’ has challenged the YDFs seriously. While the theory of SBS is very well known, photodarkening is yet to have a complete theoretical treatment. Researchers across the globe have seen photodarkening under various conditions and during the last 4-5 years, a good amount of publications have surfaced with a multitude of experimental and theoretical approaches. In order to simply define photodarkening in YDFs, one can say that it is an optical degradation of the active core, which results in gradual increase in threshold power and drop in output power over time. When one expects a stable and reliable long term operation, such an optical degradation can be very challenging.

Most of the studies on photodarkening in YDFs were based on the use of conventional pump sources (~915 nm or ~976 nm). Literature review on photodarkening in Yb doped silica glass is given in chapter 3 of this thesis. It is worth mentioning that photodarkening in trivalent ytterbium doped silica glass is not limited to the pumping at the absorption bands only. To look at the physics of photodarkening from a different perspective, a 488 nm CW source was chosen for this thesis work. It is shown that Yb doped silica glass suffers photodarkening while being pumped at non-resonant 488 nm too. Most interestingly and as an important part of this thesis, it is found that photodarkening doesn’t instantaneously stop even after stopping the 488 nm irradiation. Rather, it grows up to a certain saturation level. Another important finding is that the above mentioned ‘post-irradiation temporal evolution in loss’ can be highly influenced by external temperature. It was clearly observed that ytterbium doped phosphosilicate fibers were highly resistant to photodarkening unlike their aluminosilicate counterparts. Apart from pumping at 488 nm, in some experiments the ytterbium doped fibers (YDF) were pumped at 976 nm and simultaneously probed by a 633 nm diode laser. Photodarkening was observed in terms of diminished ASE as well as the 633 nm throughput. Pumping at 976 nm caused a bluish fluorescence, which was more prominent in the

aluminosilicate fibers than in the phosphosilicate one. Such bluish fluorescence could possibly be attributed to the Yb^{3+} ion-pair effect, or in other words, a multi-photon process that causes photodarkening. Also, it is worth mentioning that, as was seen earlier with the 488 nm irradiation, photodarkening depended on the concentration of the Yb^{3+} in the aluminosilicate host. High doping concentration can cause clustering of the Yb^{3+} ions, which is a precursor of the aforesaid ion-pair effect. Some preliminary investigations were performed on hydrogen loaded YDFs as well and those are discussed in chapter 7.

1.2 Thesis Outline:

Chapter 1 gives an introduction to ytterbium doped fiber lasers, including spectroscopic properties, MCVD and solution doping techniques for perform fabrication, fiber drawing and different core-cladding geometries.

Chapter 2 is based on the discussion on the basics of laser guide stars and the possibilities and challenges in generating 1178 nm line using ytterbium doped fibers.

Chapter 3 presents the background study and literature review on photodarkening in ytterbium doped fibers.

Chapter 4 gives details of the photodarkening experiments performed on different kinds of ytterbium doped fibers irradiated by 488 nm CW source, under different thermal conditions. Simultaneous probing at another wavelength and post-irradiation temporal loss evolution are also described.

Chapter 5 reports the experimental results obtained by using NIR pumping.

Chapter 6 is based on the results obtained from hydrogen-loaded fiber samples.

Chapter 7 concludes the thesis with a summary of the experimental works along with some ideas for future work in the same direction.

Appendix A contains the list of publications.

It is worth mentioning that all the experimental works and most of the literature review for this thesis were done between October 2006 and November 2008.

Chapter 2

Ytterbium Doped Fiber Lasers

2.1 Ytterbium doped fiber lasers: A brief introduction

The first lasing action in ytterbium activated glass was reported in 1962. In that case a flashbulb pumped host glass rod was kept at a temperature of 78 K [2.1, 2.2]. After that, it took around 26 years for the first successful demonstration of Yb-doped fiber laser (YDFL) [2.3]. Since then, the highly efficient Yb-doped fiber lasers have attracted the attention of many research groups around the world and the power scaling was enormous. The contributions of the University of Southampton to the field of fiber lasers have been extraordinary. In 2004, researchers at the Optoelectronics Research Centre (ORC), University of Southampton, achieved a record 1.36 kW CW output power at 1.1 μm , from a double-clad silica fiber doped with ytterbium and the slope efficiency 83% and near diffraction limited beam quality [2.4]. SPI Lasers, a spin-out company from the University of Southampton, has played a key role in the development of high-power industrial YDFL. At present, the record of maximum CW output power from YDFL is held by IPG Photonics [W 2.1].

2.2 Spectroscopic properties of ytterbium-doped silica: a brief overview

Yb^{3+} ion has a simple energy level structure and quantum efficiency is high (> 90%). The ground level ($^2\text{F}_{7/2}$) and excited level ($^2\text{F}_{5/2}$) are roughly 11,000 cm^{-1} apart. The typical absorption & emission bands of Yb^{3+} are shown in Fig. 2.1 which is drawn based on the data from [2.5]. The Stark levels are marked with a, b, c, d, e, f & g. Of course, the levels vary, to some extent, from host to host (e.g. aluminosilicate to phosphosilicate). A detailed description is given in [2.5].

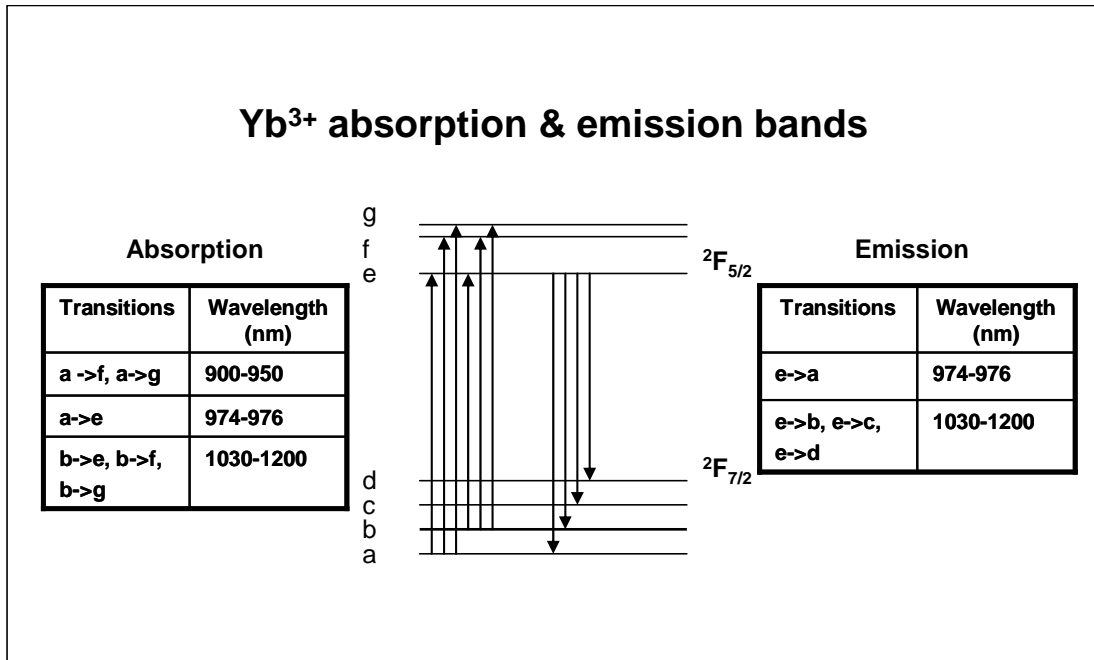


Fig. 2.1: Absorption and emission bands of Yb³⁺ (data ref. [2.5])

It is worth mentioning that YDFs are more flexible in terms of pump wavelength as compared to Neodymium doped fiber lasers (NDFLs). The fluorescence lifetime of Yb³⁺ is roughly taken to be equal to the radiative lifetime and that is approximately 0.8 ms in aluminosilicate host [2.1, 2.6]. The absorption & emission cross sections of a typical Yb-doped aluminosilicate fiber are shown in Fig. 2.2.

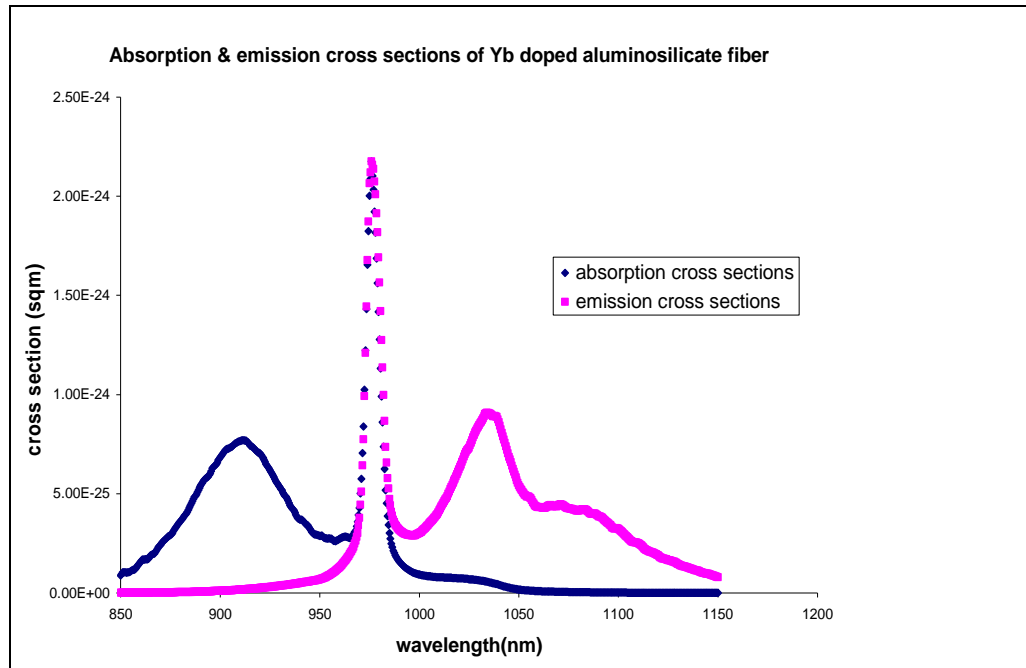


Fig. 2.2: Absorption and emission cross-sections of Yb^{3+}

It is evident from the above figure that Yb^{3+} has two major absorption peaks around 915 nm and 975 nm respectively, with the later being sharper and greater than the former. A typical YDFL can work either in 3-level or quasi-4-level scheme. The 980 nm emission in YDFL follows a 3-level scheme. The widely used 975 nm pumped YDFL lasing around 1.06 μm , can be explained as a quai-4-level system.

It is worth mentioning that temperature dependence of absorption and emission cross sections of Yb^{3+} can have great impact on higher wavelength generation (e.g. 1178 nm) from YDF while being pumped at higher pump wavelengths (e.g. 1080 nm). This particular issue is discussed in details in Chapter 3.

2.3 Double clad fiber (DCF) structure & High power fiber laser (HPFL):

Unlike optical fiber communication applications, where small core size is required for single mode operation, small core is a limiting factor for power scaling in typically multimode diode laser pumped fiber lasers. Various DCF structures have

been able to overcome this limitation by enhancing pump absorption, while maintaining good output beam quality. Fig. 2.3 is a schematic description of a simple DCF structure and it also shows different DCF geometries.

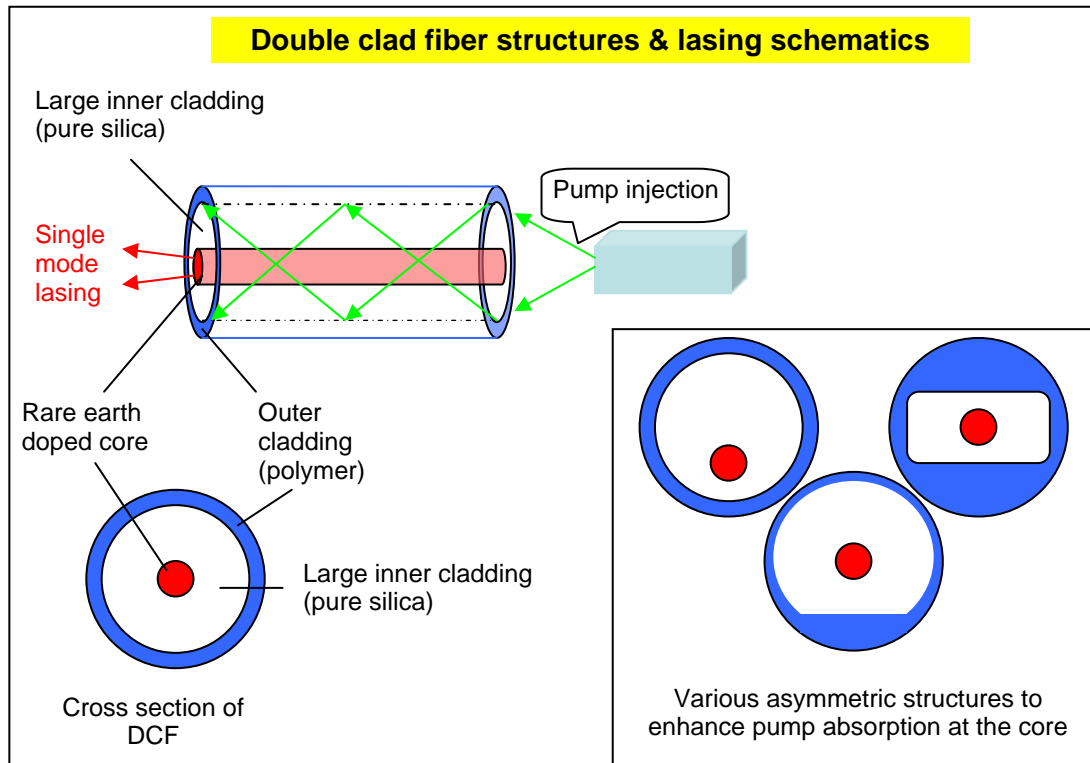


Fig. 2.3: Double-clad optical fiber schematics

It is very important to choose an optimal area ratio of the inner cladding and the core in order to have efficient pump absorption, while maintaining the size of the core for a single mode operation at the signal wavelength. The area ratio varies depending on the requirements of the applications concerned but, as a rough estimate, this range could be from 10 to 1000 [2.1]. Typical pump absorption in DCFs can vary from 0.1 to 10 dB/m [2.1]. In highly RE-doped cores, the background loss at the signal wavelength can be around 100 dB/km or more [2.1]. Depending on the background loss and pump absorption, the doping concentration and fiber length should be optimized. It is mostly preferable to have higher doping concentration and shorter length of the fiber for high power fiber lasers, in order to avoid nonlinear effects. It is worth mentioning that the doping concentration is also constrained due to cluster

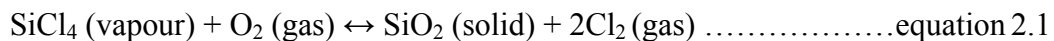
formation (solubility issues in host glass) and eventual ion-pair effects [2.6] which can seriously degrade laser operation.

There are various beam combiners available for high power pumping into the fiber and GTWave fiber [W 2.2] is one of the most popular ones.

2.4 Ytterbium doped fiber: MCVD fabrication technique

Outside Vapour Deposition (OVD), Vapour Axial Deposition (VAD) and Modified Chemical Vapour Deposition (MCVD) are the most common techniques for fiber fabrication. Out of these three, the most widely used technique is MCVD as it can produce high quality silica fibers in a comparatively cost-effective manner [2.7]. The YDFs involved in the photodarkening (PD) experiments reported here, were fabricated by the SILICA group members at the ORC, using MCVD and solution doping technique.

In MCVD, high purity oxides are deposited on the inside wall of a high purity silica glass tube. This tube is rotated about its axis in a glass-lathe machine. Oxygen (O₂) or nitrogen (N₂) gases carry the vapourized reactants SiCl₄, GeCl₄, POCl₃ (or BBr₃) into this tube, using a bubbler system and mass flow controllers (MFCs). An oxy-hydrogen burner moves back and forth along the tube and heats it at around 2200 °C in order to promote the following reactions and subsequent deposition of the oxides inside the silica tube.



The bubblers, containing the chemicals, are glass containers and are kept at constant temperature baths. The oxide deposition rate is controlled by the MFCs. The following Fig. 2.4 shows schematic description of a typical MCVD system.

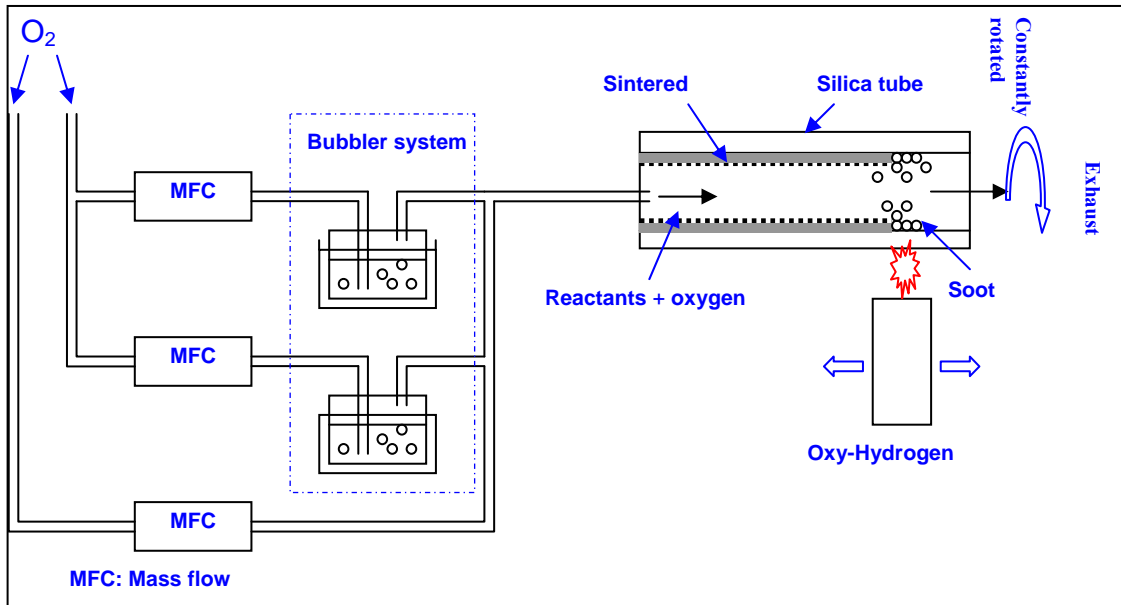


Fig. 2.4: Schematic diagram of a typical MCVD preform fabrication system

In the MCVD process, the silica tube is cleaned by etching using a flow of SF_6 and around $100\ \mu m$ of silica is etched out in this process from the internal cylindrical surface of the tube. The operating temperature for this is $\sim 2000\ ^\circ C$. In the next step, at around $2050\ ^\circ C$, deposition of cladding and core are achieved with excellent precision, by controlling the flow of the chemicals concerned. Due to lower vapour pressures of the chlorides of the rare earth ions (e.g. $ErCl_3$, $NdCl_3$, $YbCl_3$) than that of $SiCl_4$ or $GeCl_4$, it is very difficult to use the bubblers for the rare earth chlorides for vapour phase deposition in the core. Instead, solution doping technique [2.7] is used due to its simplicity, doping uniformity and cost-effectiveness. To prepare the glass tube for solution doping, the soot deposition is finished at a lower temperature ($\sim 1500\ ^\circ C$) to maintain porosity in the core (no sintering). This tube is then taken for solution doping.

2.5 Solution doping technique:

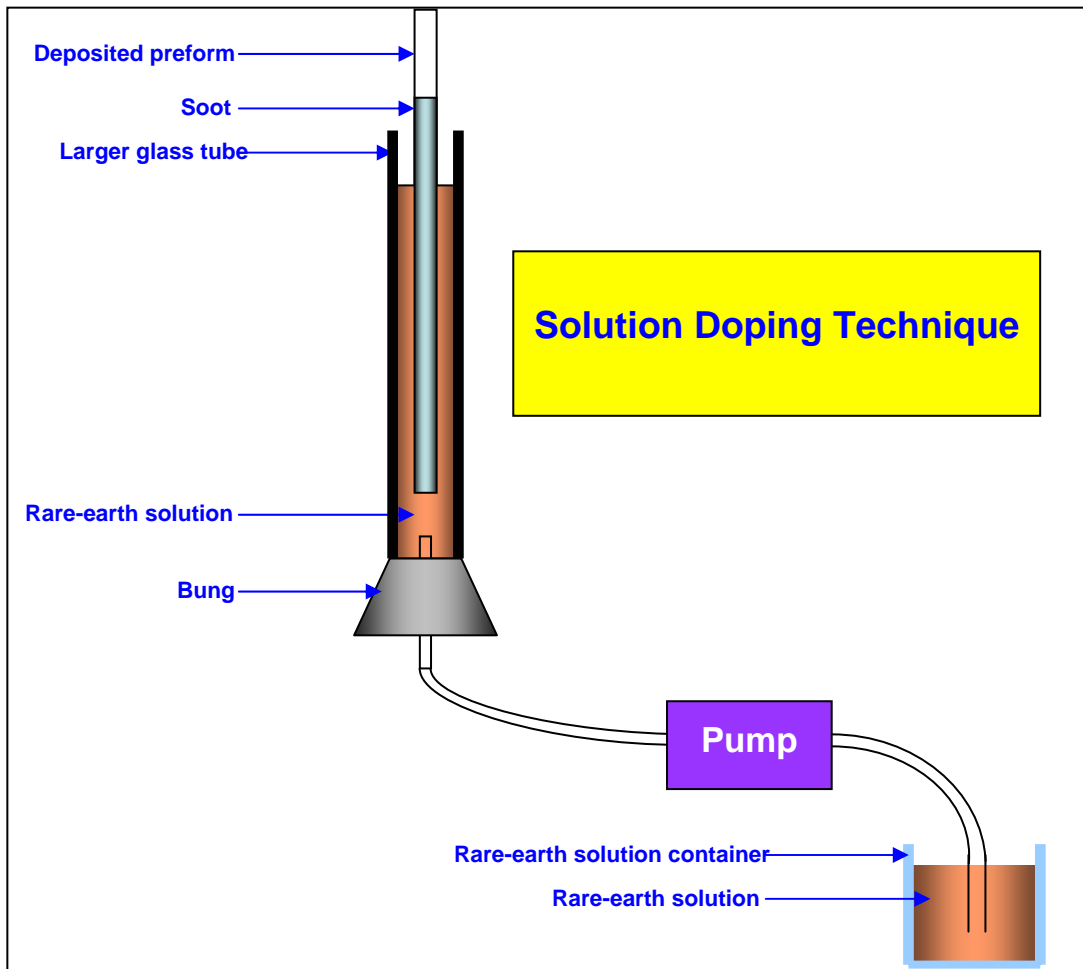


Fig. 2.5: Schematics of Solution Doping Technique

A solution of rare-earth chlorides and methanol or aqueous alcohol is prepared, in a calculated proportion, keeping in mind the application-requirement of the fiber. To enhance the solubility of the rare-earth ions, AlCl_3 is added into the solution. This solution is then slowly pumped into the porous (core) glass rod and left for soaking for ~ 1 hr. This time is good enough for complete diffusion of the rare earth ions into the soot [2.7]. Once the soaking is complete, the solution is expelled out and the tube is dried for several hours, sometimes using N_2 , O_2 gas flow in the lathe to accelerate the drying. After drying, this rare-earth doped porous glass tube is sintered at around 1850°C to obtain a transparent layer. Temperature control is very essential at this

stage in order to prevent evaporation of the rare-earth chloride(s) and AlCl_3 before oxidation can take place [2.7]. Then the tube is collapsed at $\sim 2100^\circ\text{C}$ to finalize the preform. In the sintering stage or during the final collapsing Cl_2 gas can be used to reduce the amount of water from the preform [2.7]. After collapsing, the preform is etched to obtain a suitable core: cladding ratio (thickness wise). The next step is fiber drawing where the dimensions and the coating of the fiber are finalized.

2.6 Fiber drawing:

Fig. 2.6 shows is a simplified schematic diagram of a fiber drawing tower and accessories. The heating element in the furnace is high purity carbon kept in an inert gas environment. The furnace is operated at a temperature (e.g. $>2000^\circ\text{C}$) and when the preform starts to soften, the temperature is kept fixed and the preform feeding speed and the drawing speed are controlled in order to achieve the sought diameter of the fiber. This is calculated using the concept of conservation of volume of the glass. The working formula is given below.

$$(\mathbf{V}_p/\mathbf{V}_f) = (\mathbf{d}_f/\mathbf{d}_p)^2$$

In the equation above, \mathbf{V}_p and \mathbf{V}_f are the feeding speed of the preform and the drawing speed of the fiber respectively. \mathbf{d}_f and \mathbf{d}_p are the diameters of the fiber and the preform respectively.

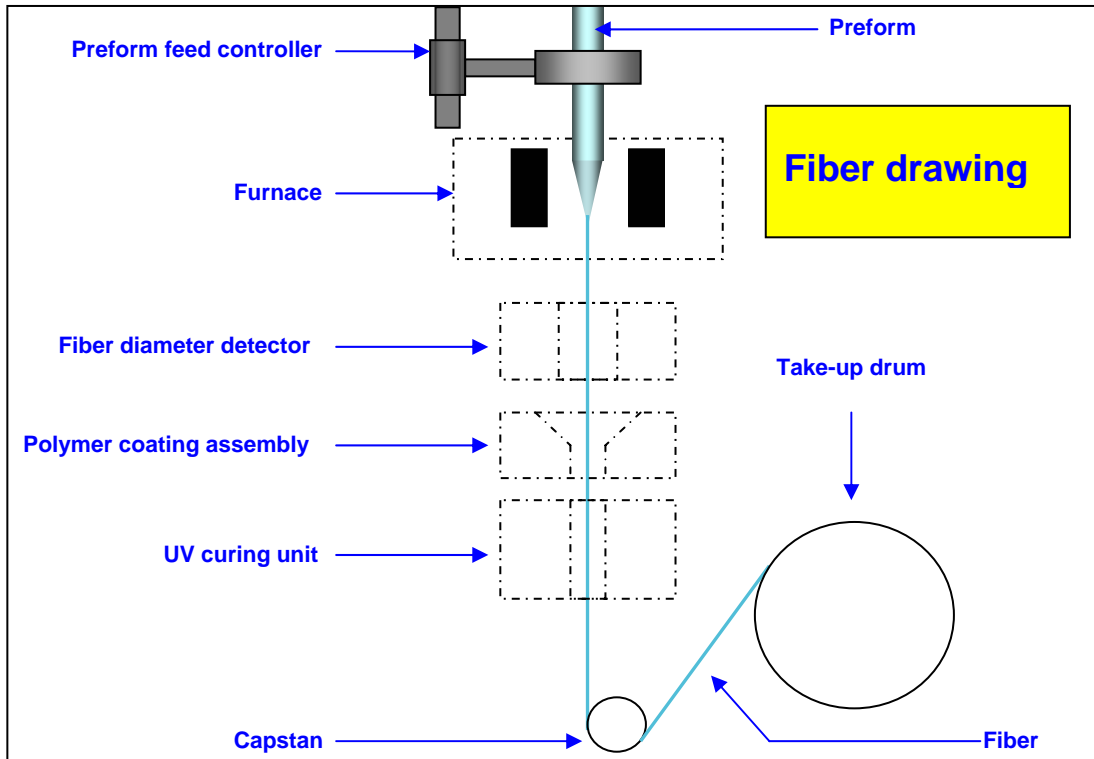


Fig. 2.6: Schematics of optical fiber drawing tower system

Taking a feedback from the diameter gauge below the furnace, the take up speed of the fiber is controlled and hence the diameter of the fiber is controlled. To avoid fluctuation in the diameter of the fiber being drawn, temperature fluctuation in the furnace and mechanical vibration in the drawing system must be avoided. The fiber is taken through the viscous polymer coating assembly and using different coating dies in the assembly, coating thickness is adjusted. It is very important to remember that the mechanical stress, in the fiber being drawn, can induce excess scattering losses [2.7] and hence the temperature fluctuations and mechanical vibrations should be carefully handled in order to produce high-quality fiber. Fig. 2.7 schematically describes the fiber fabrication steps discussed above.

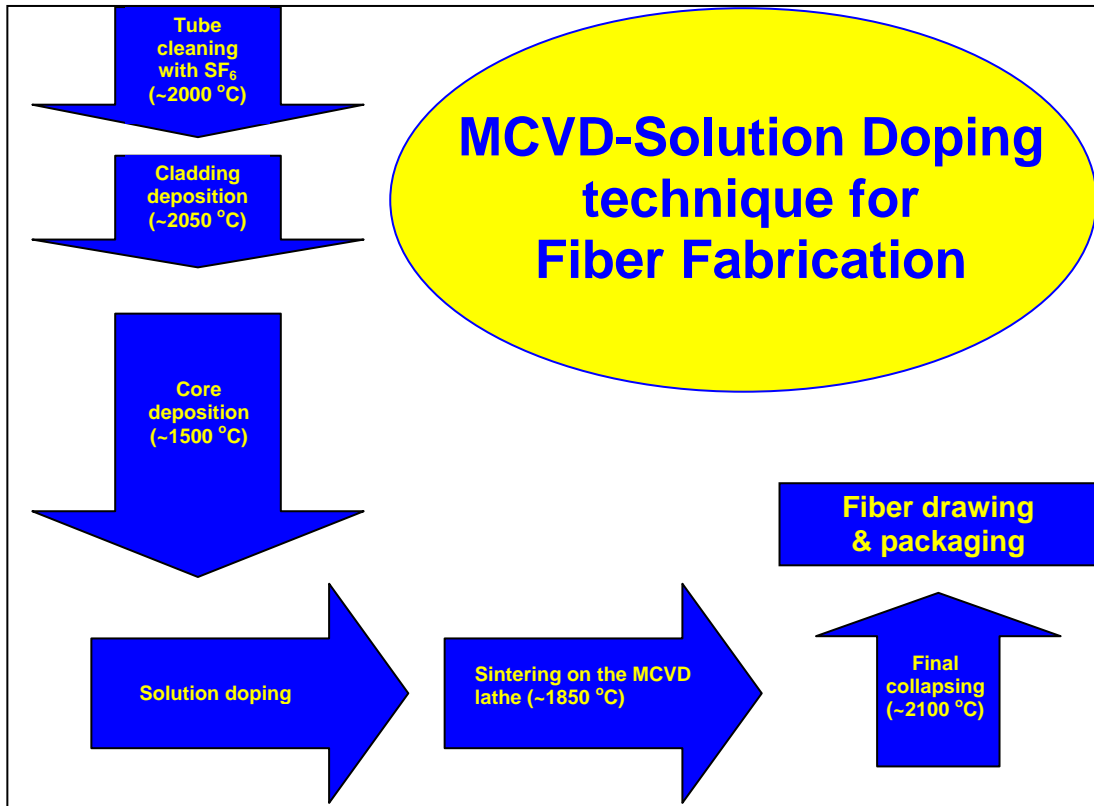


Fig. 2.7: MCVD & Solution doping based fiber manufacturing: schematics

2.7 Conclusions:

In this chapter, spectroscopic properties of trivalent ytterbium ion and the basics of ytterbium doped fiber lasers, including double clad fiber structures, have been discussed. Also, preform fabrication using MCVD technique, followed by Solution Doping and Fiber Drawing are explained briefly.

References (Chapter 2):

2.1 Romeo de Jesus Selvas-Aguilar: Cladding-Pumped Neodymium and Ytterbium Doped Fiber Lasers; PhD thesis -2004, ORC-University of Southampton (available at: <http://eprints.soton.ac.uk/41526/>)

2.2 H W Etzel, H W Gandy and R J Ginther: Stimulated Emission of Infrared Radiation from Ytterbium Activated Silicate Glass; Applied Optics, Vol. **1**, Issue 4, pp. 534-536, 1962

2.3 D C Hanna, R M Percival, I R Perry, R G Smart, P J Suni, J E Townsend and A C Tropper: Continuous-Wave Oscillation of a Monomode Ytterbium-Doped Fibre Laser; Electronics Letters, Vol. **24**, No. 17, pp 1111-1113, 1988

2.4 Y Jeong, J K Sahu, D N Payne, and J Nilsson: Ytterbium-doped large-core fiber laser with 1.36 kW continuous-wave output power; Optics Express, Vol. **12**, Issue 25, pp. 6088-6092, 2004

2.5 A S Kurkov: Oscillation spectral range of Yb-doped fiber lasers; Laser Physics Letters, Vol. **4**, No. 2, pp 93-102, 2007

2.6 H M Pask, Robert J Carman, David C Hanna, Anne C Tropper, Colin J Mackechnie, Paul R Barber and Judith M Dawes: Ytterbium-Doped Silica Fiber Lasers: Versatile Sources for the 1-1.2 μm Region; *Invited Paper*, IEEE Journal of Selected Topics in Quantum Electronics, Vol. **I**, No. I, 1995

2.7 Jae Sun Kim: Hollow optical fibres and W-type fibres for high power sources and Suppression of the stimulated Raman scattering; PhD Thesis-2006, ORC-University of Southampton.

(Abstract available at: <http://www.orc.soton.ac.uk/viewpublication.html?pid=3808>)

W 2.1

[http://www.ipgphotonics.com/Collateral/Documents/EnglishUS/PR_Final_10kW_S
M_laser.pdf](http://www.ipgphotonics.com/Collateral/Documents/EnglishUS/PR_Final_10kW_S
M_laser.pdf)

W 2.2

[http://www.spilasers.com/Media_and_resource_centre/News/Latest_News.aspx?INe
wsID=160](http://www.spilasers.com/Media_and_resource_centre/News/Latest_News.aspx?INe
wsID=160)

Chapter 3

Laser Guide Stars

3.1 Laser Guide Stars: A brief knowhow & the possibilities for frequency doubled YDFL as a source:

A Laser Guide Star (LGS) is an artificial bright spot or ‘star’, created using suitable laser sources, for adaptive optical imaging (AOI) of astronomical objects, especially the faint ones. Due to the absence of sufficiently bright stars at various regions of the sky, the use of ‘natural’ guide stars are quite limited. In contrast to that, LGS can be created almost anywhere close to the field of view of the telescope and it gives a great flexibility in the adaptive optical imaging of the objects of interest throughout a larger fraction of the sky.

Mainly two types of LGSs are used. One is the sodium beacon, which is created by using a laser source to shine the mesospheric sodium. The other one is a Rayleigh beacon which is much simpler and cheaper to create but not as good as the sodium beacon.

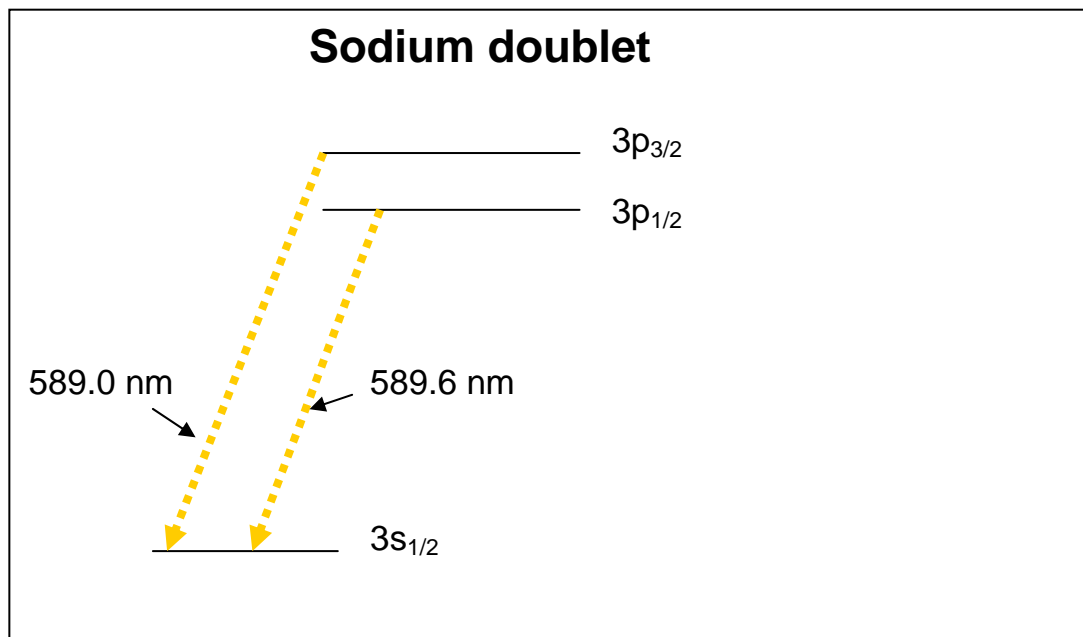


Fig. 3.1: Sodium doublet energy diagram

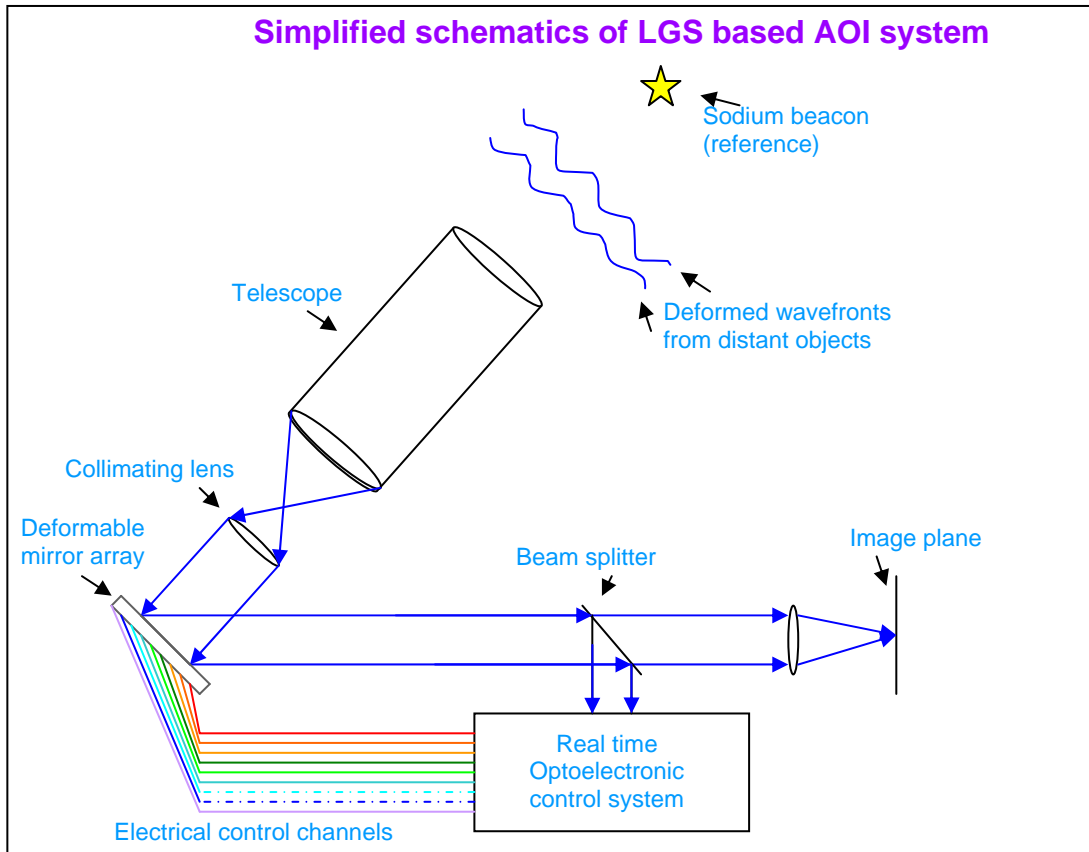


Fig. 3.2: A Simplified schematic diagram of LGS base AOI (drawn with ref. to http://www.nalux-world.com/subaru_e.htm)

Fig. 3.1 shows the energy level diagram related to sodium D2 line. Fig. 3.2 is a simplified schematic description of an LGS based AOI system.

3.2 Status of LGS:

As a field of research, LGS based AOI systems are quite young. Though many laser sources for LGS have been demonstrated, only a few astronomical observatories have adopted LGS systems [W3.1]. California based Lick and Palomar observatories, Hawaii based Keck observatory, Caltech Palomar observatory are some of the most promising places using LGS-sodium beacons [W3.1]. La Palma based William Herschel Telescope (WHT) uses a Rayleigh guide star [W3.1]. Amongst others, the Very Large Telescope (VLT) at European Southern Observatory (ESO), the Gemini

north at Hawaii & the Multiple Mirror Telescope Observatory (MMTO) are actively involved in LGS based AOI systems research [W3.1].

3.3 Sodium beacon & laser requirements:

Sodium beacon is created using a laser source operating at 589 nm which causes the yellow fluorescence (sodium D2 line) from the mesospheric sodium at an altitude of ~90 km. But this approach requires a very high power, narrow linewidth source centred at 589 nm and this kind of sources are not very straightforward to fabricate. Typical technical specifications of such a laser are given below [3.1]:

$\lambda=589.159$ nm (tunable over a 3 pm)

$\Delta\nu \sim 1$ GHz

Power > 4W (CW or quasi-CW (mode-locked))

Beam profile = TEM₀₀ ($M^2 < 1.2$)

Unfortunately, no solid-state source directly operates at 589 nm. Sum frequency generation (SFG) from 1319 nm & 1064 nm Nd:YAG sources, solid dye laser, frequency doubled crystal Raman laser, Li:LiF⁻² lasers and recently frequency doubled fiber lasers are amongst the various approaches towards the development of all-solid-state yellow/orange lasing line [3.2]. The SFG approach (1319 nm & 1064) and frequency doubling, though attractive, is quite complicated and expensive [3.2].

High power fiber laser sources are very promising in terms of size, price and ease of operation. 1178 nm lasing from YDF has recently gained much attention as this kind of sources can fulfill the demand for a reliable, cheap and compact source for LGS. An Yb-doped fiber laser operating at 1178 nm with a high power level, followed by a frequency doubling technique, can generate the 589 nm spectral line desired for laser guide star. Photodarkening in Yb-doped fibers, pumped by a high power 976 nm source, is one of the issues/problems to resolve. Another problem is ASE suppression in the shorter, 1030-1100 nm, spectral range.

3.4 Yb-doped fiber laser operating at 1178 nm:

High power visible laser sources are increasingly in demand now-a-days for various applications. A very common choice for achieving this is by the utilization of a high power laser operating at the NIR spectral range followed by frequency doubling with a suitable nonlinear crystal [3.3]. The 589 nm laser wavelength is very important, particularly for creating a laser guide star or some medical applications and also for spectroscopic study of sodium.

Although dye lasers or solid state lasers, with additional frequency doubling techniques, are already available, generating the 589 nm lasing line, they are generally very expensive and complex [3.3]. Naturally, with the advent of high power fiber lasers, there has been a strong interest to develop a 589 nm laser, based on compact and low cost fiber lasers. There have been various strategies applied to achieve this. Sum frequency generation from two different fiber lasers operating at 938 nm and 1583 nm was demonstrated to produce a 589 nm laser line. Another approach was to develop a fiber Raman-laser generating 1178 nm but, it was not very suitable because of broad bandwidth and the lack of enough conversion efficiency in the frequency doubling stage [3.3]. Recently, applying coherent beam combining technique (with more than 95% efficiency) on two narrow linewidth Raman fiber amplifiers, generation of more than 29 W at 1178 nm and further SHG of more than 25W at 589 nm (from an external cavity) have been reported [3.4].

An Yb-doped fiber laser, operating directly at 1178 nm, was reported to produce 6.5 W of output power [3.3] and this was quite remarkable. When scaling up the power, parasitic lasing posed as a problem and another obvious drawback was photodarkening due to the high pump power at 976 nm. To generate 1178 nm directly from an Yb-doped fiber laser, ASE suppression is a key issue. Reliable theoretical modelling of such a laser becomes very difficult when ASE is considered. Cladding pumped Yb-doped solid core photonic bandgap fiber (PBGF) was reported to be a promising tool for suppressing ASE around 1030 nm and lasing at higher wavelengths (e.g. 1178 nm) [3.5]. Another interesting approach, to address

the same issues along with polarization maintenance, using an all-solid PBGF, was reported [3.6]. The cladding of this particular kind of fiber was realized using a triangular lattice of germanium doped high index micro-rods in silica background [3.6]. To address the ASE suppression issue, an Ytterbium doped solid core PBGF based amplifier was reported with the generation of 30W at 1178 nm (58% efficiency) without any parasitic lasing [3.7].

It was shown that the lasing peak in a Yb-doped fiber laser tends to shift towards higher wavelengths if the fiber is heated suitably, for example, from room temperature to 100 °C or more, and if an appropriate FBG is used [3.8]. Using this technique, lasing at 1180 nm with ~ 1w of output power was reported with more than 30% slope efficiency at 200 °C [3.8]. But, for cladding pumped fiber lasers, such a high temperature can degrade the outer cladding (made of polymer) and damage the laser [3.8]. This can be avoided if a different scheme is adapted where the Yb-doped active medium is pumped at longer wavelengths [3.8]. Following this technique, a 1070 nm pumped (core-pumped configuration) YDFL with 3.2 W of maximum output at 1160 nm, having 45% slope efficiency, was reported [3.8].

In another case, an YDFL generating 3.2W maximum output power at 1160 nm, with 0.2 nm linewidth, has been reported with 45% slope efficiency at 70 °C [3.9].

A linearly polarized, diode-pumped, narrow linewidth Yb-doped fiber laser generating 1150 nm and then frequency doubled to produce 40 mW at 575 nm has been demonstrated [3.10].

In another report, effects of temperature on the emission properties of Yb-doped fibers have been discussed [3.11].

A bismuth doped fiber laser, lasing at 1178 nm with 6.4W CW power and 15% slope efficiency, and then frequency doubled to generate 589 nm output (125 mW) has

also been reported [3.12]. A Bismuth doped fiber amplifier, pumped at 1090 nm, has been reported to produce more than 3 W at 1179 nm [3.13].

Unfortunately, the number of reports on direct higher wavelength (~1178 nm) generation in YDFL, is very limited. This fact, in a positive sense, makes it more challenging and interesting for further rigorous investigation.

Although no direct investigation on lasing at 1178 nm from YDFL was pursued in this thesis work, it is worth clarifying why that particular application is mentioned in relation to this thesis. Yb^{3+} doped phosphosilicate fibers have been shown to be highly resistant to photodarkening as compared to their aluminosilicate counterparts. As long as one requires an ytterbium doped fiber laser operating around the conventional ~ 1030-1060 nm band, phosphosilicate fibers can be the best choice in order to avoid photodarkening. But, the limitation of Yb^{3+} doped phosphosilicate fibers is that the emission cross-section may not be suitably stretched beyond 1080 nm. In that case, generation of 1178 nm would not be possible. On the other hand, Yb^{3+} doped aluminosilicate fibers can be thermally influenced to shift the emission cross-section towards higher wavelength regime and can generate 1178 nm. For such an application one has to understand photodarkening in Yb^{3+} doped aluminosilicate fibers properly in order to mitigate it. That forms the basis of this thesis work, where photodarkening was mostly investigated using a non-resonant pump wavelength of 488 nm. In other words, this thesis work attempts to partially fill up the gap in understanding photodarkening in YDFLs, as most of the research works on photodarkening were primarily pursued using the conventional 915 nm or 976 nm pump wavelengths.

References (Chapter 3):

3.1 Norihito Saito, Kazuyuki Akagawa, Yutaka Hayano, Yoshihiko Saito, Hideki Takami, Masanori Iye and Satoshi Wada: Coherent 589-nm-light Generation by Quasi-Intracavity Sum-Frequency Mixing; Japanese Journal of Applied Physics, Japanese Journal of Applied Physics, Vol. **44**, No. 47, 2005, pp. L 1420–L 1422

3.2 589 nm Light Source Based on Raman Fiber Laser: Yan Feng, Shenghong Huang, Akira Shirakawa and Ken-Ichi Ueda; Japanese Journal of Applied Physics Vol. **43**, No. 6A, 2004, pp. L 722–L 724

3.3 Jun Ota, Akira Shirakawa and Ken-ichi Ueda: High-Power Yb-Doped double-clad fiber laser directly operating at 1178 nm; Japanese Journal of Applied Physics, Vol. **45**, No. 4, 2006, pp. L117–L119

3.4 Yan Feng, Luke R Taylor and Domenico Bonaccini Calia: 25 W Raman-fiber-amplifier-based 589 nm laser for laser guide star; Optics Express, Vol. **17**, No. 21, pp 19021-19026, 2009

3.5 R. Goto, K. Takenaga, K. Okada, M. Kashiwagi, T. Kitabayashi, S. Tanigawa, K. Shima, S. Matsuo and K. Himeno: Cladding-Pumped Yb-Doped Solid Photonic Bandgap Fiber for ASE Suppression in Shorter Wavelength Region; OTuJ5.pdf, OFC/NFOEC 2008.

3.6 C B Olausson, C I Falk, J K Lyngsø, B B Jensen, K T Therkildsen, J W Thomsen, K. P. Hansen, A. Bjarklev and J. Broeng: Amplification and ASE suppression in a polarization-maintaining ytterbium-doped all-solid photonic bandgap fibre; Optics Express, Vol. **16**, No. 18 , pp. 13657-13662

3.7 A Shirakawa, H Maruyama, K Ueda, C B Olausson, J K Lyngsø, and J Broeng: High-power Yb-doped photonic bandgap fiber amplifier at 1150-1200 nm Optics Express, Vol. **17**, No. 2, pp 447-454, 2009

3.8 A S Kurkov: Oscillation spectral range of Yb-doped fiber lasers; Laser Physics Letters, Vol. **4**, No. 2, pp 93-102, 2007

3.9 A S Kurkov , V M Paramonov, O I Medvedkov: Ytterbium fiber laser emitting at 1160 nm; Laser Physics Letters, Vol. **3**, No. 10, pp 503–506, 2006

3.10 S Sinha, C Langrock, M J Digonnet, M M Fejer, and R L Byer: Efficient yellow-light generation by frequency doubling a narrow-linewidth 1150 nm ytterbium fiber oscillator; Optics Letters, Vol. **31**, Issue 3, pp. 347-349, 2006

3.11 T C Newell, P Peterson, A Gavrielides, M P Sharma: Temperature effects on the emission properties of Yb-doped optical fibers; Optics Communications, 273, pp 256–259, 2007

3.12 A B Rulkov, A A Ferin, S V Popov, J R Taylor, I Razdobreev, L Bigot, and G Bouwmans: Narrow-line, 1178nm CW bismuth-doped fiber laser with 6.4W output for direct frequency doubling; Optics Express, Vol. **15**, Issue 9, pp. 5473-5476, 2007

3.13 Mridu P. Kalita, Seongwoo Yoo and Jayanta Sahu: All Fiber Narrow Linewidth High Power Bismuth Doped Fiber Amplifier at 1179 nm; CThGG, *CLEO/IQEC* 2009 Baltimore, 31 May - 5 Jun 2009

W3.1 http://www.rp-photonics.com/laser_guide_stars.html

Chapter 4

Photodarkening in Ytterbium Fiber Lasers: Literature review and brief theoretical background

This chapter gives a brief review on most of the key papers, available over the duration of this work, on the topic of photodarkening in YDFs.

4.1 Background loss in optical fibers:

The background loss in optical fibers is an intrinsic property of the material used in the core. In the case of a double clad fiber, the inner cladding also contributes to this. The background loss is an exponentially decaying function of the length and is given by the well known **Lambert-Beer law**:

$$I(z) = I_0 \exp(-\alpha' cz) \quad \text{eqn (4.1)}$$

Where I_0 is the intensity at $z=0$ and $I(z)$ is the intensity measured at a distance z . α' is the absorptivity or extinction coefficient and c is the concentration of absorbing species in the material. For fiber related background loss measurement, this can be re-written as

$$I(z) = I_0 \exp(-\alpha z) \quad \text{eqn (4.2)}$$

where $\alpha = \alpha' c$

This assumption is valid since the concentration of the absorbing species is fixed in a given fiber and hence a loss parameter α , often called the absorption coefficient, is defined for simplicity, without explicitly using the concentration parameter c .

With a given fiber, this α is supposed to be a constant for a given wavelength but, when a fiber is photodarkened, it is observed in general that α increases.

It was interesting to compare the parameter α of a photodarkened fiber with that of an identical pristine fiber. This was done using the cutback technique.

4.2 Literature review and the status of the topic area:

This part is broadly divided into sub-sections, for discussing photodarkening in Yb-doped silica fibers and photobleaching as well.

4.2.1 Photodarkening in Yb-doped silica fibers:

Ytterbium doped fiber lasers and amplifiers operating at the 1.0-1.1 μm wavelength region are interesting for materials processing, nonlinear wavelength conversion and military applications [4.1]. But, Yb^{3+} doped silica fibers are shown to suffer photodarkening [4.2]. Tm^{3+} , Ce^{3+} , Pr^{3+} and Eu^{3+} doped silica fibers are also reported to show photodarkening [4.1]. Photodarkening is a permanent damage (unless thermally or optically bleached later on) of the doped core in terms of increased background loss and higher laser threshold. The most apparent result is the drop in output power in such a photodarkened fiber laser or amplifier. This is a big threat to the long term reliability of operating high power YDFs.

The first experimental evidence of photodarkening in Yb-doped silica fibers dates back to 1996-97 [4.3]. Since then, several publications have reported the photodarkening phenomena in Yb-doped silica fibers but there has been no experimental or theoretical reasoning to fully disclose the underlying physical mechanism of photodarkening. It is often stated that color centers or defect centers cause photodarkening [4.4]. The formation of such color centers and the photodarkening caused are also correlated to the oxygen deficiency in the silica matrix of the fibers [4.5].

The induced background loss due to photodarkening in Yb-doped fiber is shown to have its peak around 450 nm [4.6].

Photodarkening in YDF in correlation with the amount of population inversion has also been studied and reported [4.7].

The disturbing fact is that photodarkening in active fibers can lead to higher thresholds for lasing and a permanent loss can be induced, which is not desirable for fiber lasers and amplifiers.

4.2.1(a) Materials related facts on photodarkening of Yb-doped fibers

It has been shown that the introduction of a high concentration of aluminium into Yb-doped silica fibers can reduce photodarkening [4.6, 4.8] and that photodarkening depends on population inversion [4.6, 4.8-4.10].

Oxygen deficient centers (ODC) inside the Yb-Al-Si matrix are also proposed to be a precursor of photodarkening and oxygen loading has been successfully shown to reduce the amount of photodarkening in Yb-doped aluminosilicate fibers [4.5]. These ODCs have a characteristic peak around 240 nm in germanosilicate glasses whereas the peak is believed to be around 220 nm in the case of aluminosilicate glass [4.5]. Alternatively, this kind of absorption band, around 230nm, has been attributed to a strong charge transfer mechanism leading to photodarkening [4.11].

Also, the presence of non-bridging oxygen hole centre (NBOHC) has been reported to be a possible precursor in YDFs [4.12]. In this report, red fluorescence due to green (532 nm) input irradiation in a YDF was discussed.

Most importantly, Yb doped phosphosilicate fibers have been shown to be highly resistant to photodarkening, as compared to their aluminosilicate counterparts [4.13-4.15]. This was verified and reported (in case of 488 nm irradiation induced PD) as a part of this thesis work [4.15].

As far as color centre formation in Yb-doped silica fiber, through multi-photon processes, is concerned, it is very important to study the cooperative luminescence and Yb^{3+} - Yb^{3+} ion pair effects [4.16-4.19] in order to understand the probable underlying mechanism of photodarkening.

The presence of Yb^{2+} ions in Yb-doped aluminosilicate glass has been reported recently and this may also influence photodarkening in Yb-doped aluminosilicate fiber lasers [4.20]. $\text{Yb}^{3+} \rightarrow \text{Yb}^{2+}$ conversion and $\text{Yb}^{2+} \rightarrow \text{Yb}^{3+}$ conversion in Yb-doped aluminosilicate fiber have also been studied and reported in relation to photodarkening and photobleaching respectively [4.21].

Liekki, a Finland based specialty fiber manufacturing company, has reported that their Yb-doped fibers produced by Direct Nanoparticle Deposition (DND) technique show less photodarkening than the similar fibers produced by usual MCVD process [W4.0]. They claim that their patented DND technique is better as it can minimize clustering of Yb inside the silica matrix and can offer better homogeneity.

4.2.1(b) Photobleaching

Once a fiber is photodarkened by irradiation with a particular wavelength, it can be almost reset to its original background loss level by another irradiation process with a different wavelength source. This is known as photobleaching. Yb-doped silica LMA fiber has been reported to be photodarkened by a 980 nm pump source and almost fully photobleached by a UV, 355 nm source [4.22].

Partial bleaching of the photodarkening loss in Yb-doped aluminosilicate fiber, by the pump (915 nm) power itself, has been reported [4.23].

Thermal bleaching is another interesting possibility, where a photodarkened fiber can be heated up within a certain temperature range, in order to return its original pristine-like condition [4.24].

Although photobleaching can help reduce the induced background loss by a significant amount, there is no online photobleaching mechanism implemented till date, to the best of my knowledge. For practical purposes, it is not very promising to use a high power fiber laser and take out the dark fiber for photobleaching and re-install the fiber inside. Neither is it economic to pack an auxiliary laser for

photobleaching inside a fiber laser box. If photobleaching is the last resort to get rid of photodarkening, the photobleaching mechanism has to be incorporated in a compact and economic way.

References (Chapter 4):

4.1 J J Koponen, M. J. Söderlund, S K T Tammela and H Po: Photodarkening in ytterbium-doped silica fibers ; SPIE Security & Defense Europe '05 Symposium

4.2 J J Koponen, M Söderlund, S Tammela, and H Po, Measuring photodarkening from Yb-doped fibers; CLEO/Europe Conference '05, No. CP2-2-THU, 2005.

4.3 R Paschotta, J Nilsson, P R Barber, J E Caplen, A C Tropper and D C Hanna: Lifetime quenching in Yb doped fibers; Optics Communications, Vol. **136**, Number 5, pp. 375-378, 1997

4.4 L B Glebov: Linear and Nonlinear Photoionization of Silicate Glasses; Glass Science and Technology, Vol. **75**, No. C2, 2002

4.5 S Yoo, C Basu, A J Boyland, C Sones, J. Nilsson, J K Sahu, and D. Payne: Photodarkening in Yb-doped aluminosilicate fibers induced by 488 nm irradiation: Optics Letters, Vol. **32**, No. 12, pp 1626-1628, 2007

4.6 B Morasse, S Chatigny, É Gagnon, C Hovington, J P Martin, J P de Sandro : Low photodarkening single cladding ytterbium fiber amplifier; Proceedings of SPIE, Vol. 6453, 64530H-1-9 (2007) (Photonics West 2007)

4.7 J Koponen, M Laurila and M Hotoleanu: Inversion behavior in core- and cladding-pumped Yb-doped fiber photodarkening measurements; Applied Optics, Vol. **47**, No. 25, 2008

4.8 T Kitabayashi, M Ikeda, M Nakai, T Sakai, K Himeno, K Ohashi: Optical Fiber Communication Conference and Exposition and The National Fiber Optic Engineers Conference on CD-ROM (Optical Society of America, Washington, DC, 2006), OThC5.

- 4.9** I Manek-Hönniger, J Boulet, T Cardinal, F Guillen, S Ermeneux, M Podgorski, R Bello Doua and F Salin: Photodarkening and photobleaching of an ytterbium-doped silica double-clad LMA fiber; *Optics Express*, Vol. **15**, Issue 4, pp. 1606-1611, 2007
- 4.10** J J Koponen, M Söderlund, H J Hoffman: Measuring photodarkening from single-mode ytterbium doped silica fibers ; *Optics Express* ,Vol. **14**, No. 24 , pp. 11539-11544, 2006
- 4.11** M Engholm and L Norin: Preventing photodarkening in ytterbium-doped high power fiber lasers; correlation to the UV-transparency of the core glass; *Optics Express*, Vol. **16**, No. 2, pp 1260-1268, 2008
- 4.12** Peter D Dragic, Chad G Carlson and André Croteau : Characterization of defect luminescence in Yb doped silica fibers: part I NBOHC; 31 March 2008 / Vol. 16, No. 7 / *Optics Express*, Vol. **16**, No. 7, pp 4688-4697, 2008
- 4.13** Y W Lee, S Sinha, M J F Digonnet, R L Byer and S Jiang : 20 W single-mode Yb³⁺-doped phosphate fiber laser ; *Optics Letters*, Vol. **31**, No. 22, pp 3255-3257, 2006
- 4.14** A V Shubin, M V Yashkov, M A Melkumov, S A Smirnow, I A Bufetov, and E M Dianov: Photodarkening of aluminosilicate and phosphosilicate Yb-doped fibers; Conf. Digest of CLEO Europe-EQEC 2007, CJ3-1-THU
- 4.15** J K Sahu, S Yoo, A J Boyland, M P Kalita, C Basu, A Webb, C L Sones, J Nilsson, and D N Payne: 488 nm irradiation induced photodarkening study of Ybdoped aluminosilicate and phosphosilicate fibers; poster-CLEO USA (2008)

4.16 S Magne, Y Ouerdane, M Druetta, J P Goure, P Ferdinand, G Monnom: Cooperative luminescence in an ytterbium-doped silica fibre; Optics Communications, Vol. **111**, pp. 310-316, 1994

4.17 Y G Choi, Y B Shin, H S Seo, K. H. Kim: Spectral evolution of cooperative luminescence in an Yb³⁺-doped silica optical fiber; Chemical Physics Letters, Vol. **364**, pp. 200–205, 2002

4.18 T G Ryan, S D Jackson: Cooperative luminescence and absorption in ytterbium doped aluminosilicate glass optical fibers and preforms; Optics Communications, Vol. **273**, pp. 159–161, 2007

4.19 A V Kir'yanov, Y O Barmenkov, I L Martinez, A S Kurkov, and E M Dianov: Cooperative luminescence and absorption in Ytterbium-doped silica fiber and the fiber nonlinear transmission coefficient at $\lambda=980$ nm with a regard to the Ytterbium ion-pairs' effect; Optics Express, Vol. **14**, Issue 9, pp. 3981-3992, 2006

4.20 M Engholm and L Norin : Divalent Ytterbium in Ytterbium Doped Aluminosilicate Glass- Aspects on Photodarkening in Fiber Lasers; Poster- Conference on Lasers and Electro-Optics (CLEO), Baltimore, Maryland, USA, May 2007 (JTUA61).

4.21 A D Guzman Ch'avez, A V Kir'yanov, Y O Barmenkov and N N Il'ichev: Reversible photo-darkening and resonant photo-bleaching of Ytterbium-doped silica fiber at in-core 977-nm and 543-nm irradiation; Laser Physics Letters, Vol. **4**; No.10, pp. 734-739, 2007

4.22 I Manek-Hönninger, J Boulet, T Cardinal and F Guillen, S Ermeneux, M Podgorski, R Bello Doua, F Salin : Photodarkening and photobleaching of an ytterbium-doped silica double-clad LMA fiber ; Optics Express, Vol. **15**, No. 4, 1607, 2007

4.23 S Jetschke, S Unger, U Röpke, J Kirchhof: Photodarkening in Yb doped fibers: experimental evidence of equilibrium states depending on the pump power; Optics Express, Vol. **15**, Issue 22, pp. 14838-14843, 2007

4.24 M Leich, U Röpke, S Jetschke, S Unger, V Reichel, J Kirchhof: Non-isothermal bleaching of photodarkened Ybdoped fibers; OPTICS EXPRESS 2009, Vol. **17**, No. 15 / pp 12588-12593

Web Reference-W4.0 (accessed on 26.10.2009):

http://www.liekki.fi/docs/whitepapers/Liekki%20white%20paper_Photodarkening%20Understanding%20and%20Mitigating_050719.pdf

Chapter 5

Photodarkening in YDF by 488 nm CW irradiation

5.1 Introduction:

The following flow-chart gives a clear idea of the experimental road map, followed in the early stage photodarkening experiments, involving 488 nm CW irradiation on Yb-doped aluminosilicate fibers. 488 nm wavelength was chosen as this was not within the typical Yb^{3+} absorption band and apart from avoiding high inversion or ion-pair related issues caused by the pump wavelengths (915 nm or 976 nm), the underlying physics of photodarkening could still be addressed from a different angle.

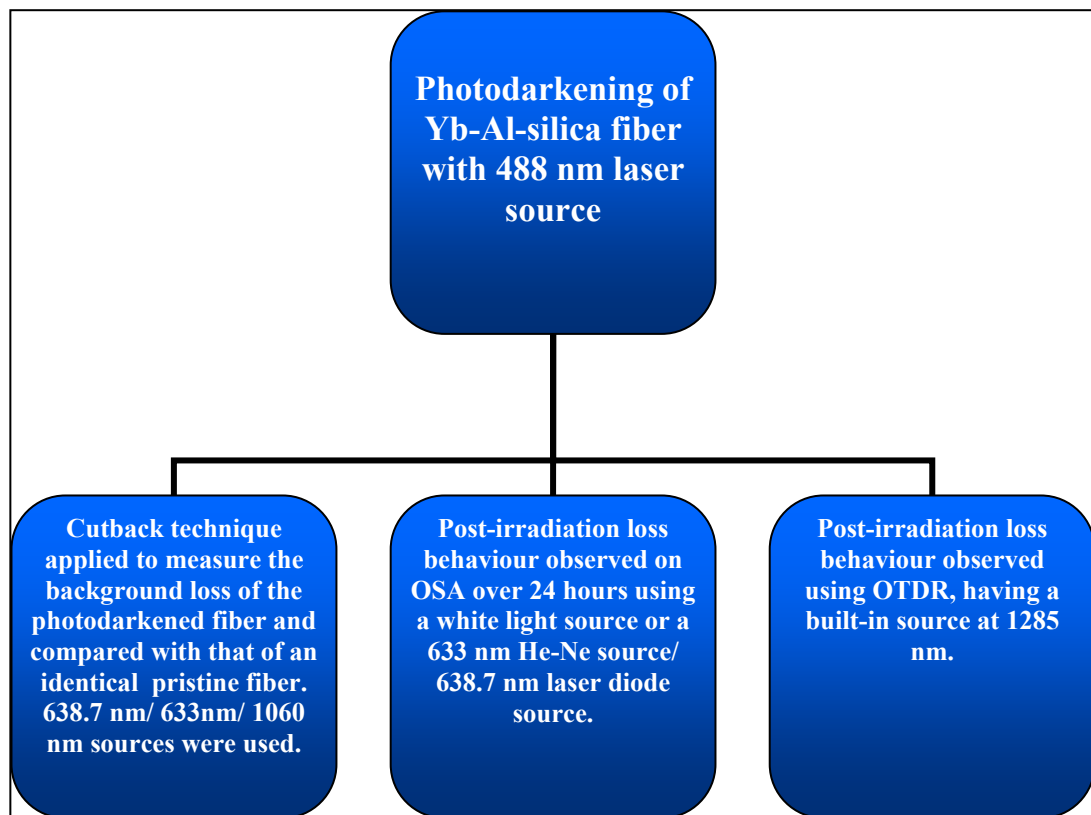


Fig. 5.1: Schematic description of the main photodarkening experiments performed

5.2.1 Photodarkening experiment

The following figure schematically shows the basic/initial experimental setup used to photodarken the Yb-doped aluminosilicate fibers.

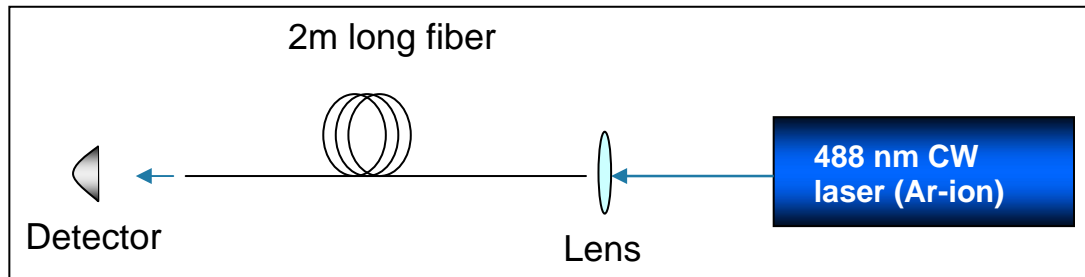


Fig. 5.2: Schematic diagram of the photodarkening experimental setup

The details of the fibers used under this setup are summarized below and the results obtained are summarized in table T5.1. These fibers were coated with high index polymer and in-core pumping scheme was followed. In this thesis, ppm means ppm by weight or simply ppm-wt.

Fiber # F628LF235:

Yb-doping level=16000 ppm

Co-dopant: Aluminium

Core diameter= 6.9 μm .

Outer diameter=100 μm

N.A= 0.14;

Length used =2m (unless stated otherwise)

Fiber # T0116L30059:

Yb-doping level=3500 ppm

Co-dopant: Aluminium

Core diameter= 9.05 μm .

Outer diameter=148.8 μm

N.A= 0.067

Length used =2m (unless stated otherwise)

Fiber # T0138L30091:

Yb-doping level=5500 ppm

Co-dopant: Aluminium

Core diameter= 8.5 μm

Outer diameter= 125 μm

N.A= 0.075

Length used =2m (unless stated otherwise)

Fiber # T0155L30100:

Yb-doping level=17000 ppm

Co-dopant: Aluminium

Core diameter= 8.3 μm .

Outer diameter=125 μm

N.A= 0.15

Length used =2m (unless stated otherwise)

Other than the experiments (488 nm irradiation) performed for OTDR measurements on the irradiated fibers, all the 488 nm irradiations, summarized in table T5.1, were continued for 90 minutes. The approximate in-core power, in all other experiments involving 488 nm pump and/or 633 nm probe, was measured by chopping an identical sample of the fiber at a distance of 10 to 11 cm from the launching end after finalizing the maximum launching efficiency at low input power (e.g. ~30 mW at 488 nm) and then instantly increasing to the desired higher input power level. The 10-11 cm length could not be minimized due to the launching fiber mount size. After finishing the 488 nm irradiation, the fiber was monitored under a white light source and OSA or a 633 nm He-Ne source (~15 mW) or a 638.7 nm laser diode (~5 mW) source (using suitable detectors) for a long time (typically 24 hours or more). Then, the final background loss was monitored (mostly in the visible wavelengths), using cutback technique.

One of the most important observations in this project was the post-irradiation temporal loss evolution in the irradiated fibers, i.e., even after finishing the 488 nm irradiation, a saturable increase in loss was observed at various wavelengths ranging from visible to near infrared.

In order to monitor the post-irradiation temporal loss evolution, in the irradiated fibers, using an OTDR, longer lengths of fibers were used (6 m of F628LF235; 10m of T0155L30100) and the 488 nm irradiations were done for a longer duration (190 minutes) as well. The other two fibers (T0116_L300599, T0138_L30091), mentioned in the table T5.1, were not suitable for the OTDR measurements due to low NA. It is important to note that the OTDR had a 1285 nm in-built LED source. Below, some of the early stage experiments on the highly Yb-doped F628LF235 & T0155L30100 fibers are described briefly (the results are summarized in table T5.1).

5.2.2 Experimental results with fiber F628-LF235

Fig. 5.3 shows the drop (~32%) in throughput power in the fiber F628LF235 over a 90 minute time duration, while irradiated with 488 nm CW source (~570 mW). The power into the core of the fiber was ~345 mW. This clearly indicates a high amount of photodarkening in the fiber caused by the 488 nm irradiation. The irradiated fiber was then probed by a white light source and the transmission was monitored on the OSA. This showed a significant amount of temporal drop in the transmitted power at various wavelengths, in other words, gradual increase in loss at various wavelengths, even after stopping the 488 nm radiation was monitored. This is shown in Fig. 5.4. It is important to notice that this post-irradiation temporal loss evolution is dominant, as shown on the OSA, in the visible wavelengths.

In another experiment, a similar photodarkened fiber was probed by a 638.7 nm laser diode source (5 mW) just after irradiation by the 488 nm source was finished (with a 31% drop in throughput power within first 25 minutes of irradiation, but the 488 nm laser output power started fluctuating after that until the 90 minute time period of irradiation). This experiment also showed a similar trend of post-

irradiation temporal evolution in loss, at 638.7 nm. This is shown in Fig. 5.5. After finishing this particular experiment, the same fiber was used for a cutback measurement with the 638.7 nm laser diode source. The cutback data clearly revealed, as expected, the increase in loss as compared to an identical pristine fiber, using cutback technique, under the same 638.7 nm source. This result is shown in Fig. 5.6. At 638.7 nm, the background loss in the pristine fiber was 0.3dB/m whereas the loss in the photodarkened fiber was 4.7 dB/m.

A 6m long sample of this fiber was irradiated by the 488 nm source, at ~570 mW and the throughput power dropped by 67% over 190 minutes. This fiber was then immediately taken for OTDR measurements. OTDR measurements also confirmed the post-irradiation temporal evolution of loss. This result is shown in Fig. 5.7. As probed by the OTDR with 1285 nm LED source, the loss in the photodarkened fiber, just after finishing the 488 nm irradiation was just 47 dB/km and gradually increased to 107 dB/km in ~24 hours, which was almost at saturation point. It was surprising to see that the loss in the fiber, measured by the OTDR, just after irradiation was finished, was 47 dB/km which was just 7 dB/km higher than that of the pristine sample and the post-irradiation temporal evolution of loss itself showed a huge change from 47 dB/km to 107 dB/km. But, this particular fiber (F628LF235) was no more available and so further clarification was not possible. Another fiber (T0155L30100) with almost similar composition and configuration was then picked up to carry on further investigation.

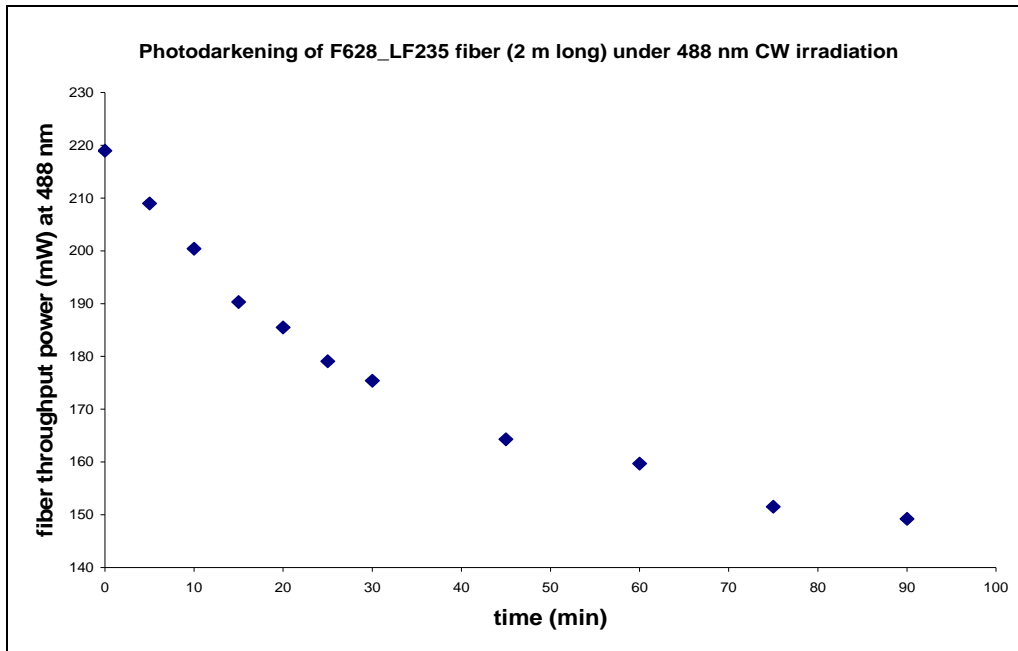


Fig. 5.3: Typical photodarkening trend in Yb-doped fiber (F628-LF235) irradiated with 488 nm CW source

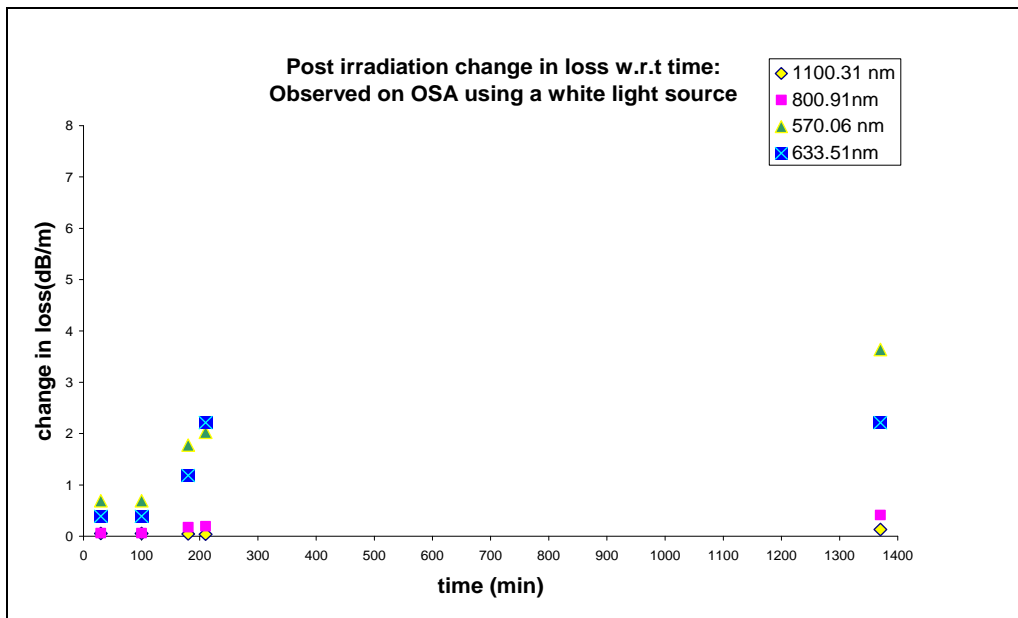


Fig. 5.4: Post-irradiation temporal evolution of loss in F628-LF235, observed on OSA

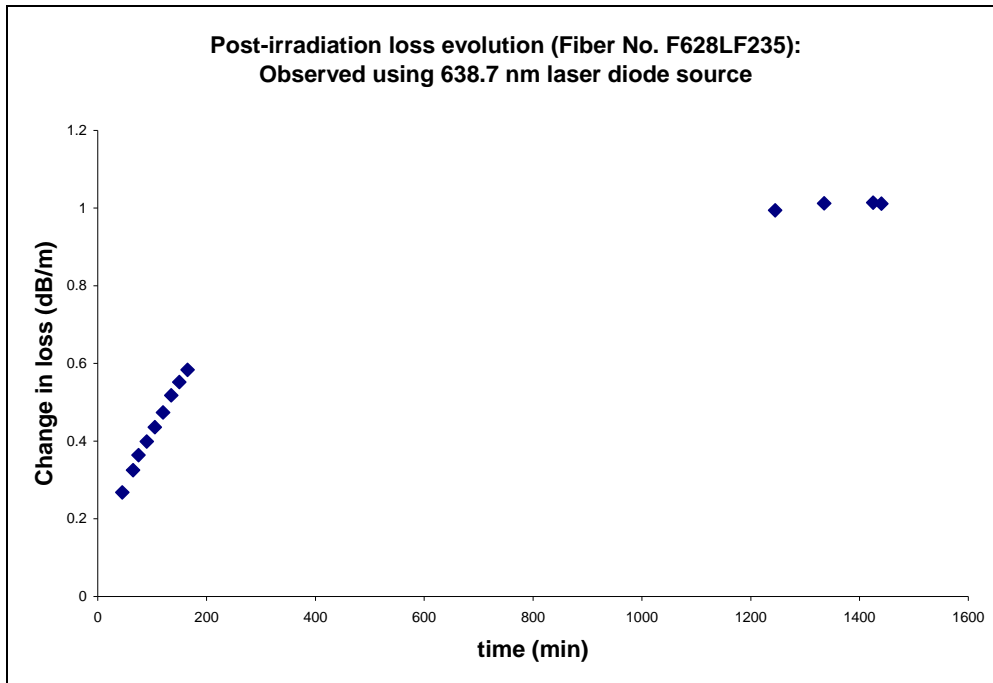


Fig. 5.5: Loss evolution probed with 638.7 nm source on F628-LF235 fiber

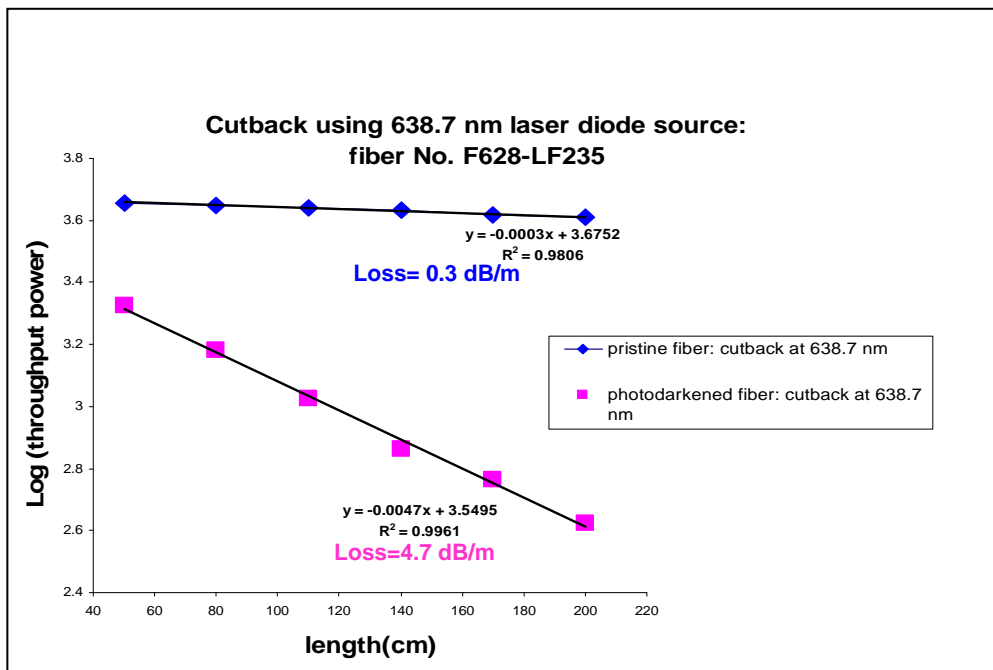


Fig. 5.6: Background loss in F628-LF235 observed using cutback technique with a 638.7 nm source: comparison between a pristine and a photodarkened fiber

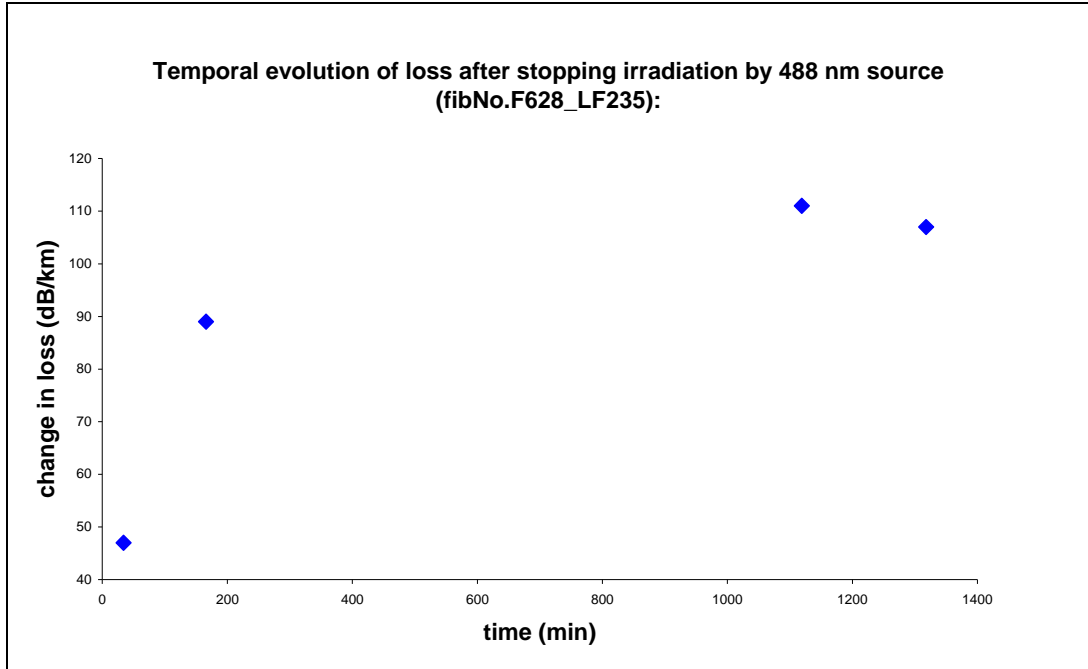


Fig. 5.7: Post-irradiation temporal evolution of loss measured by OTDR

5.2.3 Experimental results with fiber T0155-L30100

Fig. 5.8 shows the drop in throughput power in the fiber T0155-L30100 over time, while being irradiated with 488 nm CW source (~570 mW). This clearly shows high amount of photodarkening in the fiber (throughput power drop ~22%), caused by the 488 nm radiation. The power into the core of the fiber was ~346 mW. The irradiated fiber was probed by a white light source, just after irradiation by the 488 nm source was finished. This experiment also showed significant post-irradiation temporal evolution in loss in the visible region, as observed on the OSA. Fig. 5.9 shows the post-irradiation temporal evolution of loss particularly at 633 nm, as observed on the OSA. After finishing this experiment up to a loss saturation point, cutback measurement was done on the same fiber, using a 633 nm He-Ne laser source. The cutback data clearly revealed, as expected, the increase in loss as compared to an identical pristine fiber which was also cutback under the same 633 nm He-Ne source. These results are shown in Fig. 5.10. At 633 nm, the background loss in the pristine fiber was ~1.0 dB/m whereas the loss in the photodarkened fiber was ~7.3 dB/m.

A 10m long pristine sample of this fiber was irradiated by the 488 nm source, at ~570 mW and the throughput power dropped by 61% over 190 minutes. This fiber was then immediately taken for OTDR measurements. OTDR measurements clearly pointed to the post-irradiation temporal evolution of loss. This is shown in Fig. 5.11. The loss in the pristine fiber, as shown by the OTDR, was 17.4 dB/km. As probed by the OTDR with 1285 nm LED source, the loss in the photodarkened fiber, just after finishing the 488 nm irradiation was 122 dB/km and gradually grew up to almost a saturation level at 155 dB/km over 24 hours.

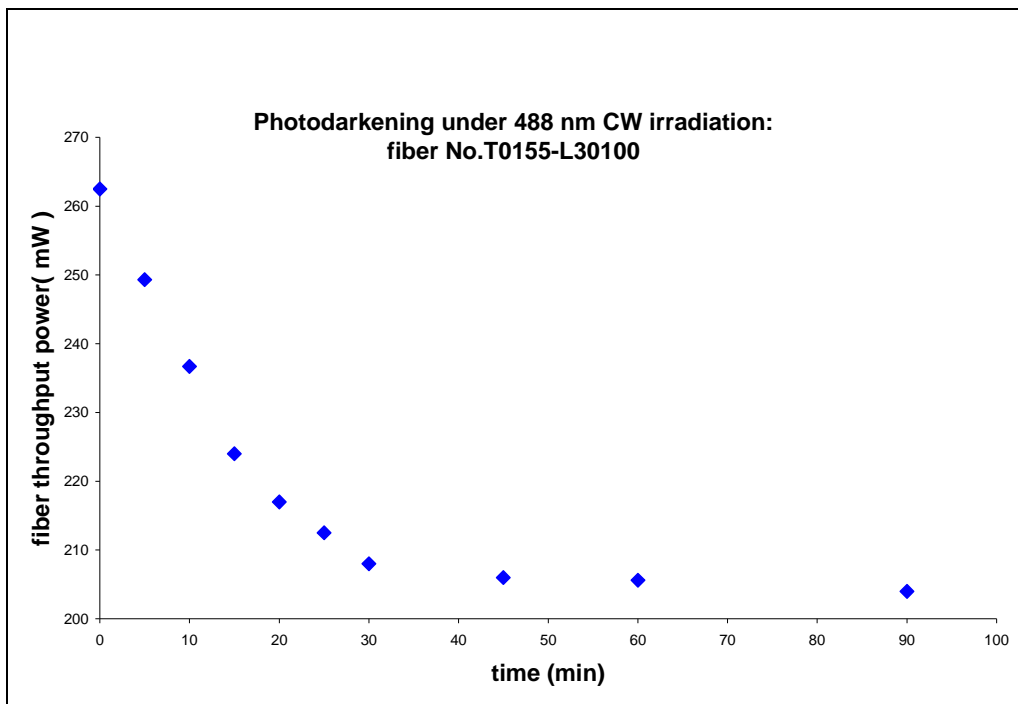


Fig. 5.8: Drop in throughput power in the fiber T0155-L30100

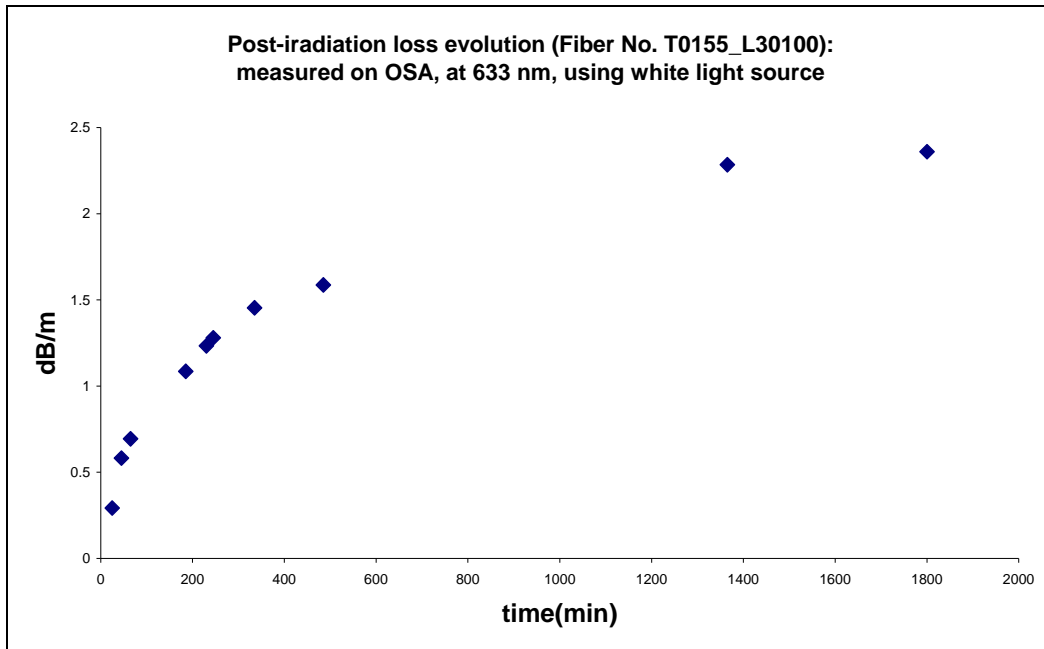


Fig. 5.9: Post irradiation loss evolution in fiber T0155 L30100

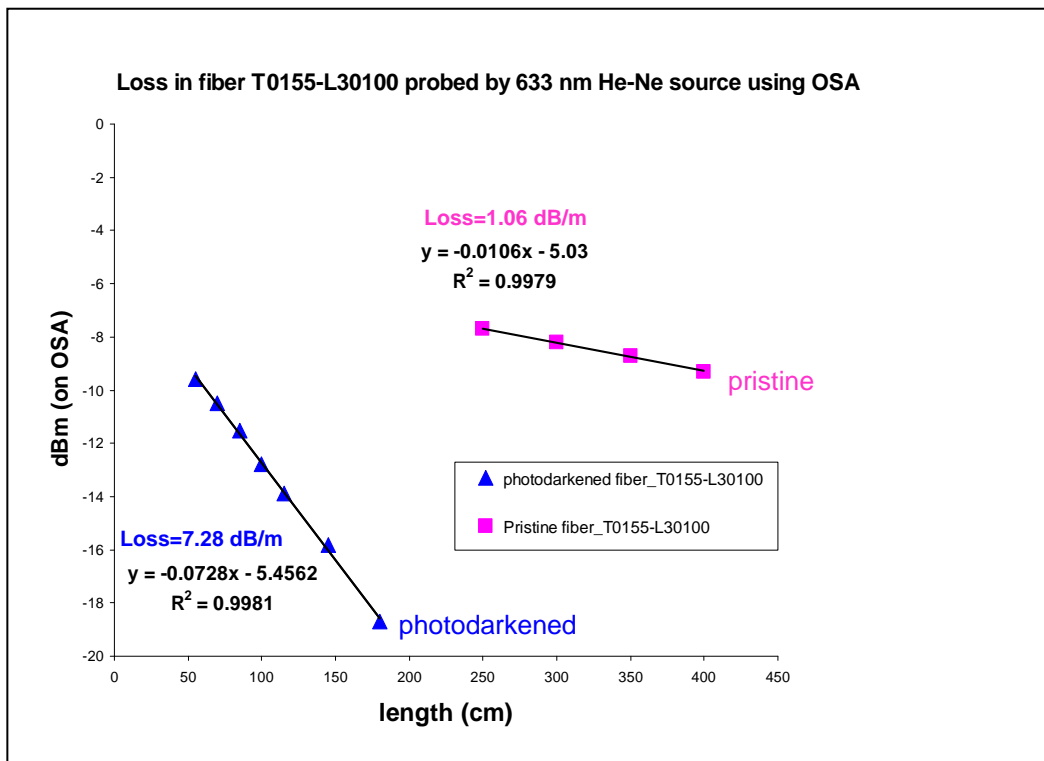


Fig. 5.10: Loss comparison by cutback technique

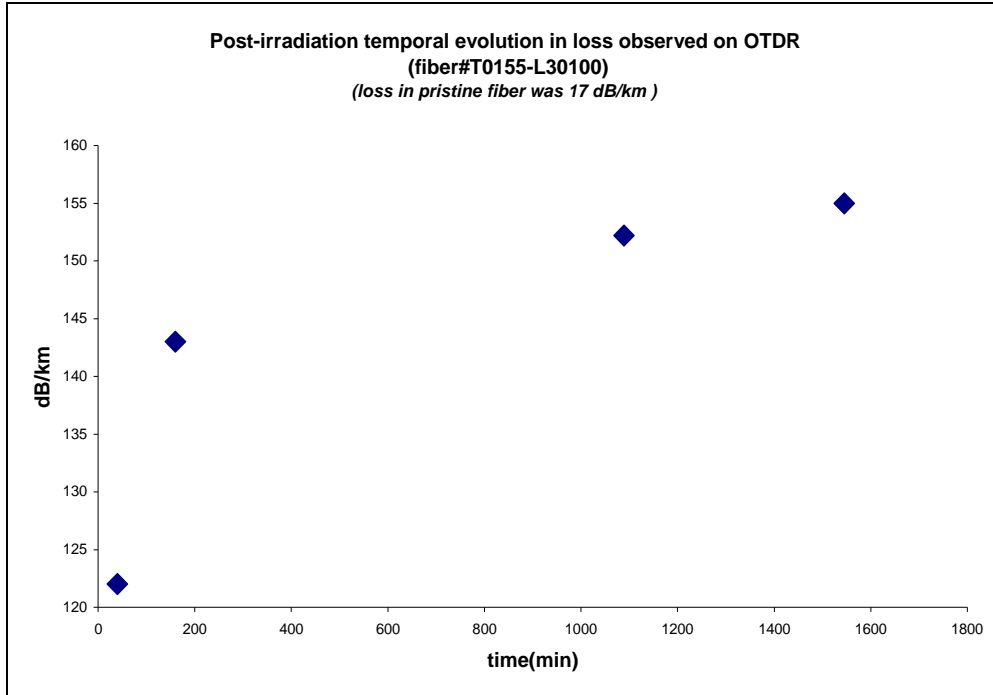


Fig. 5.11: Post-irradiation temporal loss evolution observed on OTDR

5.2.4 Phosphosilicate fiber:

A phosphosilicate fiber was tested under 488 nm CW irradiation and was found to show very low photodarkening (5.2%) under 488 nm irradiation for 90 minutes. The laser output was ~590 mW and the in-core power was ~475 mW. The loss in both the photodarkened sample and an identical pristine one was then measured using cutback technique with 1047 nm source and the result is shown in Fig. 5.12. The fiber had ~20,000 ppm of Yb^{3+} and a core diameter of ~8.3 μm (with ~125 μm outer diameter, N.A~0.16). The result shows its higher resistance to photodarkening as compared to similar aluminosilicate fibers. It is important to note that the 1047 nm source was used at low power (30-50 mW), for cutback on both the irradiated and the pristine phosphosilicate fibers, in order to avoid ambiguity in the loss measurement, arising from probable ASE generated by 1047 nm pump. In another experiment with a 2 m long sample of the same fiber, the post-irradiation cutback at 633 nm source showed very little increase of the background loss (0.5 dB/m to 0.7 dB/m) as compared to that of the pristine sample. This is shown in Fig. 5.13.

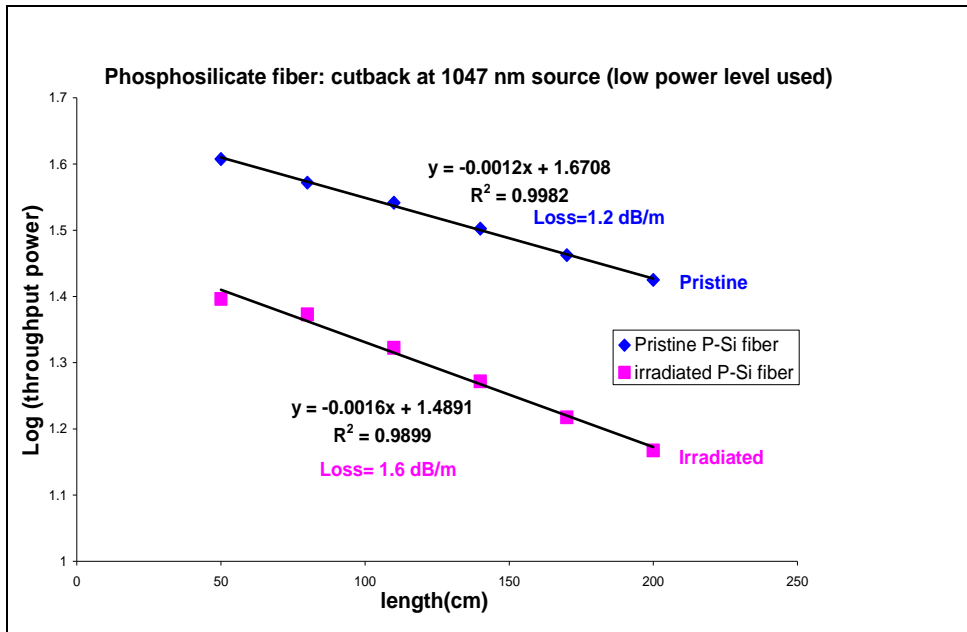


Fig. 5.12: Loss comparison by cutback technique (at 1047 nm)

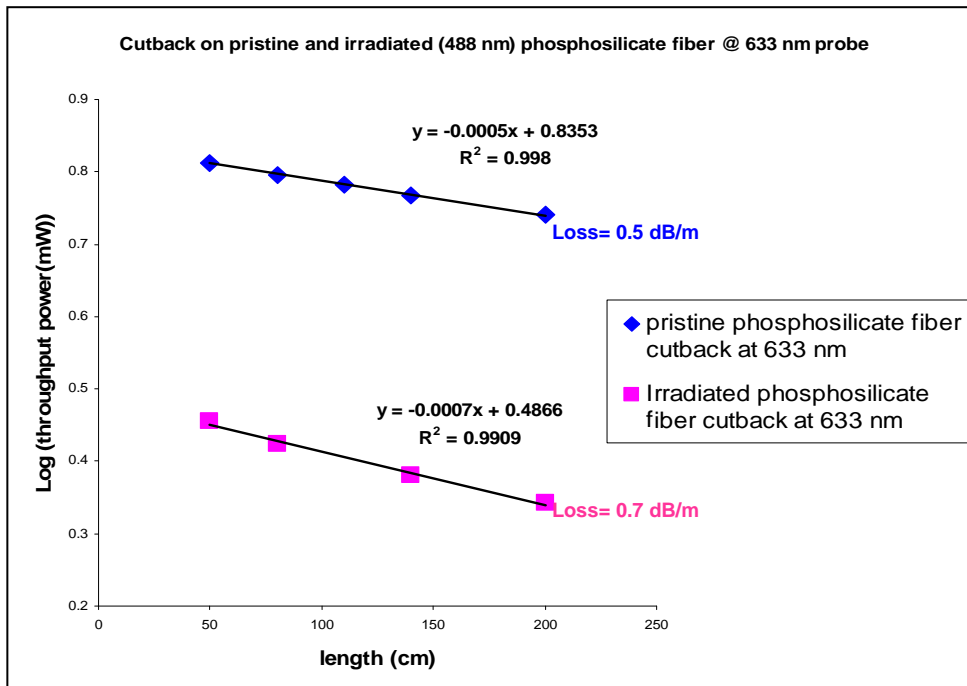


Fig. 5.13: Loss comparison by cutback technique (at 633 nm)

Fiber number	Doping conc. in ppm (approx.)	Post-irradiation temporal change in loss only (Δ - in dB/m)	Cutback : loss just after irradiation (after subtracting Δ)	Typical power drop (@488 nm) in 2m long fiber during irradiation	Temporal OTDR measurements (after 488 irradiation for longer durations; see text for details)
F628_LF235	16000	Probe: 638.7 nm source /OSA Δ =1 dB/m (@638.7 nm)	Loss in pristine(@638.7nm): 0.3 dB/m Loss after irradiation: 3.7 dB/m Laser output(488nm)=570 mW In-core-power (@488nm) ~345 mW	31% (for the corresponding set of data on the left side)	Loss in pristine:40 dB/km Post PD increase in loss: 47 to 107 dB/km (<i>PD loss at 488 nm =67% , during irradiation</i>)
T0116_L30059	3500	Probe: He-Ne/OSA Δ =1.3 dB/m (@633 nm)	Loss in pristine(@638.7nm): 0.5 dB/m Loss after irradiation: 5 dB/m Laser output(488nm)=570 mW In-core-power (@488nm) ~360 mW	19%	X
T0138_L30091	5700	Probe: White light/OSA Δ = 4 dB/m (@633.5 nm)	Loss in pristine (@633nm): 0.93 dB/m Loss after irradiation: 7 dB/m Laser output(488nm)=577 mW In-core-power (@488nm) ~350 mW	38%	X
T0155_L30100	17000	Probe: White light/OSA Δ =2.35 dB/m (@633.5 nm)	Loss in pristine (@633nm): 1 dB/m Loss after irradiation: 4.93 dB/m Laser output(488nm)=513 mW In-core-power (@488nm) ~346 mW	22%	Loss in pristine: 17.4 dB/km Post PD increase in loss: 122 to 154.7 dB/km (<i>PD loss at 488 nm =61% , during irradiation</i>)

Table: T5.1: Summary of photodarkening in Yb-doped aluminosilicate fibers under 488 nm CW irradiation

5.3 Photodarkening experiments with simultaneous probing at 633 nm:

In some of the experiments, while the fiber was being irradiated by the 488 nm source, simultaneous probing by a 633 nm HeNe source was also incorporated using dichoric mirrors (DM) and an additional power meter. The following figure is a schematic description of such experiments.

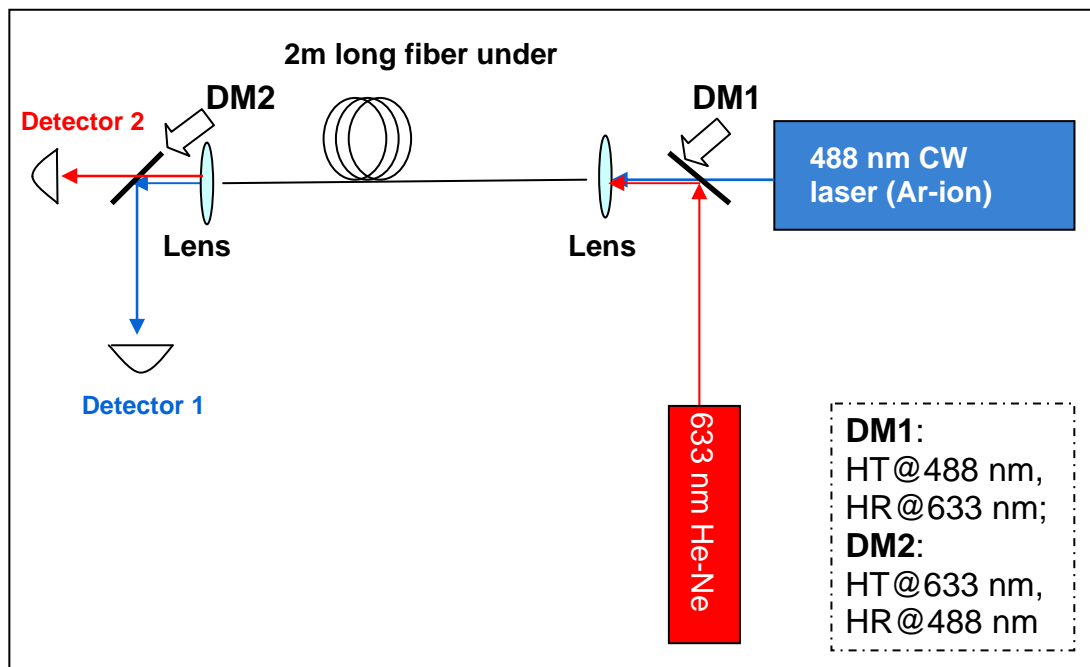


Fig. 5.14: Photodarkening by 488 nm CW irradiation and simultaneous probing at 633 nm

It's worth mentioning that less than ~0.2 % and ~10% errors, in the detector 1 & detector 2 respectively, were observed due to the transmission of 488 nm line and reflection of 633 nm line at DM2, at the beginning of irradiation when the throughput power (and hence leakage power) at both 488 nm and 633 nm were maximum.

Samples of the fiber **T0155L30100** have been used for the following experiments and each sample, used for photodarkening, was ~2 m (unless otherwise stated). The

in-core pump power (488 nm CW) was $\sim 3.7 \text{ mW}/\mu\text{m}^2$, as measured at the start of the experiment.

Digital Multimeter (DMM) - A PC interfaced DMM (Uni-Trend UT60) was used for data logging (633 nm throughput data) from the analog output of the Newport power meter (model-840C) which was connected to the Detector 2 (Newport detector-818 SL).

Detector 1- ILX detector-OMH 6722B Silicon used with ILX Lightwave optical multimeter (power meter), OMM6810B. Detector 2- 818 SL Newport detector with (attenuator attached-883 SL; OD3) used with Newport handheld power meter, Model 840C.

5.3.1 No heating of fibre during or after irradiation by 488 nm CW source:

In these 3 sets of experiments, 2m long samples of the fiber T0155L30100 were irradiated by the 488 nm CW source and a 633 nm CW source was also used to probe the background loss dynamics during and after stopping the 488 nm irradiation. Fig. 5.15 shows the throughput power drop at 488 nm over 90 minutes of irradiation. Fig. 5.16 shows the throughput power drop at 633 nm, during and after 488 nm irradiation. The post-irradiation evolution in the background loss at 633 nm is clearly visible. The table

T5.2 gives comparative details of the loss measurements, including the data obtained by cutback technique.

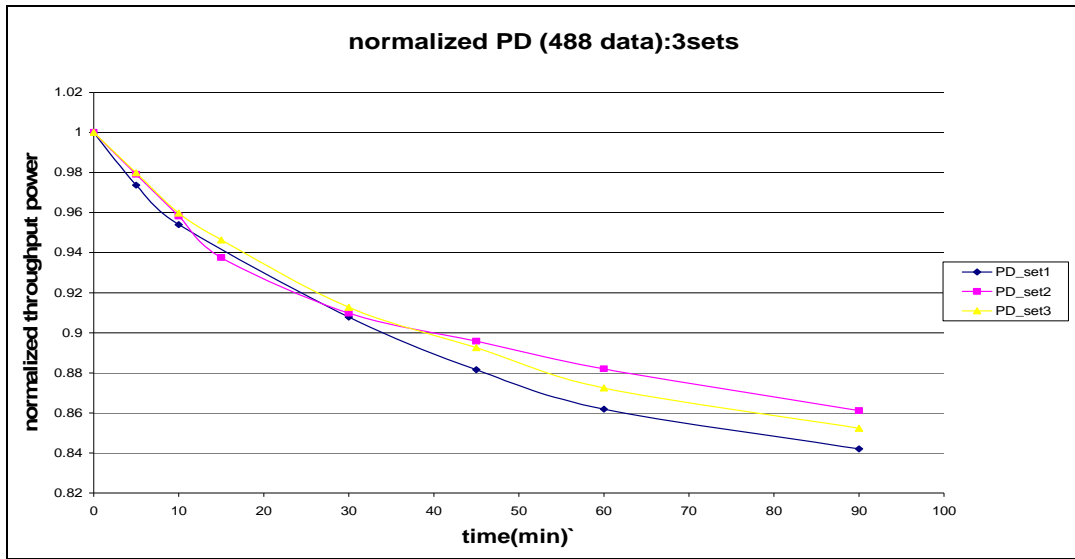


Fig. 5.15: Throughput power drop at 488 nm due to photodarkening, without any external heating

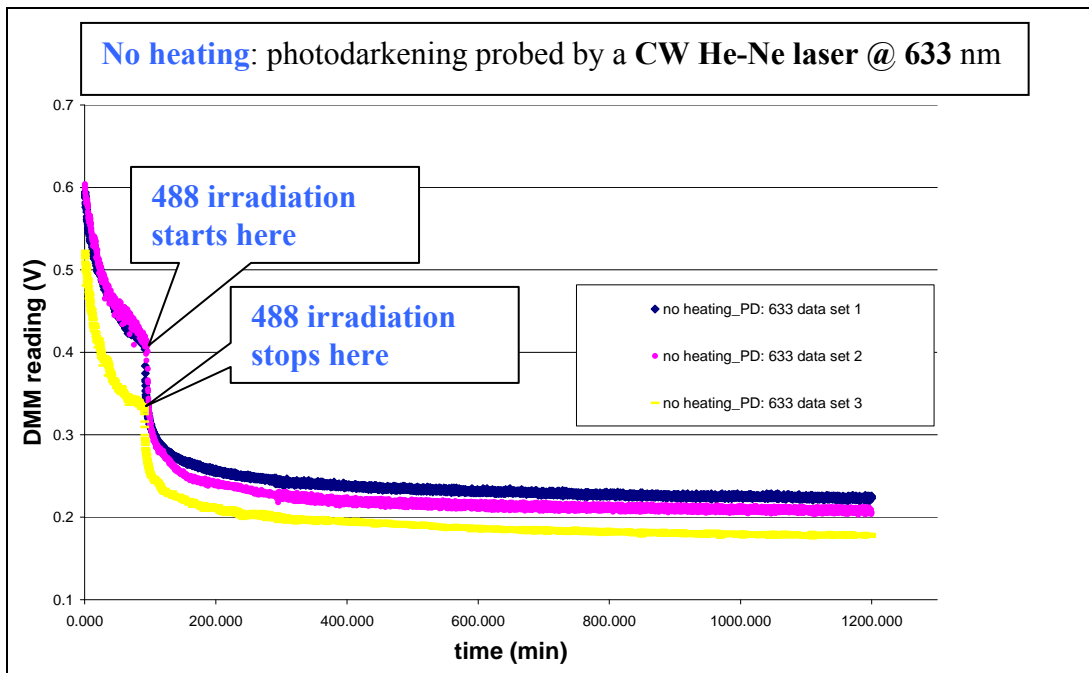


Fig. 5.16: Throughput power drop of the probe (633 nm) due to photodarkening, without any external heating

Sl. No.	Loss @633 nm during 488 nm irradiation (dB/m)	Post-irradiation loss @633 nm (dB/m)	Total PD induced loss @633 nm (dB/m)	Final cutback loss @633 nm (dB/m)
Set 1	0.78	1.31	2.09	3.5
Set 2	0.82	1.49	2.31	3.7
Set 3	0.99	1.35	2.34	3.8

Table T5.2: Summary of PD induced loss in T0155L30100 fiber without external heating. The cutback loss, measured with a pristine sample @633 nm, was 1.06 dB/m

In another experiment, a 2m long T0155L30100 fiber was photodarkened under 488 nm CW irradiation for 90 minutes (no probing by He-Ne) and after that white light transmission was monitored on the OSA. Fig. 5.17 shows that result and the post-irradiation temporal evolution in the background loss, over the range 500-800 nm is clearly observed. Fig. 5.18 shows a fitting plot on the temporal loss data obtained from the same experiment (Fig. 5.17).

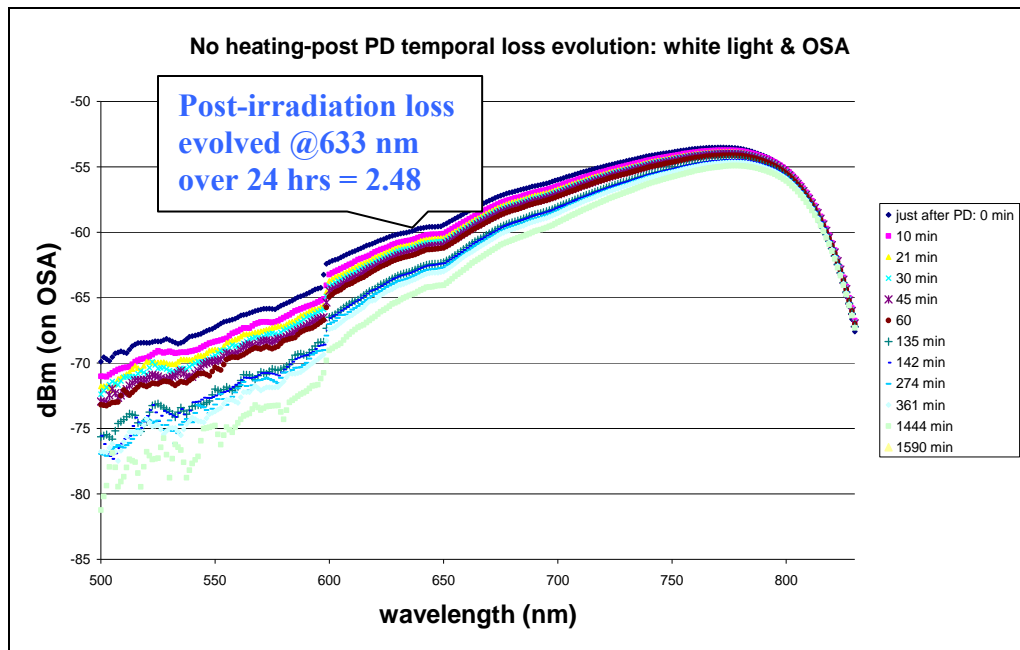


Fig. 5.17 Post irradiation temporal loss evolution observed on OSA (using a white light source)

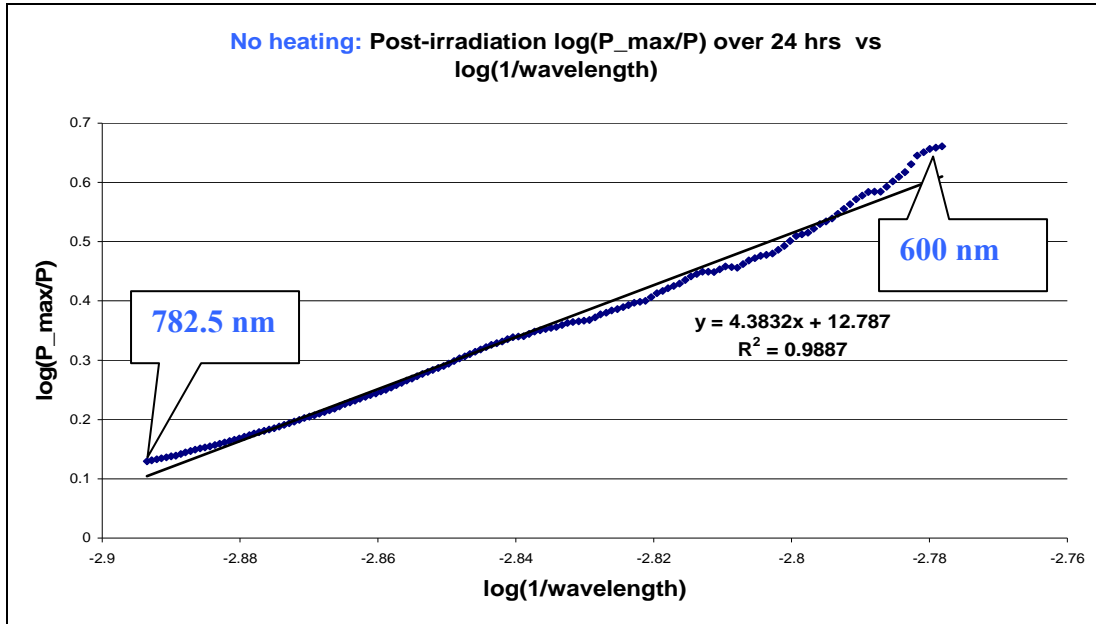


Fig. 5.18: Fitting to identify Rayleigh scattering centres

The slope of the curve in Fig. 5.18 is very close to ‘4’ and this can be an indication of generation of new scattering centres (Rayleigh scattering centres) even after stopping the 488 radiation. **P_max** denotes the maximum throughput power, at a certain wavelength, observed at time $t=0$ min and **P** denotes the power at the same wavelength after 24 hours. This may not be the only reason for post-irradiation loss evolution in the photodarkened fiber and the overall effect can be expected to be a combination of scattering and absorption by newly formed colour centres, if there are any.

5.3.2 Influence of heat on photodarkening of normal Yb-doped fibers

5.3.2.1 Heating during irradiation:

In this case, every fiber under test was heated at 120° C, while being irradiated by the 488 nm CW source. The coiled portion of the fiber was kept on a hot-plate and was properly enclosed with a suitable metal cover. Simultaneous probing by 633 nm

CW He-Ne source was also in place and that continued for hours, even after stopping the 488 nm irradiation. Fig. 5.19 and Fig. 5.20 show the data obtained from these photodarkening experiments. The summary of the losses measured at 633 nm, is shown in Table T5.3. Post-irradiation temporal growth in loss and the overall final loss measured by cutback method at 633 nm, are lesser in case of heating during irradiation. This is not well understood but might be an indication that generation of traps or precursors are reduced on heating during irradiation. Further investigation is definitely required for better clarity.

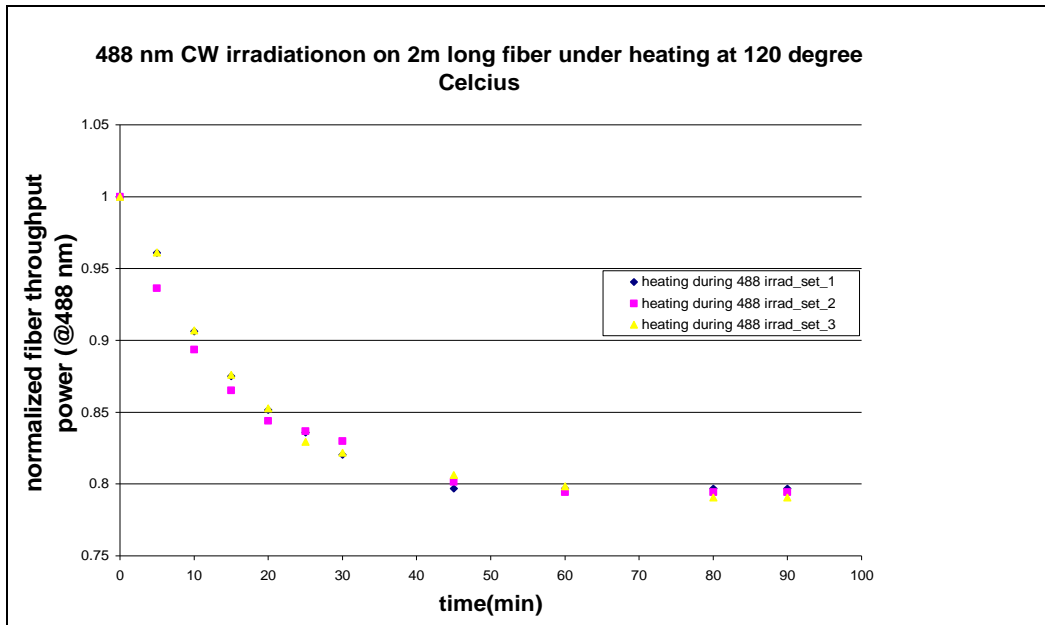


Fig. 5.19: Photodarkening in a fiber under external heating during 488nm irradiation

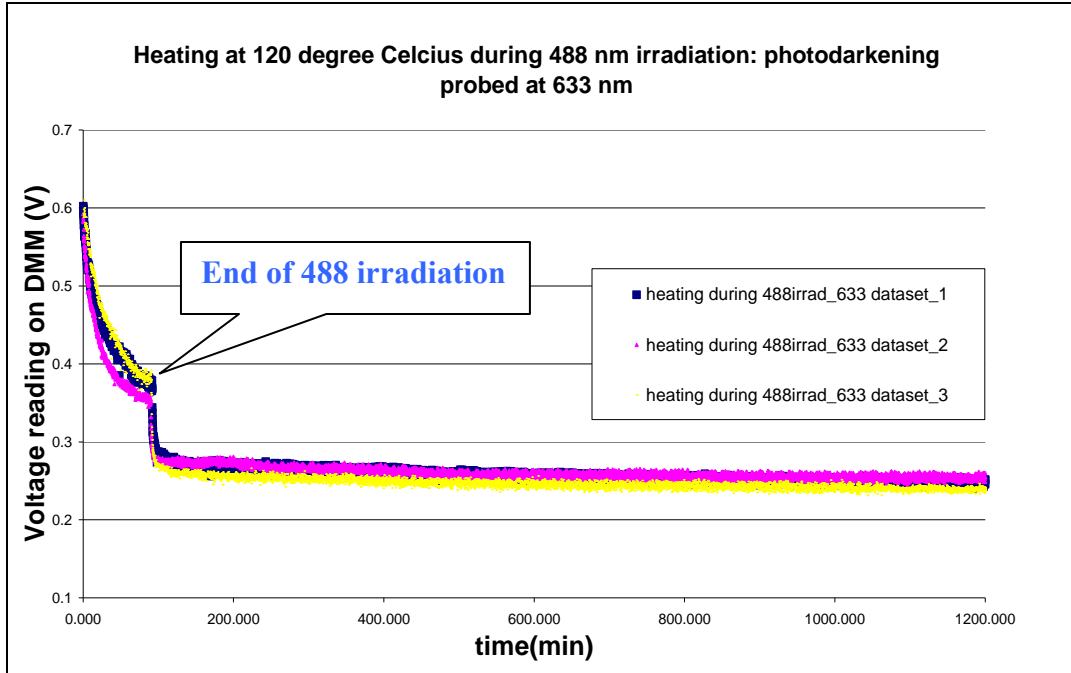


Fig. 5.20: Drop in the probe (633 nm) throughput power in T0155L30100 fiber, during 488 nm irradiation with simultaneous external heating and afterwards.

Sl.No.	Loss@633 nm due to 488 irradiation (dB/m)	Loss@633 nm (post-irradiation only) (dB/m)	Total loss @ 633nm (dB/m)	Loss shown by cutback @ 633nm (dB/m)
Set1	1.04	0.83	1.87	2.0
Set2	1.13	0.58	1.71	2.3
Set3	0.96	0.91	1.81	2.4

Table T5.3: Summary of the PD loss in T0155L30100 fiber due to 488 nm irradiation with simultaneous external heating.

5.3.2.2 Heating after irradiation:

Fig. 5.21 shows the two particular sets of experiments where the fibers were kept at 120° C for ~2 hours, just after finishing the 488 nm CW irradiation for post irradiation study. The cutback data (using 633 nm He-Ne source) were obtained after ~24 hours and those data showed significantly higher loss (4.8 dB/m and 5.3 dB/m

@633 nm respectively) than that of the no-heating cases described in section 5.3.1. In short, post-irradiation heating seems to cause more photodarkening and also faster saturation of the normal post-irradiation loss evolution as compared to that in the no-heating cases. Fig. 5.22 shows the data where post-irradiation loss monitoring was performed using a white light source and OSA and the fiber was heated at 120° C for the first 30 minutes after finishing the 488 nm CW irradiation. Fig. 5.24 gives a comparison on heating and no-heating cases, as far as post-irradiation loss evolution is concerned. In Fig. 5.24 (a), the deep blue line shows the white light throughput spectrum just after finishing 488 nm irradiation. The pink one is the spectrum recorder after 30 mins at room temp. And finally, the green one is the spectrum recorded after 24 hours from the start of OSA measurements. The temporal growth in loss after 24 hours was 2.5 dB/m at 633 nm. In Fig. 5.24 (b), just within 30 minutes of heating after finishing irradiation, the loss grew up to 2.6 dB/m. The heater was switched off then and the final loss after 24 hours was measured to be 3.1 dB/m. It clearly shows that post-irradiation temporal evolution of loss can be accelerated and enhanced by heating, below the threshold temperature for thermal bleaching.

No concrete model to explain this phenomenon is available so far, to the best of my knowledge. The overall PD in YDFs, due to 488 nm irradiation, can be hypothesized as a combination of two different loss mechanisms as shown in process 1 & process 2 in Fig. 5.25. It should be noted that process 2, as shown in Fig. 5.25, can be expedited with external heating within a certain temperature limit and faster post-irradiation temporal loss evolution can be observed. Beyond that limit thermal bleaching will prevail.

Fig. 5.23 shows a straight line-fitting of the data obtained from Fig 5.22. This was done in order to verify whether the slope of the line measures close to 4, which could have been an indication of a dominant effect of Rayleigh scattering. Similar fittings yielded inconclusive results as far as presence or generation of scattering centres were concerned. Since the overall post-irradiation temporal evolution of loss

is monitored, which comprises of contributions from different kinds of absorption centres, along with the scattering centres if there are any, such fittings would not be able to pin-point Rayleigh scattering centres. Nevertheless, further investigation in this direction might be useful.

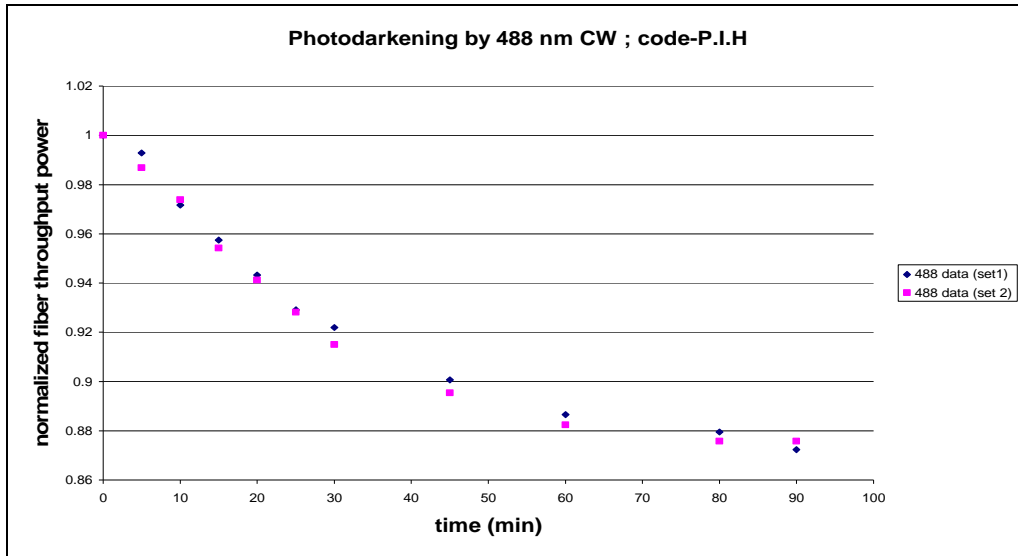


Fig. 5.21: Drop in throughput power of the 488 nm irradiation in T0155L30100 fiber. The fiber samples were heated after finishing 488 nm irradiation.

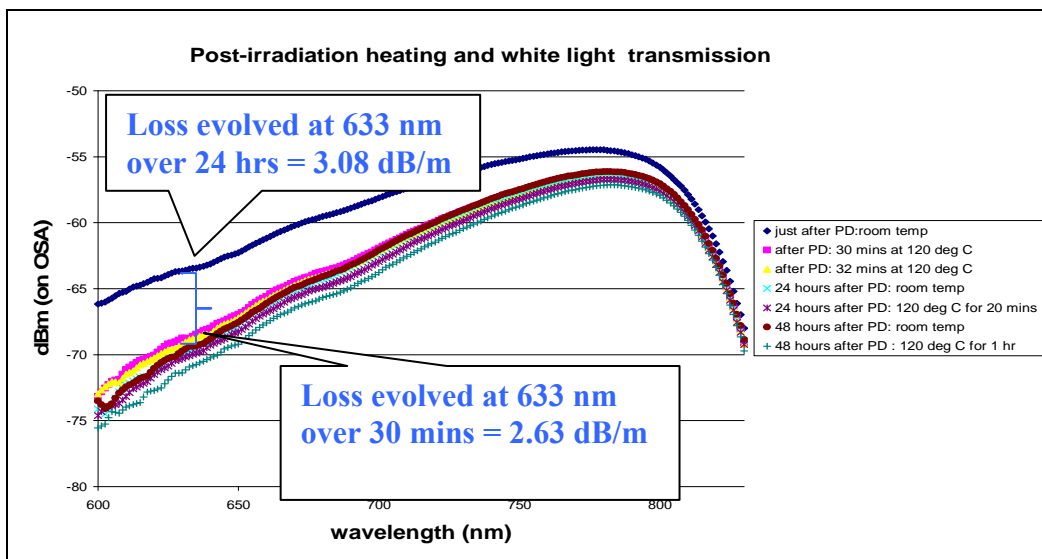


Fig. 5.22: Post-irradiation heating and effect on temporal loss evolution observed on an OSA, using a white light source

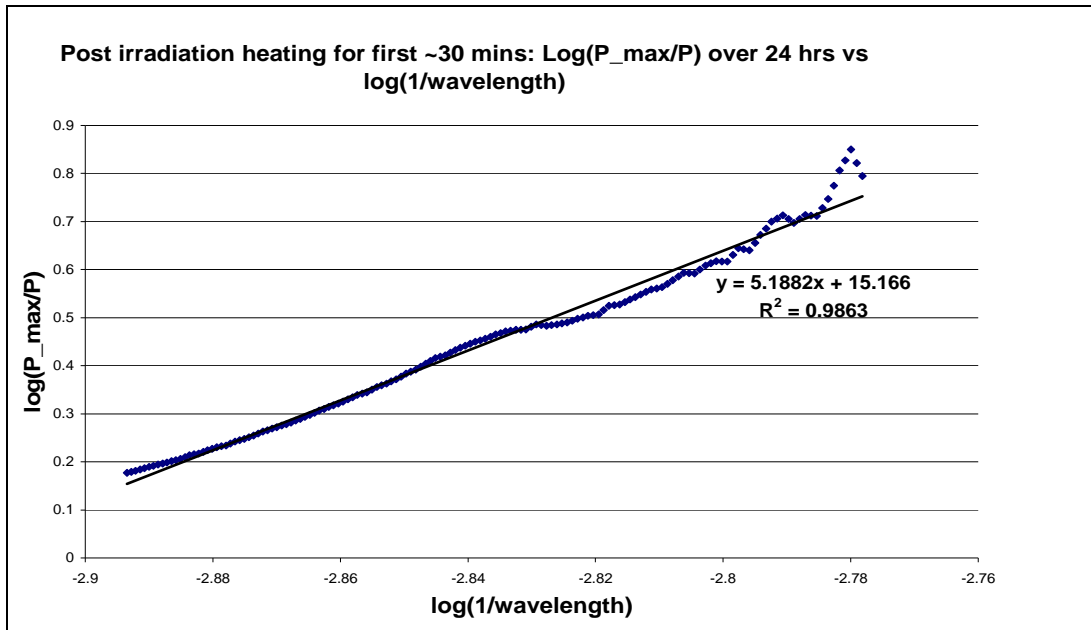


Fig. 5.23: Plot to identify whether Rayleigh scattering centres are formed and are dominant in the post irradiation temporal loss evolution process, Please see text for details.

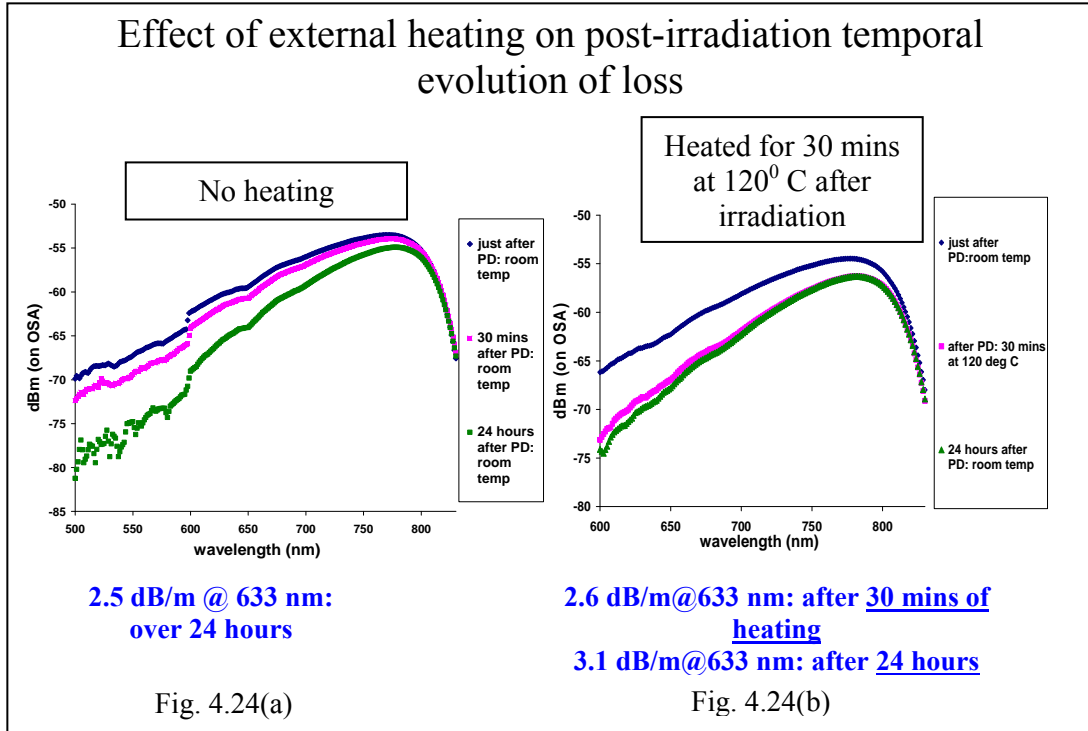


Fig. 5.24: Effect of external heating on post-irradiation temporal loss evolution

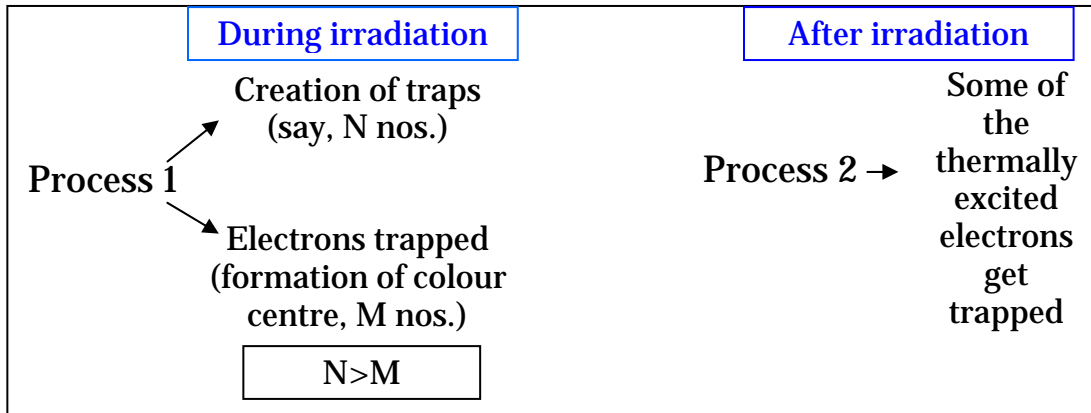


Fig. 5.25: Schematic of a probable path for post-irradiation temporal loss evolution

5.4 Influence of probing sources on pristine Yb-doped fibers:

It was verified that the 633 nm CW He-Ne source (in-core power in the test fibers ~55 $\mu\text{W}/\text{Sq-micron}$) or the white light source, used on the test fibers for hours, did not themselves cause any photodarkening in the fiber. Fig. 5.26 depicts a direct verification, where a 2m long, pristine T0155L30100 fiber, irradiated by a white light source continuously for 7 hours, did not show any observable variation in the broad transmission spectrum monitored on the OSA. This can also be seen as a fact that, having UV-VIS photons from a source is not enough to cause photodarkening in Yb-doped fibers but there has to be a threshold power level (can vary depending on the glass composition) above which photodarkening takes place. Photodarkening varies nonlinearly with input power level and this nonlinearity also varies with the pump wavelength used.

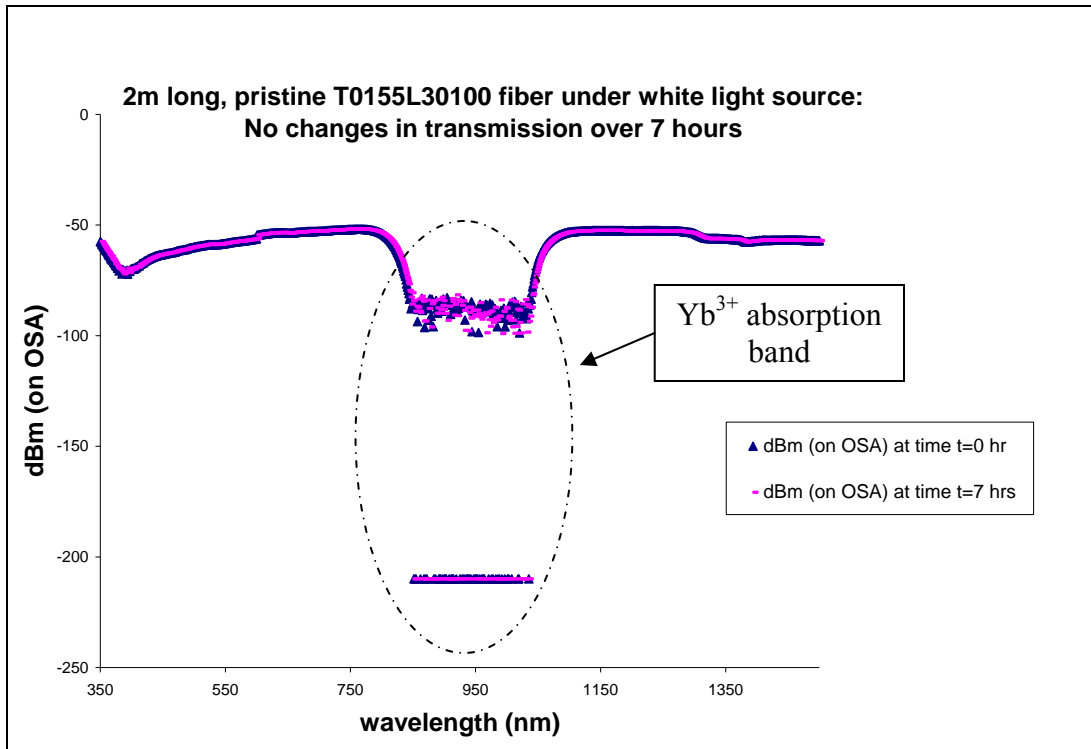


Fig. 5.26: Pristine YDF monitored on an OSA, using a white light source

5.5 Conclusion:

Photodarkening in Yb-doped aluminosilicate fibers under 488 nm CW radiation has been studied on various fibers. The background loss in the irradiated fibers were significantly higher than their pristine counterparts, as expected and this was more intensely observed in the VIS region, as probed by a white light source or a standard 633 nm CW He-Ne laser. Experimental results on phosphosilicate fibers have confirmed the host's high resistance towards photodarkening and that is very good for conventional wavelength lasers (1030-1060 nm) using Yb-doped fibers. Yb-doped aluminosilicate fibers are more suitable than the Yb-doped phosphosilicate ones as the latter is not good for generating wavelengths above 1080 nm. Some smart techniques should be adapted in order to address photodarkening in Yb-doped aluminosilicate fibers in the high power domain.

Post-irradiation (i.e. after stopping the radiation from the 488 nm CW source) temporal evolution of loss in Yb-doped fibers was also observed in the VIS as well

as in the NIR regions (using OTDR). This is a very interesting phenomenon and perhaps the first of its kind as far as Yb-doped fibers are concerned. Similar result was shown in case of germanosilicate fibers [5.1]. Also, this chapter describes some experiments where acceleration and enhancement of post irradiation temporal evolution of loss were observed due to external heating. Analysis of photodarkening in YDF, from a thermodynamic point of view, has recently drawn increasing amount of research interest. In this context, our conference paper [5.2] followed by two more publications [5.3, 5.4] from other researchers are worth mentioning. To the best of my knowledge, no full-proof-theory exists to explain this phenomenon presently and future works can improve the level of understanding on this and a theoretical model may be developed.

In this context, it is worth to mention the published article [5.5] where oxygen deficient centres (ODC) have been proposed to as a precursor of photodarkening in Yb-doped aluminosilicate fibers. Fig. 4.27 shows the ODC peak around 220 nm, in a Yb-doped aluminosilicate fiber preform. This particular experiment is credited to Dr. S Yoo and Dr. A J Boyland, both from the ORC, University of Southampton, UK.

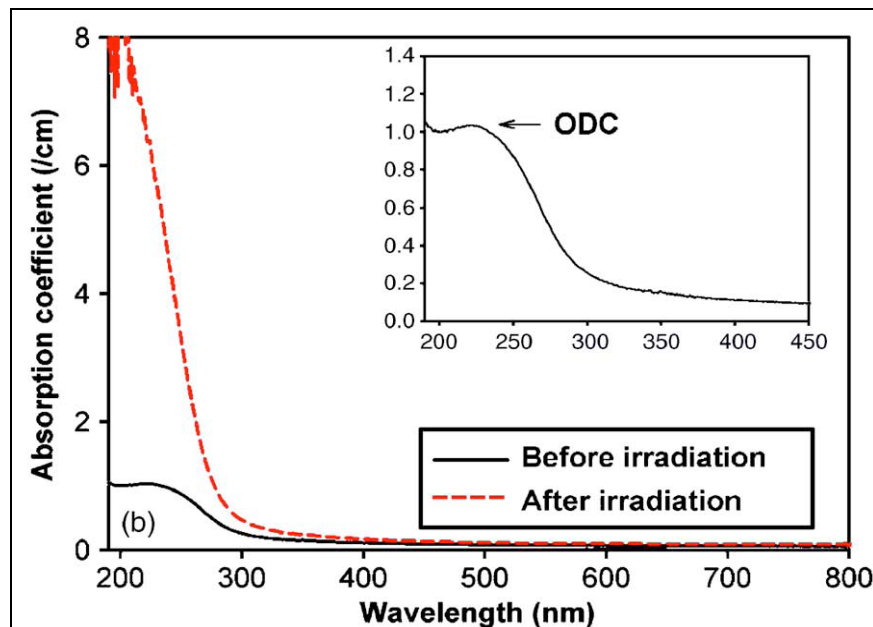


Fig. 5.27: Optical absorption in an Yb-doped fiber preform before and after 488 nm irradiation (Inset: enlarged section to highlight the ODC peak at 220 nm)

References (Chapter 5):

5.1 L.J. Poyntz-Wright and P.ST.J .Russel: Spontaneous Relaxation Processes in Irradiated Germanosilicate Optical Fibers; Electronics Letters, 1989, Vol. **25** , No.7, pp. 478-480

5.2 C Basu, S Yoo, A J Boyland, A Webb, C L Sones , J K Sahu: Influence of temperature on the post-irradiation temporal loss evolution in Yb-doped aluminosilicate fibers, photodarkened by 488 nm CW irradiation; CLEO/Europe-EQEC 2009 Munich 14-19 Jun 2009 CJ1.2

5.3 M J Söderlund, J J Montiel i Ponsoda, J P Koplow and S Honkanen : Heat-induced darkening and spectral broadening in photodarkened ytterbium-doped fiber under thermal cycling; OPTICS EXPRESS 2009, Vol. **17**, No. 12 / pp. 9940-9946

5.4 M Leich, U Röpke, S Jetschke, S Unger, V Reichel, J Kirchhof: Non-isothermal bleaching of photodarkened Ybdoped fibers; OPTICS EXPRESS 2009, Vol. **17**, No. 15 / pp 12588-12593

5.5 S Yoo, C Basu, A J Boyland, C Sones, J Nilsson, J K Sahu, and D Payne: Photodarkening in Yb-doped aluminosilicate fibers induced by 488 nm irradiation: Optics Letters, Vol. **32**, No. 12, 2007

Chapter 6

NIR pump induced photodarkening

6.1 Introduction:

NIR pumped YDFs often show visible fluorescence in blue/green region, due to Yb-ion pair effect. This can be correlated to the photodarkening in YDFs under NIR pumps. In this chapter, some experiments on the photodarkening of different YDFs due to NIR (976 nm) pumping, have been reported and the presence of distinct blue-fluorescence have been discussed. It has already been shown that such visible fluorescence occurs even in highly purified silica glass and so can not always be attributed to thulium contamination [6.1]. Moreover, in silica fibers, such kind of Tm^{3+} contamination would have led to stronger absorption/emission lines around 780 nm and 480 nm. 780 nm corresponds to the Tm^{3+} absorption and 480nm corresponds to the emission. But that was not observed in the following experiments. So, the blue-fluorescence can be attributed to ytterbium ion pair (IP) effect [6.1-6.4]. Hydrogen loaded (HL) YDFs were also tested under the same scheme, but the absorption was too high which is in good agreement with [6.5]. It is worth mentioning that blue fluorescence was observed in the HL fibers as well.

At the end of this chapter, some additional experimental and simple simulation results involving 1047 nm CW pump, have been reported.

6.2 Experimental setup and results:

Fig. 6.1 shows the experimental setup for investigating the NIR pumped photodarkening of YDFs. Two Wavelength Division Multiplexers (WDMs) have been used to separate out the NIR pump light (977 nm) and an additional visible probe light (633 nm). The fiber under test (FUT) had to be spliced with the suitable output ports of WDMs concerned. The WDMs (Lightel Technologies Inc.) were characterized using a white light source and OSA in order to verify the suitability for this setup. The WDM characterization plots are shown in Fig. 6.2 & Fig. 6.3.

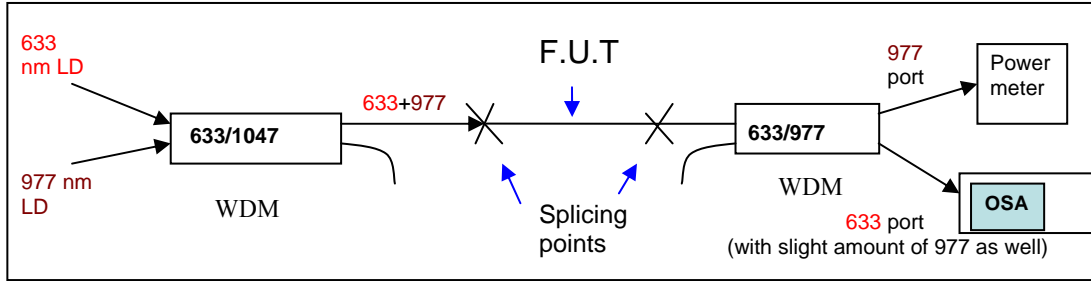


Fig. 6.1: Schematic Diagram of the NIR pumped photodarkening setup

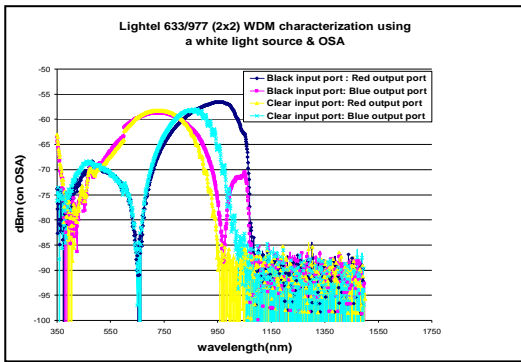


Fig. 6.2: WDM characterization

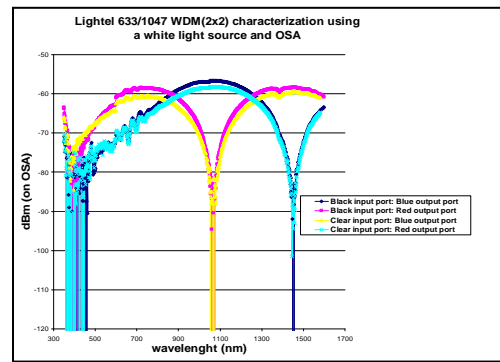


Fig. 6.3: WDM characterization

Fig. 6.4 to Fig. 6.6 show the bluish fluorescence from the various fiber samples pumped by 976 nm CW laser diode. The aluminosilicate fiber with lower concentration (3500 ppm; Fiber # T0116L30059) of ytterbium showed very little photodarkening in the VIS and no photodarkening in the NIR. In case of the phosphosilicate sample, the blue fluorescence was very faint and also no photodarkening was observed (See Fig. 6.5). The HL fiber samples were highly lossy at the pump wavelength and the power meter could not detect any throughput power at all. The blue-fluorescence was observed in HL loaded fibers also, but it was limited only to initial few centimeters from the launching end and that diminished over time. No photodarkening at the probe wavelength (633 nm) was observed, which can be attributed to the high loss of the pump in the core and weak inversion. Fig. 6.7 shows the power calibration plot of the 976 nm CW laser diode source.

The throughput power (at the 977 port of the WDM) was monitored on a Melles Griot(MG) power meter (model-13PEM001 ; detector-MG -D06K0193) and rapid drop in power was monitored only in the case of 17000 ppm YDF (Fiber # T0155L30100). Fig 6.8 shows this. Fig. 6.9 shows the similar experimental results obtained from the T0116L30059 fiber (3500 ppm).The phosphosilicate fiber, in spite of having higher Yb-concentration (20,000 ppm), showed no significant power drop, as shown in Fig. 6.10. This reinforces the findings that phosphosilicate YDF is better than aluminosilicate YDF, as far as photodarkening is concerned [5.6, 5.7]. In Fig.6.11, the throughput spectra of the phosphosilicate YDF at different pump-probe ON/OFF states and low/high pump power levels have been shown. This is helpful to understand respective origins of the peaks/troughs in the spectra. Fig. 6.12 shows the temporal throughput spectra of a hydrogen loaded sample of T0155L30100 fiber under 977 nm pump and 633 nm probe. The details of hydrogen loading are given in section 6.1.

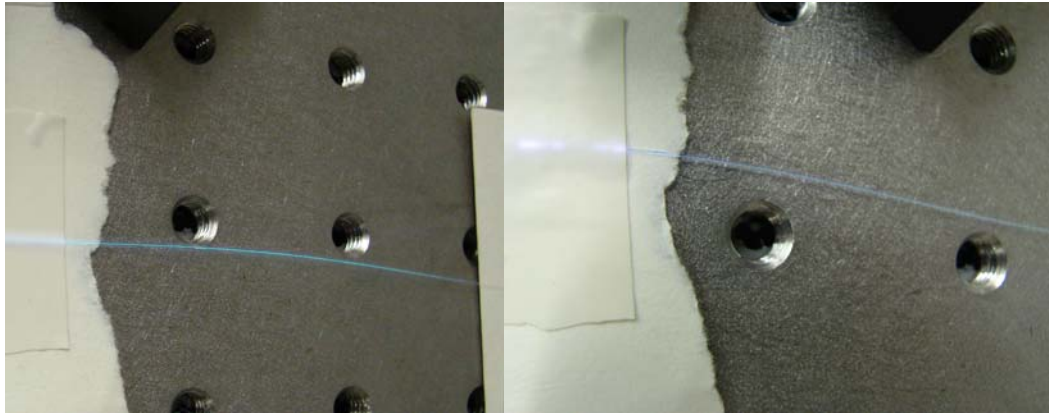


Fig. 6.4 (a)

Fig. 6.4 (b)

Fig. 6.4: bluish fluorescence from (a) Fiber # T0155L30100 (aluminosilicate) & (b) Fiber # T0116L30059 (aluminosilicate)

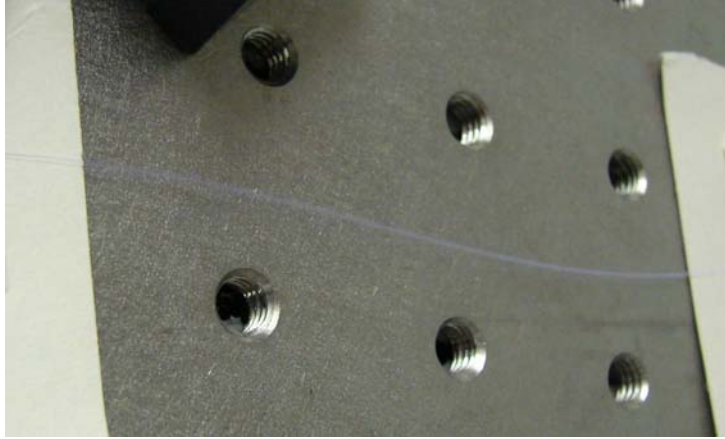


Fig. 6.5: Very faint bluish fluorescence from 20000 ppm YDF (phosphosilicate)

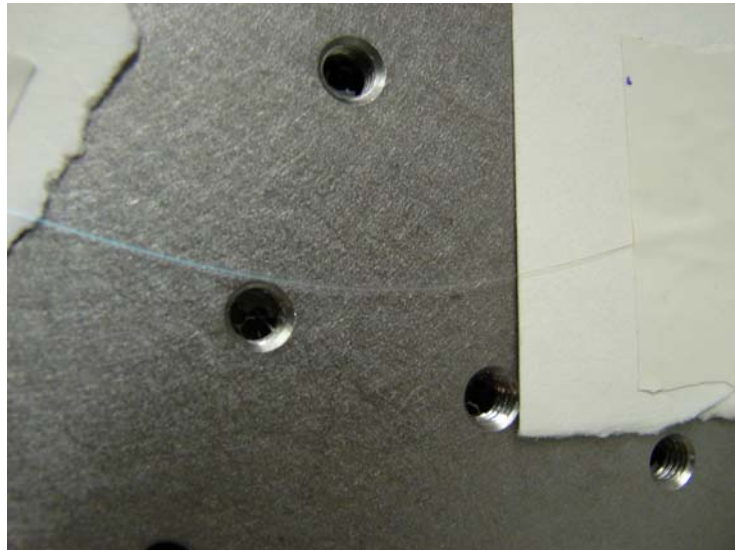


Fig. 6.6: Faint bluish fluorescence from H-loaded YDF (original sample Fiber # T0155L30100). The loss was so high that the fluorescence is visible only from the initial portion (from launching end) of the FUT.

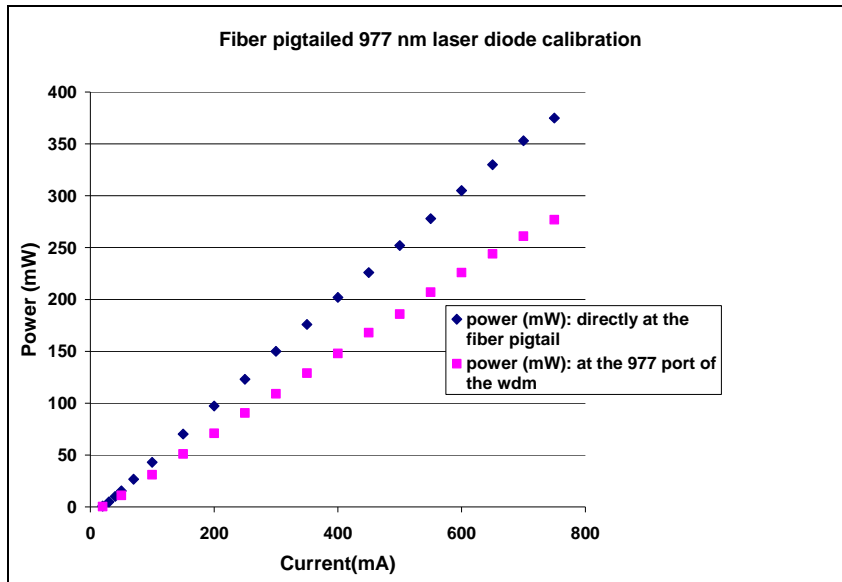


Fig. 6.7: Power calibration of the pump diode (977 nm)

The temporal drop in the throughput power (at 977 nm) of a 12 cm long sample of T0155L30100 fiber is shown in Fig. 6.13.

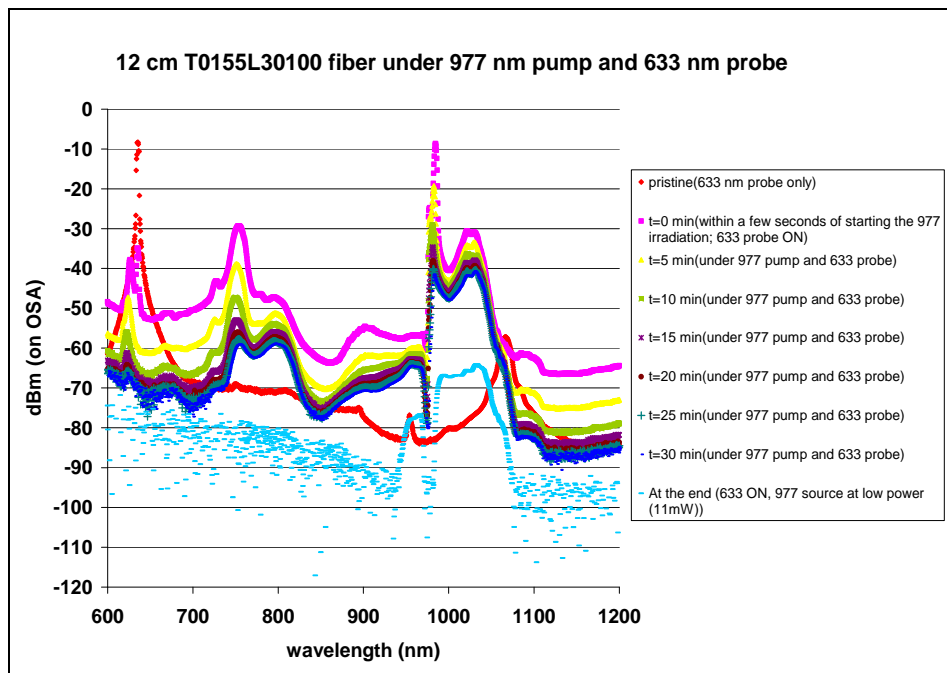


Fig. 6.8: Output spectrum observed on the OSA: Fiber # T0155L30100

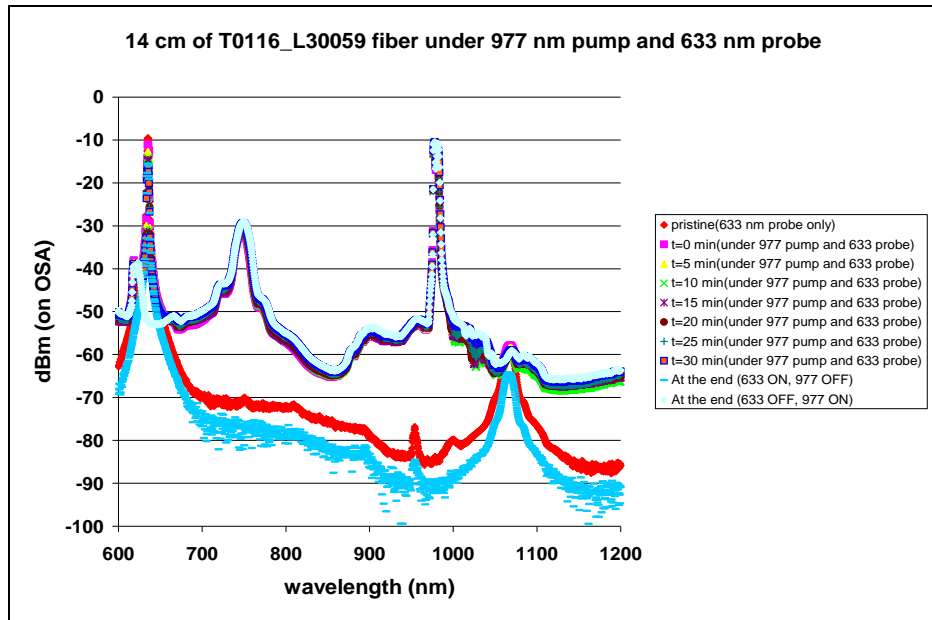


Fig. 6.9: Output spectrum observed on the OSA: Fiber # T0116L30059

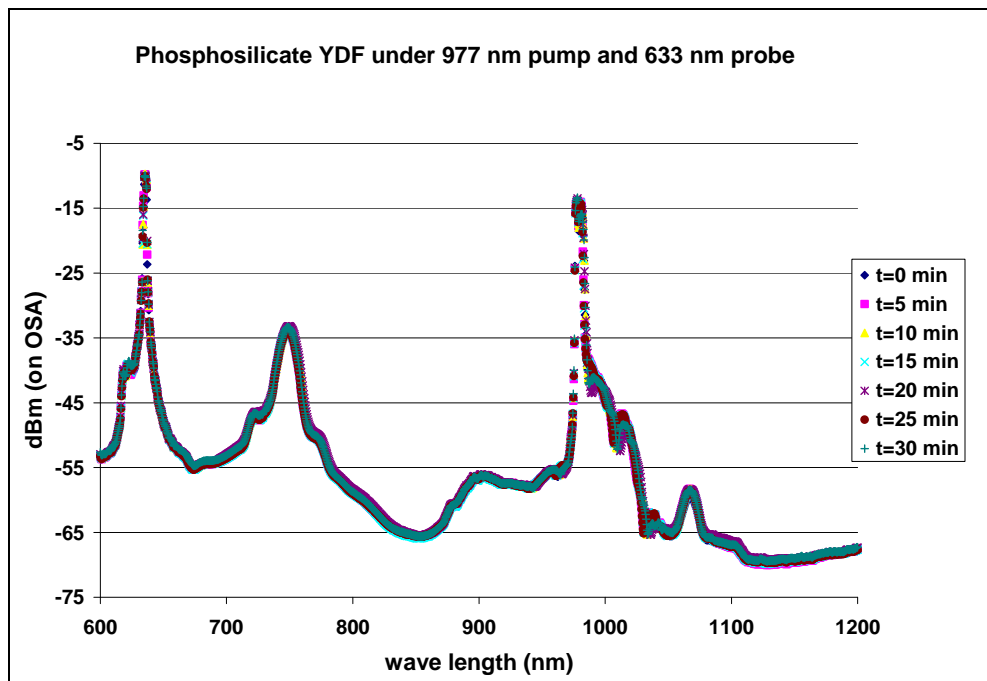


Fig. 6.10: Output spectrum observed on the OSA: 15 cm long, 20000 ppm YDF (phosphosilicate)

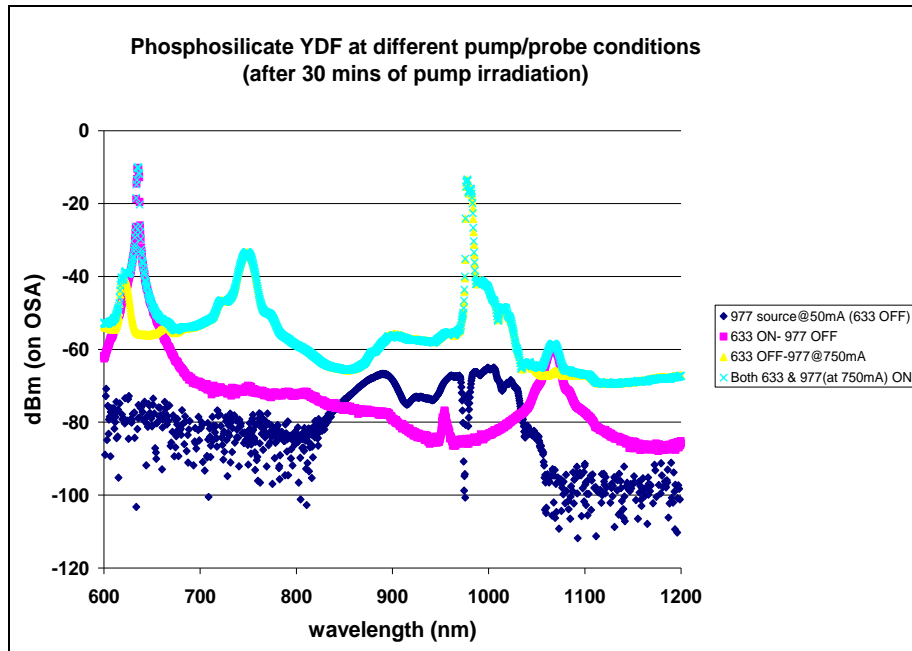


Fig. 6.11: Output spectra of the phosphosilicate YDF at different pump/probe conditions

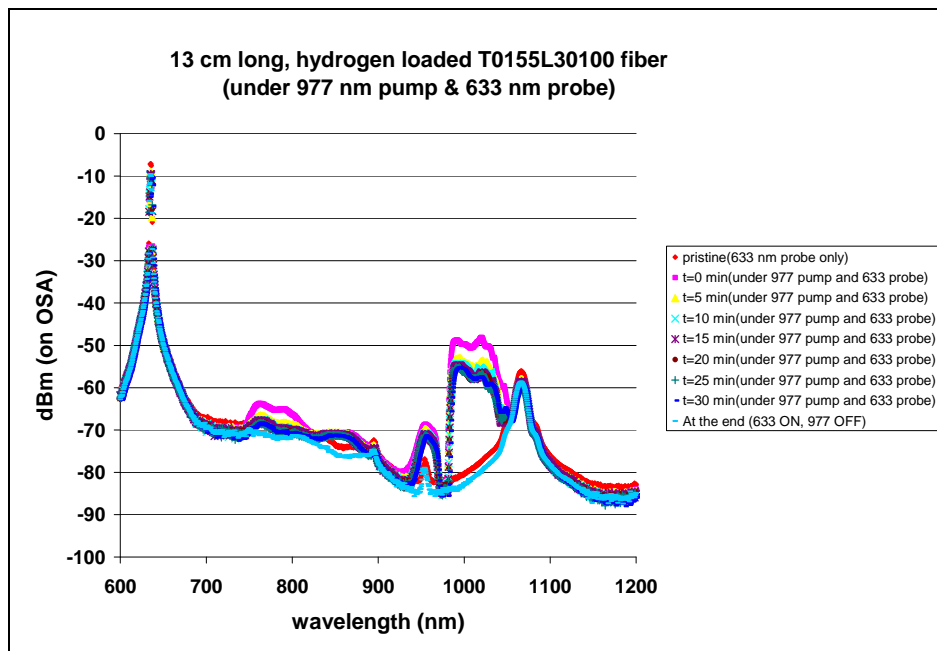


Fig. 6.12: Output spectrum from an HL fiber under 977 nm pump and 633 nm probe

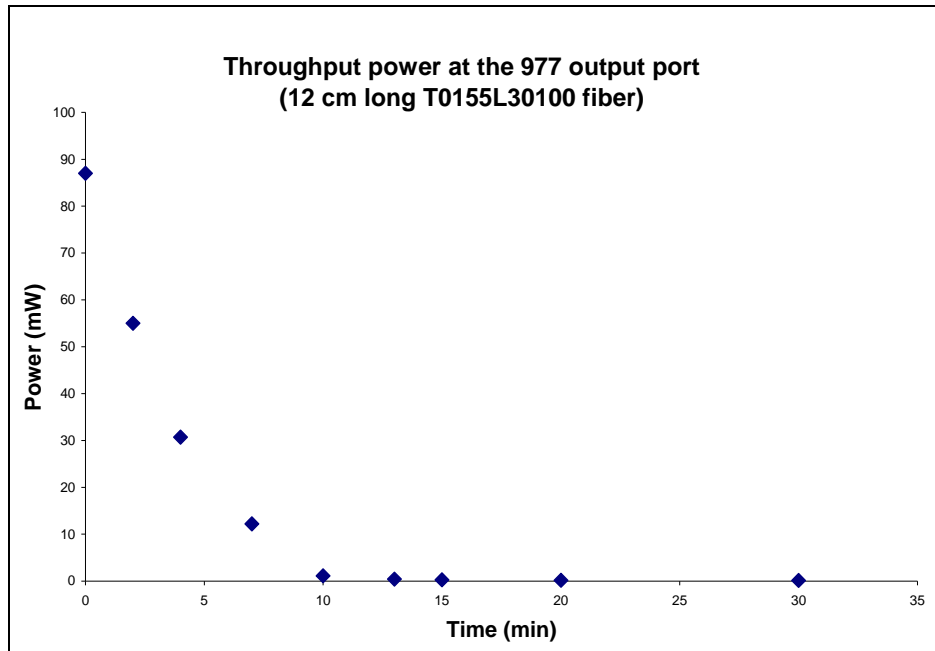


Fig. 6.13: Temporal power drop at NIR (pump and ASE combined)

To investigate the effect of pumping at higher wavelength, a sample of T0155L30100 fiber was irradiated by a 1047 nm CW Nd:YLF source. No photodarkening was observed, although the laser itself showed some instability in the throughput power (fluctuation < 5 mW). The calibration of the said laser and the throughput from the test fiber have been shown in Fig. 6.14 & Fig. 6.15 respectively. It was expected that pumping a YDF at an wavelength of 1047 nm or longer can help overcome photodarkening and, at the same time, such a scheme would be also beneficial for the generation of 1178 nm line [6.8].

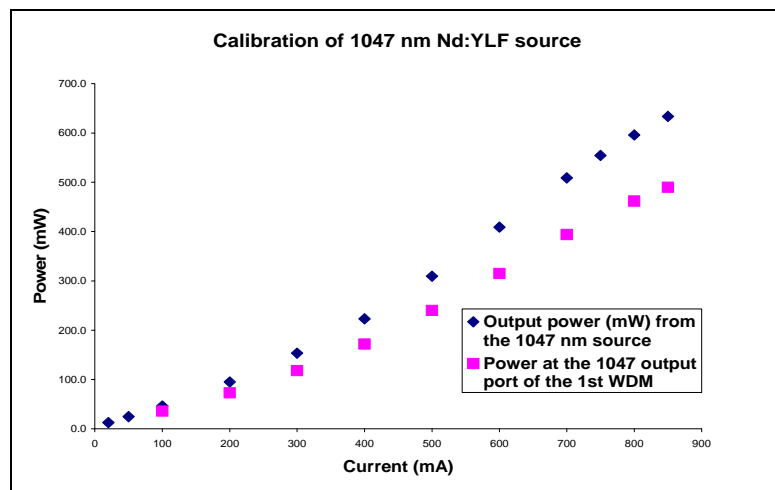


Fig. 6.14: Power calibration of the 1047 nm Nd:YLF source

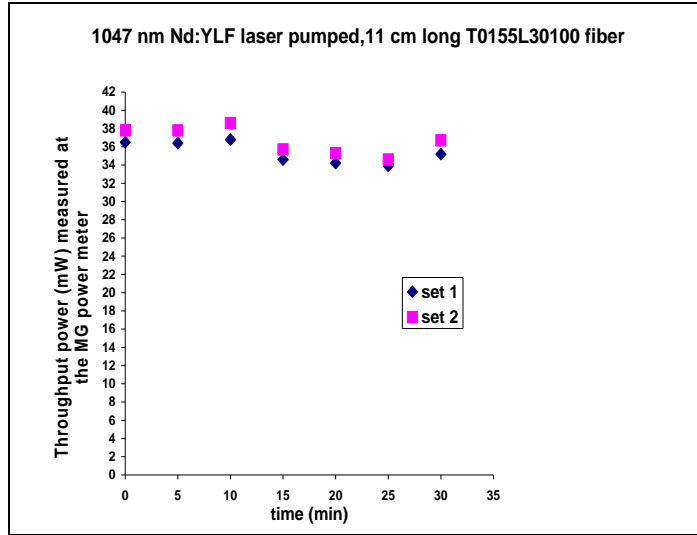


Fig. 6.15: Throughput power stability (No photodarkening observed)

6.3 Pumping at 1047 nm and external heating effect on YDF

Some experiments have been done to study the throughput spectrum from a 1047 nm pumped YDF under external heating. External heating has been shown to improve pump absorption at 1070 nm and reduce ASE [6.9]. Further investigation in this direction can be helpful in order to understand the feasibility and performance dynamics of 1047/1080 nm pumped YDFL generating 1178 nm. Fig. 6.16 schematically shows the setup.

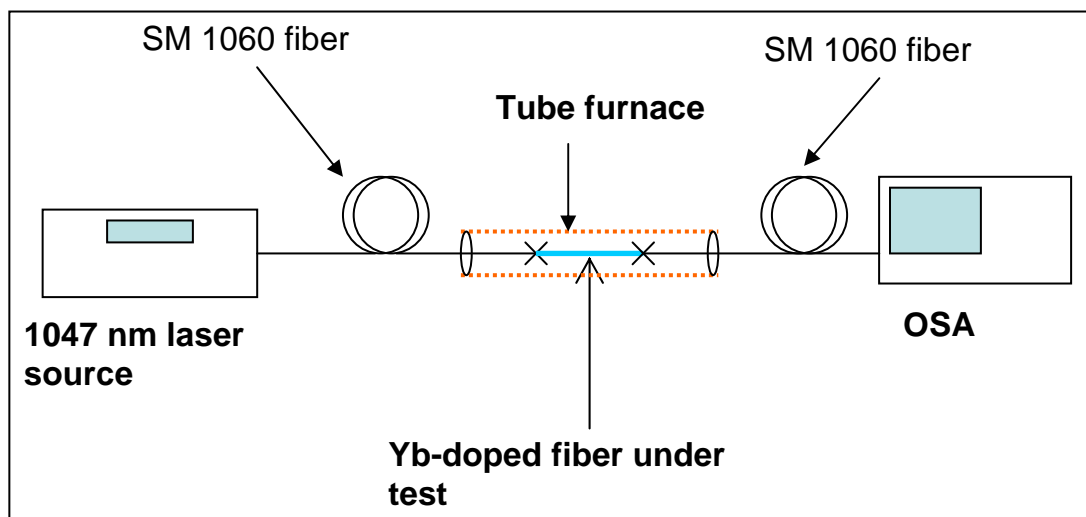


Fig. 6.16: Schematic diagram of the setup for monitoring ASE variation with temperature

Fig. 6.17 shows throughput spectrum in the range 900 nm-1200 nm of a 10 cm long fiber (T0155L30100) under 1047 nm pump. The in-core input power was ~ 14.9 mW. Fig. 6.18 shows the 1080 nm-1280 nm region of the same spectrum. The spectrum was obtained at room temperature (~ 22 °C) and 100 °C.

In these experiments, the variation of the throughput spectra with the temperature, under 1047 nm pump, was clearly observed. Longer lengths of fibers or/and higher pump power should be used for this kind of experiment to observe the ASE with good clarity. The space inside the tube furnace was limited and long length of the fiber was not spirally introduced to avoid bending loss at higher wavelengths and also to ensure uniform heating throughout the sample.

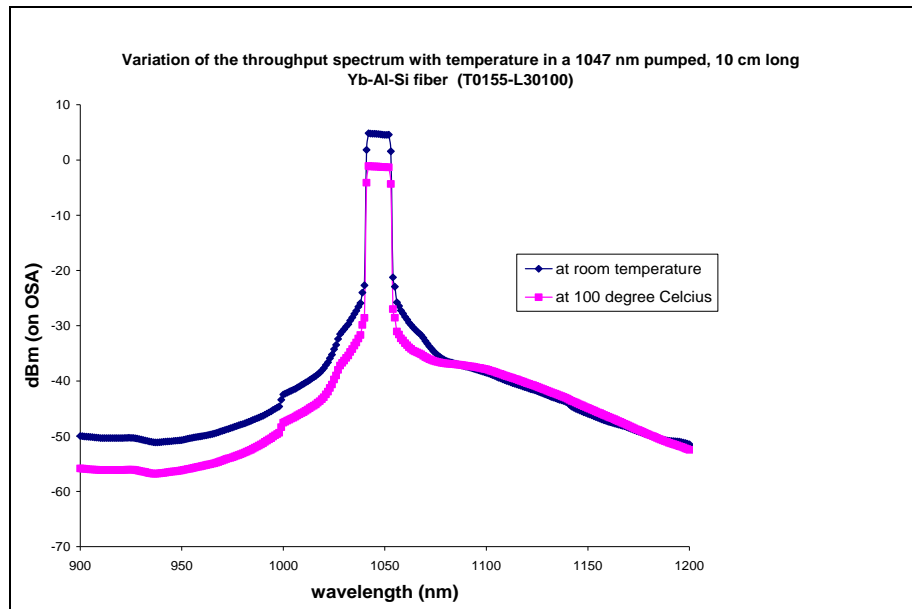


Fig. 6.17: Variation of throughput spectrum on heating the FUT

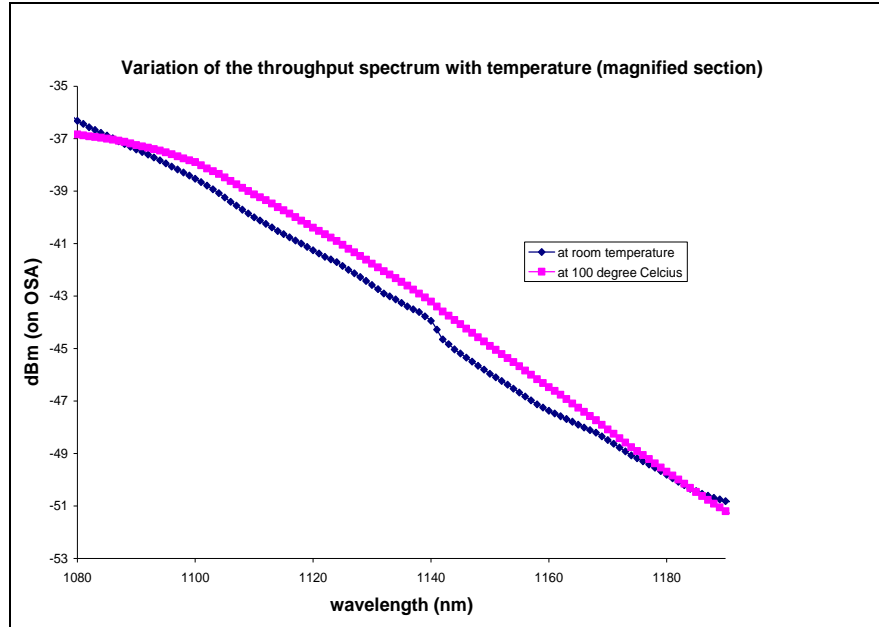


Fig. 6.18: Zoomed in version of Fig. 5.17

6.4 Simulation of YDFA:

Since photodarkening in Yb-doped aluminosilicate fibers depends on the amount of inversion of Yb^{3+} ions (discussed in chapter 2), a simple simulation was performed, based on the Yb-doped fiber amplifier model proposed by R. Paschotta et al [6.10], in order to understand the inversion in YDF at higher pump wavelength (976 nm in this case). The fractional population (n_2) in level 2 of Yb^{3+} has been computed at different pump power levels, at two different signal (1080 nm) power levels (0.08 picowatt and 8 microwatt). This is shown in Fig. 6.19. Signal power level or ASE can be neglected in the amplifier configuration if the fiber length is very short (say, a few centimeters). The amplifier configuration was relevant, given the experimental techniques followed, as the fibers were photodarkened in a non-laser configuration (Fig. 6.1). Physical parameters of the fiber # T0155L30100 were used for this simulation.

The equations used in this simulation, as stated by R. Paschotta et al [6.10], are:

$$\frac{dn_2}{dt} = (R_{12} + W_{12})n_1 - (R_{21} + W_{21} + A_{21})n_2 \quad \dots\dots\dots \text{eqn. (6.1)}$$

$$\frac{dn_1}{dt} = -(R_{12} + W_{12})n_1 + (R_{21} + W_{21} + A_{21})n_2 \quad \dots\dots\dots \text{eqn. (6.2)}$$

$$n_2 = \frac{R_{12} + W_{12}}{R_{12} + R_{21} + W_{12} + W_{21} + A_{21}} \quad \dots\dots\dots \text{eqn. (6.3)}$$

$$n_2 = 1 - n_1 \quad \dots\dots\dots \text{eqn. (6.4)}$$

Where, $R_{12} = \frac{\sigma_{12}^{(p)} I_p}{h\nu_p}$; $R_{21} = \frac{\sigma_{21}^{(p)} I_p}{h\nu_p}$; $W_{12} = \frac{\sigma_{12}^{(s)} I_s}{h\nu_s}$; $W_{21} = \frac{\sigma_{21}^{(s)} I_s}{h\nu_s}$, $\sigma_{12}^{(p)}, \sigma_{21}^{(p)}$

are the effective pump absorption and emission cross-sections at 976 nm and on the other hand, $\sigma_{12}^{(s)}, \sigma_{21}^{(s)}$ are the corresponding values at the signal wavelength (1080 nm). R_{12}, R_{21}, W_{12} & W_{21} are the transition rates. I_p, I_s denote the pump and signal intensities in W/m^2 . ν_p, ν_s are the optical pump and signal frequencies, respectively and h denotes Planck's constat. The eqn. (6.3) is the steady state solution obtained from the eqn. (6.1) and eqn. (6.2). n_1 and n_2 are the local fractional population at lower and upper levels, respectively.

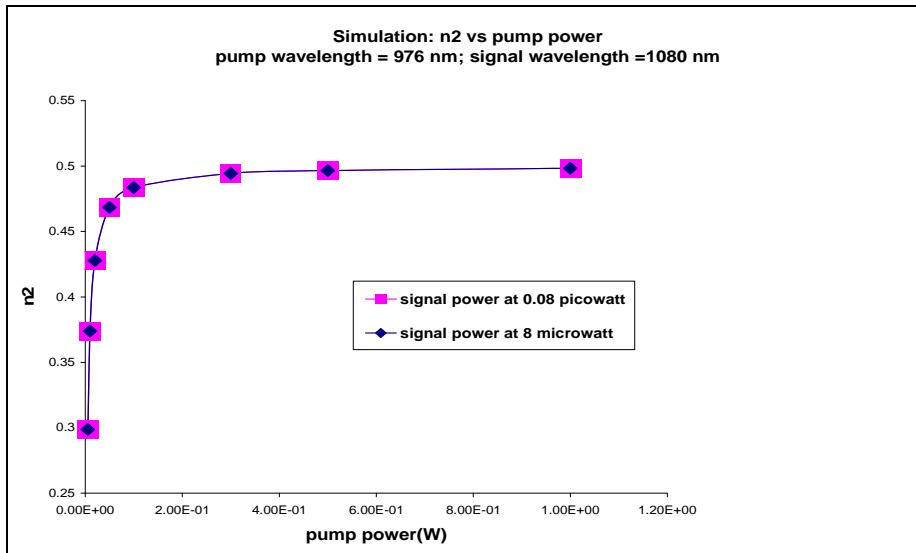


Fig. 6.19: Simulation of inversion vs pump power in a YDF.

6.5 Conclusions:

In this chapter, some investigations on the 976 pump induced visible fluorescence and photodarkening in different YDFs (including the HL ones) have been reported. Strong evidence of Co-operative luminescence or Yb-ion pair effect has been obtained. The HL ones showed very high background loss at 976 nm and 633 nm as well, even in the pristine form. But, a faint blue fluorescence was still observed. It seems that HL YDFs are not very suitable for building a laser system as such a system would demand higher pump power or, in other words, would show lower efficiency. Pumping at 1047 nm showed no signs of photodarkening or any blue fluorescence, which is actually beneficial for pumping YDFs at >1047 nm in order to obtain 1178 nm laser line.

Also, the effect of external heating on the throughput spectrum, while pumping an YDF at 1047 nm, was experimented and the result seemed to be positive, as far as shifting the throughput spectrum towards higher wavelengths is concerned. There have been reports on lasing around 1160 nm from YDFs, with external heating, in order to shift the YB^{3+} emission spectra towards higher wavelength regime [6.9, 6.11]. A basic simulation has been performed in order to see the inversion as a function of pump power (@976 nm), in an amplifier configuration.

References (Chapter 6):

6.1 A V Kir'yanov, Y O Barmenkov, I L Martinez, A S Kurkov, and E M Dianov: Cooperative luminescence and absorption in Ytterbium-doped silica fiber and the fiber nonlinear transmission coefficient at $\lambda=980$ nm with a regard to the Ytterbium ion-pairs' effect; Optics Express, Vol. **14**, Issue 9, pp. 3981-3992, 2006

6.2 S Magne, Y Ouerdane, M Druetta, J P Goure, P Ferdinand, G Monnom: Cooperative luminescence in an ytterbium-doped silica fibre; Optics Communications, Vol. **111**, pp. 310-316, 1994

6.3 Y G Choi, Y B Shin, H S Seo, K. H. Kim: Spectral evolution of cooperative luminescence in an Yb^{3+} -doped silica optical fiber; Chemical Physics Letters, Vol. **364**, pp. 200–205, 2002

6.4 T G Ryan, S D Jackson: Cooperative luminescence and absorption in ytterbium doped aluminosilicate glass optical fibers and preforms; Optics Communications, Vol. **273**, pp. 159–161, 2007

6.5 S Jetschke, S Unger, A Schwuchow, M Leich, V Reichel and J Kirchof: Photodarkening in Yb-doped silica fibers: influence of the atmosphere during preform collapsing; SPIE Proceedings vol. **6873**, 2008

6.6 A V Shubin, M V Yashkov, M A Melkumov, S A Smirnow, I A Bufetov, and E M Dianov: Photodarkening of aluminosilicate and phosphosilicate Yb-doped fibers; Conf. Digest of CLEO Europe-EQEC 2007, CJ3-1-THU

6.7 J K Sahu, S Yoo, A J Boyland, C Basu, M P Kalita, A Webb, C L Sones, J Nilsson and D N Payne: 488 nm irradiation induced photodarkening study of Ybdoped aluminosilicate and phosphosilicate fibers; JTUA27 CLEO USA (2008)

6.8 M P Kalita, S U Alam, C Codemard, S Yoo, A J Boyland, M Ibsen, J K Sahu : Multi-watts narrow-linewidth all fiber Yb-doped laser operating at 1179 nm; Optics Express, Vol.18 pp.5920-5925, 2010

6.9 A S Kurkov , V M Paramonov, O I Medvedkov: Ytterbium fiber laser emitting at 1160 nm; Laser Physics Letters, Vol. 3, No. 10, pp 503–506, 2006

6.10 R Paschotta, J Nilsson, A C Tropper and D C Hanna: Ytterbium-doped fiber amplifiers; IEEE J. Quantum Electron. 33, 1049-1056, 1997

6.11 A S Kurkov: Oscillation spectral range of Yb-doped fiber lasers; Laser Physics Letters, Vol. 4, No. 2, pp 93-102, 2007

Chapter 7

Hydrogen loaded fibers

7.1 Photodarkening in hydrogen loaded fibers under 488 nm irradiation:

Presence of divalent ytterbium in aluminosilicate host was reported, both under reducing and oxidizing environments [7.1, 7.2]. It was also perceived that the divalent ytterbium ions could play a role in the photodarkening mechanism [7.2]. Hydrogen loading on some ytterbium doped aluminosilicate fibers was performed in order to see whether that affects the characteristics of 488 nm irradiation induced photodarkening.

Some experimental results on photodarkening (no external heating) of hydrogen loaded (HL) fibers are shown in Fig. 7.1 & Fig. 7.2. It seemed that hydrogen loading damaged the coating of the fiber to a certain extent. Samples of the T0155L30100 fiber were hydrogen loaded for 4 weeks at a temperature of 70°C and 140 atm. of pressure. These fiber samples were then subjected to the 488 nm irradiation, in a similar manner as followed for non-HL fibers. Drop in throughput power due to 488 nm CW irradiation is evident from Fig. 7.1. These fiber samples were probed by a He-Ne laser at 633 nm, while being irradiated by 488 nm and also after stopping the 488 nm irradiation. The results of this simultaneous probing at 633 nm are shown in Fig. 7.2. The induced excess loss values monitored in terms of drop in throughput power as well as from cutback technique are given in Table T7.1.

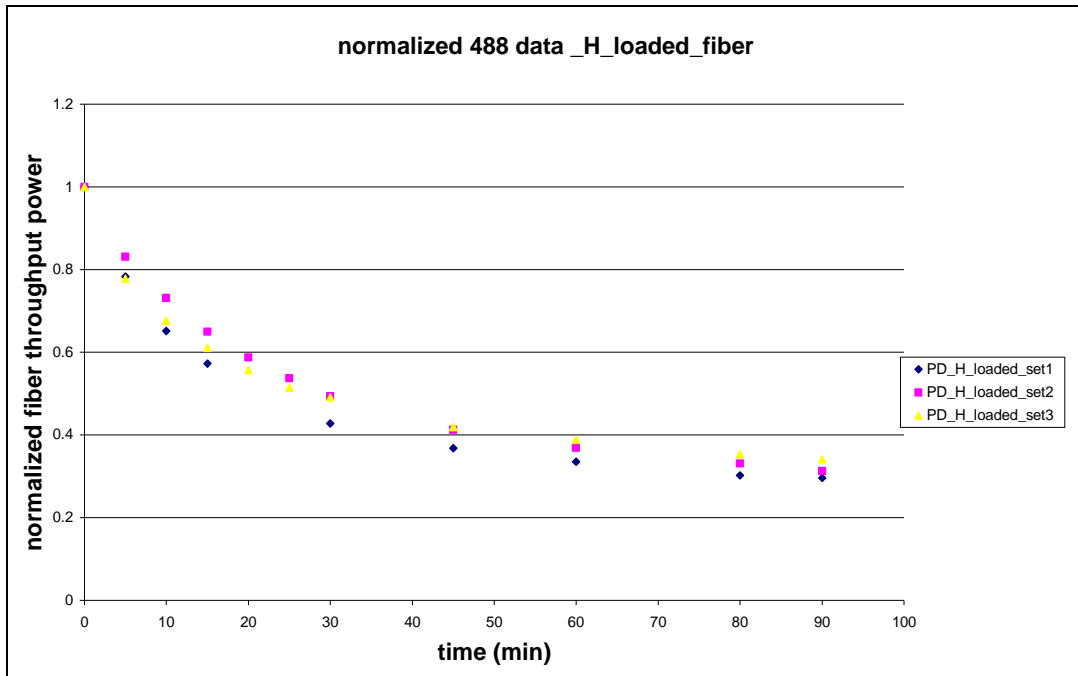


Fig. 7.1: Normalized drop in throughput power (@488 nm) in HL YDF samples (T0155L30100)

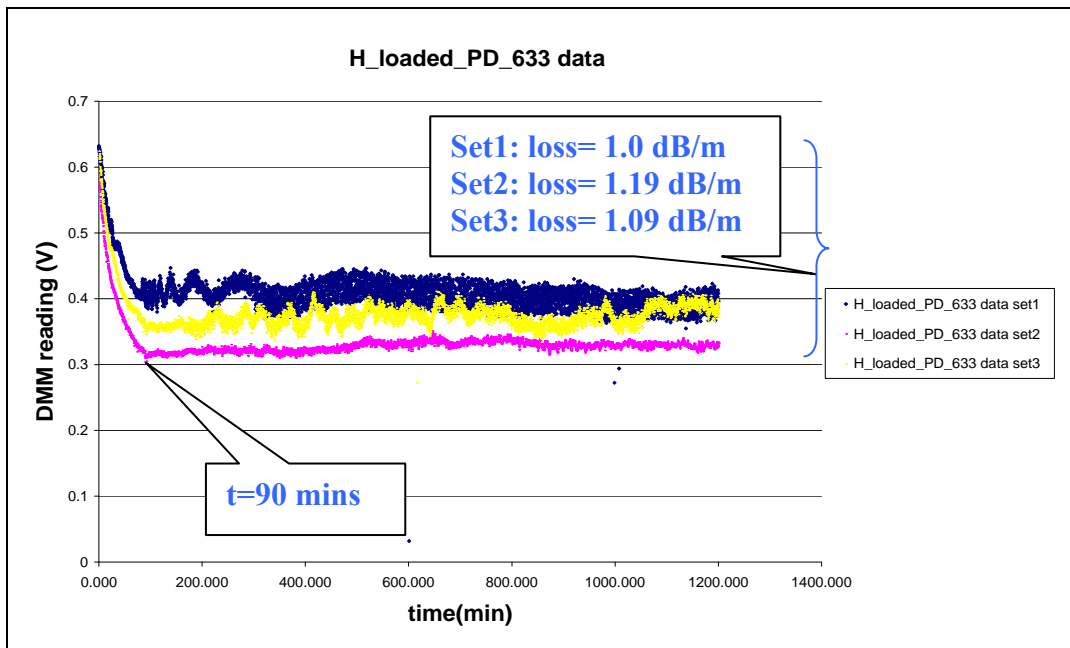


Fig. 7.2: Drop in the throughput power of the probe (@633 nm) in HL YDF samples (T0155L30100)

Sl.No.	Loss@633 nm over the 488 irradiation time (dB/m)	Post-irradiation loss@633 nm observed up to 20 hrs (dB/m)	Final loss measured by cutback at 633 nm (dB/m)
Set 1	1.00	NIL	1.1
Set 2	1.19	NIL	1.1
Set 2	1.09	NIL	1.0

Table T7.1: Summary of the results related to the data shown in Fig.1 & Fig.2

7.2 Hydrogen loading and effect on the coating material:

The HL fibers (T0155_L30100) were observed to photodarken under 488 irradiation, as far as the drop in throughput power was concerned. But the amount of induced excess loss, in each case, was almost equal to the final loss measured by cutback (~ 1 dB/m @ 633 nm). Unlike in non-HL fibers, no post-irradiation temporal evolution in loss was observed in HL fibers. In order to address this ambiguity, the HL fibers were probed under a white light source and OSA. The most important observation was the disappearance of Yb^{3+} absorption band between 850-1050 nm in the HL fiber even before or after photodarkening. This could be seen as a result of reduction of trivalent Yb to divalent Yb ions but, almost complete reduction of ~15000 ppm of trivalent Yb seemed to be unreasonable. After twisting the fiber in the middle, the Yb^{3+} absorption band was again visible on the OSA. This was a strong indication that the fiber coating material, DSM-314, might have been affected by hydrogen loading, leading to lowering of refractive index. That is to say that the guiding behaviour of the fiber was very much similar to that of a typical low-index fiber.

Fig. 6.3 shows the comparison of the white light spectra in a pristine fiber sample (50 cm), an HL fiber (unirradiated) and the same HL fiber with a small loop (twisted). Similar absorption bands were observed with the pristine fiber and the HL

fiber. However, the Yb^{3+} absorption band was missing in the straight/untwisted HL fiber. Fig. 7.4 is a zoomed in version of the absorption band shown in Fig. 7.3. Further investigation was pursued in order to see, if there was any, change in the refractive index profile (RIP) in an irradiated HL fiber, as compared to an unirradiated HL fiber. For this, a standard Photon Kinetics S14 profiler was used and no difference in the RIP was observed (Fig. 7.5). The RIP data was obtained by Mr. Rob Standish at the ORC, University of Southampton.

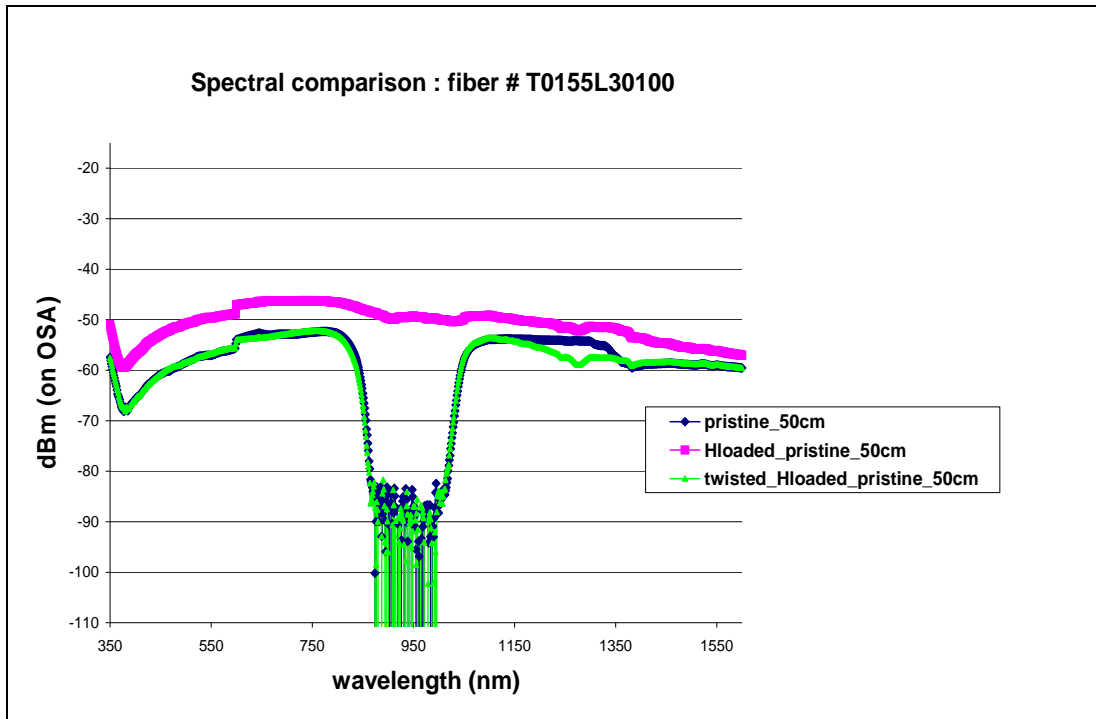


Fig. 7.3: White light throughput spectra from an HL pristine YDF sample (straight & twisted) and comparison with the same from a non-HL pristine sample.

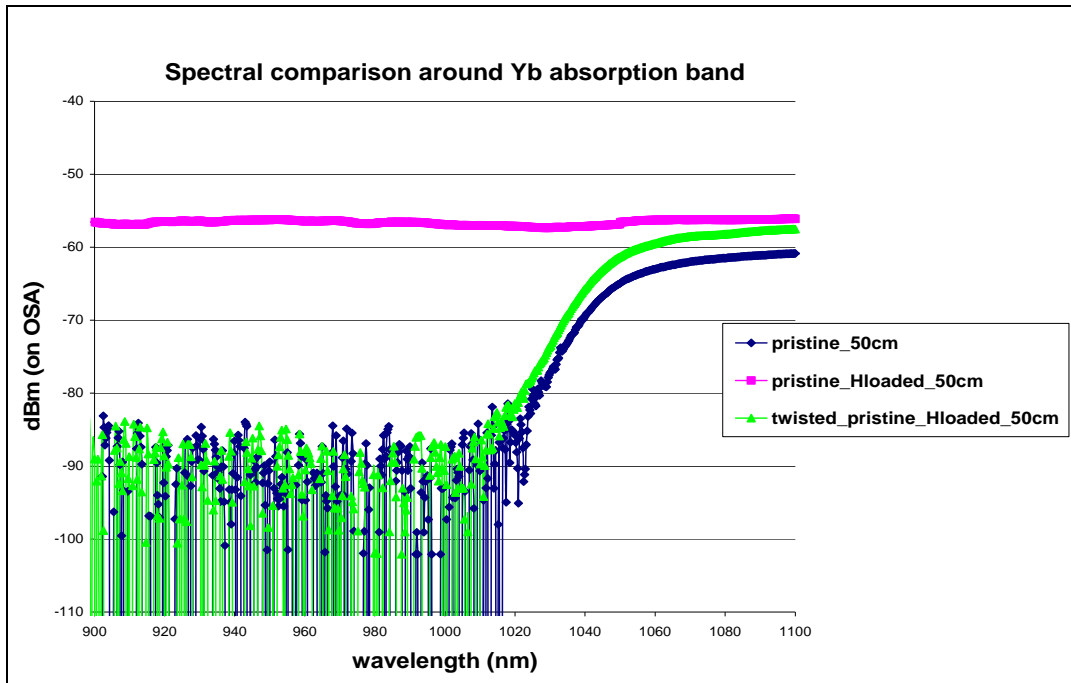


Fig. 7.4: White light throughput spectra, around the Yb^{3+} absorption band in an HL pristine YDF sample (straight & twisted) and comparison with a non-HL pristine sample.

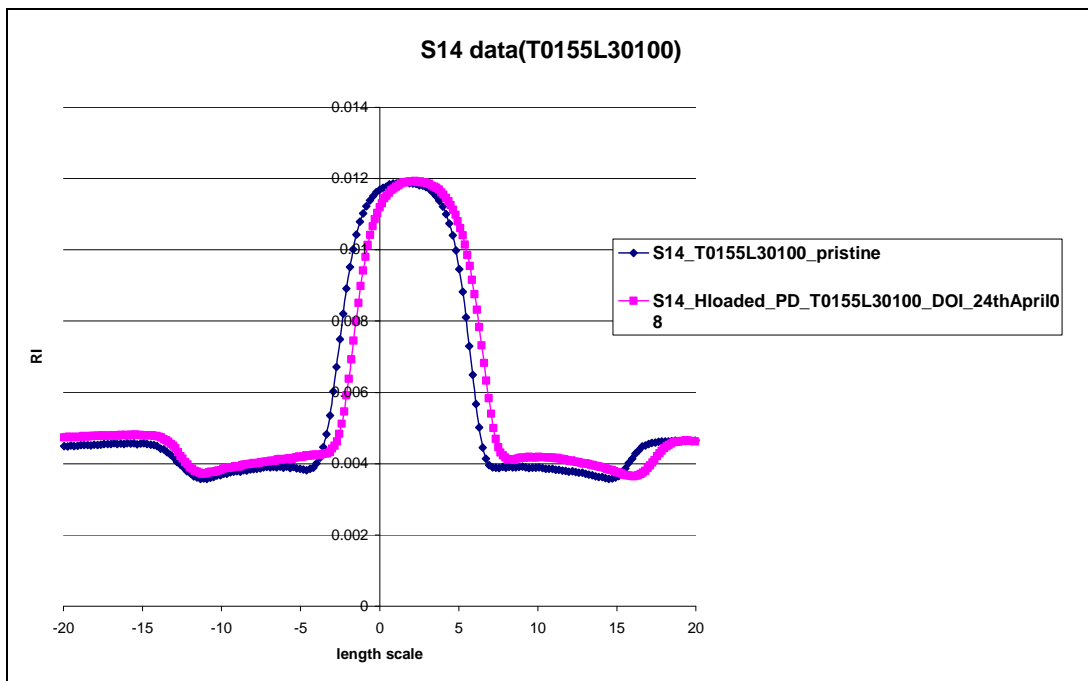


Fig. 7.5: Refractive index profile comparison between a pristine HL fiber sample and the same after being irradiated by 488 nm laser source.

7.3 Discussion & Conclusion:

Fig. 7.3 & Fig. 7.4 clearly show the apparent disappearance of the Yb^{3+} absorption band in the HL fiber whereas an identical non-HL pristine fiber sample shows the Yb^{3+} absorption band. A little twist (single loop of dial ~ 1.5 cm) in the HL fiber shows back the Yb^{3+} absorption band. This might be an indication that the coating material (DSM-314) got affected due to hydrogen loading. A possibility is that during the high pressure H_2 loading the coating got separated from the glass surface. In Fig. 7.5, the refractive index profile of a pristine T0155_L30100 fiber has been compared to that of an identical HL fiber which was photodarkened for 90 minutes under 488 nm CW irradiation but, no significant difference was observed.

References:

7.1 M Engholm, L Norin, and D Åberg, "Strong UV absorption and visible luminescence in ytterbium-doped aluminosilicate glass under UV excitation," *Optics Letters* **32**, 3352-3354 (2007)

7.2 M Engholm and L Norin, "Divalent Ytterbium in Ytterbium Doped Aluminosilicate Glass: Aspects on Photodarkening in Fiber Lasers," in Conference on Lasers and Electro-Optics/Quantum Electronics and Laser Science Conference and Photonic Applications Systems Technologies, OSA Technical Digest (CD) (Optical Society of America, 2007), paper JTUA61.

Chapter 8

Conclusions

8.1 Summary and Conclusions:

This thesis is based on the experimental works on photodarkening in ytterbium doped fibers, mostly using a 488 nm CW laser source for irradiation, although some other results obtained due to NIR pumping, are also presented.

The choice of the irradiation source (@488 nm) was interesting as the wavelength does not come under the typical Yb^{3+} absorption bands and still photodarkening was observed. Unlike photodarkening caused by NIR pumping, which involves a great amount of dependence on the population inversion, photodarkening caused by 488nm irradiation was a different way to understand the physics of photodarkening. Although phosphosilicate fiber samples were also used, mostly the focus was on aluminosilicate fibers as the motivation for this thesis was based on the idea of generating 1178 nm line which could be utilized for creating laser guide stars, after frequency doubling. Phosphosilicate YDFs are limited up to 1080 nm as evident from its emission cross sections.

Several aluminosilicate fibers, fabricated at the Optoelectronics Research Centre, University of Southampton in the UK, were utilized for the experiments reported here. The early experiments were based on the 488 nm irradiation, temporal monitoring of the drop in throughput power, followed by cutback measurements at or around 633 nm, either by using a coherent source or a by using a white light source and an OSA. The white light spectra also indicated additional broad absorption bands in the photo darkened fiber samples. Such absorption bands stretched from UV to NIR, as confirmed by OTDR measurements as well.

A highly Yb-doped phosphosilicate fiber was found to be highly resistant to photodarkening by 488 nm irradiation, unlike its aluminosilicate counterpart. This

was an interesting finding and, to the best of my knowledge, first of its kind in the given wavelength regime (488 nm). OTDR measurements, at 1285 nm probe wavelength, also confirmed this.

Post irradiation temporal evolution of loss was the most important observation in this thesis work and again, to the best of my knowledge, first of its kind in Yb-doped aluminosilicate fibers. It was clearly verified that the photodarkening loss mechanism was not very straightforward and the loss continued to grow even after stopping the 488 nm CW irradiation. Simultaneous probing (@633 nm) of photodarkening in YDFs, while being irradiated by 488 nm CW source, was carried out under several conditions.

Effect of external heating on photodarkening, during and after 488 nm irradiation, was studied with special emphasis on the of post irradiation temporal evolution of loss.

976 nm pumped YDF samples have been shown to fluoresce in blue and photodarken. Hydrogen loaded fiber samples have been shown to have very high background loss at the NIR regime.

The most important contribution of this work was the observation of the influence of external heating in speeding up the post-irradiation temporal evolution of loss in photodarkened fibers and finally leading to faster saturation. Clearly, it can be hypothesized that the post-irradiation temporal evolution of loss in photodarkened fibers is a thermal process in absence of further laser irradiation. It indicates that apart from the creation of defect centres and subsequent loss evolution during laser irradiation, some “potential defect centres” are also formed which capture thermally excited electrons/holes later on after stopping the laser irradiation.

In the plots, multiple sets of the experimental data have been presented, wherever possible. Although error bars are not added to the plots explicitly, the measurement

instruments have been clearly mentioned with respective model numbers and from that one can have an idea of the accuracy levels of the measurements concerned.

8.2 Future work:

In-depth study on the thermodynamics of photodarkening in YDFs, both during and after laser irradiation, would be an interesting aspect of further research along the line of this thesis. Also, a correlation between the thermal conditions during preform fabrication and the amount or speed of photodarkening in the YDFs concerned can possibly be drawn and if so, optimization of the fabrication conditions, in order to reduce photodarkening, may be possible.

Very limited amount of reports are available on thermal bleaching of photodarkened YDFs and this could be another area to work on. Intuitively, thermal bleaching, especially in commercial systems, should be a more viable option as compared to optical bleaching which would demand for an additional laser source and rather complicated laser architecture. The choice of coating material would be crucial for thermal bleaching.

Photodarkening in YDFs due to unconventional pump wavelengths (e.g. 1090 nm or so) for higher wavelength (1178 nm) output generation, should be compared to the results obtained with conventional pumping at 915 nm or 976 nm. This can lead to the identification of the up-conversion band which, as a consequence of ion pair effect, causes photodarkening in YDFs. Further, addition of co-dopants in order to absorb such up-conversion band(s) and thus reduce photodarkening, can be investigated. It has already been shown that cerium codoping helps improve resistance to photodarkening in YDFs [8.1].

No concrete theory or mathematical model of photodarkening in YDFs is available till date. It will be extremely beneficial to compile the individual research works in this field, where different technical approaches have been taken to understand and characterize photodarkening in YDFs and finally develop a theoretical model. It will

be extremely beneficial, for the industrial YDFs to have a well defined “photodarkening parameter” which can clearly indicate the user about the expected amount of photodarkening in the long run, under specified operating conditions like pump power density, external temperature etc.

Reference (Chapter 8):

8.1 M Engholm, P Jelger, F Laurell, and L Norin: Improved photodarkening resistivity in ytterbium-doped fiber lasers by cerium codoping; *Optics Letters*, vol. 34, pp 1285-1287, 2009

Appendix A

A. List of publications

- 1.** S Yoo, C Basu, A J Boyland, C Sones, J Nilsson, J K Sahu, and D Payne: Photodarkening in Yb-doped aluminosilicate fibers induced by 488 nm irradiation: Optics Letters, Vol. **32**, No. 12, pp 1626-1628, 2007
- 2.** J K Sahu, S Yoo, A J Boyland, C Basu, M P Kalita, A Webb, C L Sones, J Nilsson, and D N Payne: 488 nm irradiation induced photodarkening study of Yb doped aluminosilicate and phosphosilicate fibers; poster-CLEO USA (2008)
- 3.** C Basu, S Yoo, A J Boyland, A Webb, C L Sones , J K Sahu: Influence of temperature on the post-irradiation temporal loss evolution in Yb-doped aluminosilicate fibers, photodarkened by 488 nm CW irradiation; CJ1.2, CLEO/Europe-EQEC 2009 Munich, 2009